ผลของน้ำหนักโมเลกุลของสารช่วยกระจายตัวต่อการกระจายตัวและเสถียรภาพของสารแขวนลอยในน้ำของอนุภาคซิงก์ออกไซด์ระดับนาโน

นางสาวฤดีรัตน์ สันตะโก

วิทยานิพนธ์นี้เป็นส่วนหนึ่งของการศึกษาตามหลักสูตรปริญญาวิทยาศาสตรดุษฎีบัณฑิต
สาขาวิชาวัสดุศาสตร์ ภาควิชาวัสดุศาสตร์
คณะวิทยาศาสตร์ จุฬาลงกรณ์มหาวิทยาลัย
ปีการศึกษา 2555

EFFECTS OF DISPERSANT MOLECULAR WEIGHT ON DISPERSION AND STABILITY OF ZINC OXIDE NANOPARTICLE AQUEOUS SUSPENSION

Miss Rudeerat Suntako

A Dissertation Submitted in Partial Fulfillment of the Requirements
for the Degree of Doctor of Philosophy Program in Materials Science
Department of Materials Science
Faculty of Science
Chulalongkorn University
Academic Year 2012

Thesis Title	EFFECTS OF DISPERSANT MOLECULAR WEIGHT ON DISPERSION AND STABILITY OF ZINC OXIDE NANOPARTICLE AQUEOUS SUSPENSION
By	Miss Rudeerat Suntako
Field of study	Materials Science
Thesis Advisor	Assistant Professor Nisanart Traiphol, Ph.D.
Thesis Co-advisor	Assistant Professor Rakchart Traiphol, Ph.D.

Accepted by the Faculty of Science, Chulalongkorn University in Partial Fulfillment of the Requirements for the Doctoral Degree

…….. Dean of the Faculty of Science

(Professor Supot Hannongbua, Dr. rer. nat.)

THESIS COMMITTEE

……. Chairman

(Assistant Professor Sirithan Jiemsirilers, Ph.D.)

…….. Thesis Advisor

(Assistant Professor Nisanart Traiphol, Ph.D.)

……. Thesis Co-advisor

(Assistant Professor Rakchart Traiphol, Ph.D.)

……. Examiner

(Assistant Professor Pornapa Sujaridworakun, Ph.D.)

……. Examiner

(Karn Serivalsatit, Ph.D.)

……. External Examiner

(Assistant Professor Benya Cherdhirunkorn, Ph.D.)

ฤดีรัตน์ สันตะโก : ผลของน้ำหนักโมเลกุลของสารช่วยกระจายตัวต่อการกระจายตัวและเสถียรภาพของสารแขวนลอยในน้ำของอนุภาคซิงก์ออกไซด์ระดับนาโน. (EFFECTS OF DISPERSANT MOLECULAR WEIGHT ON DISPERSION AND STABILITY OF ZINC OXIDE NANOPARTICLE AQUEOUS SUSPENSION) อ.ที่ปรึกษาวิทยานิพนธ์หลัก : ผศ.ดร. นิศานาถ ไตรผล, อ. ที่ปรึกษาวิทยานิพนธ์ร่วม : ผศ.ดร. รักชาติ ไตรผล, 129 หน้า.

งานวิจัยนี้เตรียมสารแขวนลอยในน้ำของอนุภาคซิงก์ออกไซด์ (ZnO) ระดับนาโนเมตรที่ปริมาณของแข็งร้อยละ 0.5 โดยน้ำหนัก โดยใช้พอลิอะคริลิคแอซิด (PAA) เป็นสารช่วยกระจายตัว ผง ZnO ที่ใช้มีขนาดอนุภาคเดี่ยวเฉลี่ย 65.31 174.56 และ 224.54 นาโนเมตร และ PAA มีน้ำหนักโมเลกุล 1.8k 450k และ 3000k กรัม/โมล จากนั้นทำการศึกษาการกระจายตัวของอนุภาคและความเสถียรของสารแขวนลอย ZnO ในน้ำ พบว่า PAA(1.8k) มีประสิทธิภาพดีที่สุดในการทำหน้าที่เป็นสารช่วยกระจายตัวสำหรับ ZnO ทุกขนาด โดยสามารถเตรียมสารแขวนลอยที่มีการกระจายตัวของอนุภาคที่ดีและมีเสถียรภาพสูงที่ปริมาณ PAA(1.8k) ร้อยละ 0.5 โดยน้ำหนัก สารแขวนลอยที่เตรียมได้มีค่ากลางขนาดของกลุ่มอนุภาคเท่ากับ 0.18 0.37 และ 1.02 ไมครอน เมื่อเตรียมจากผง ZnO ขนาด 65.31 174.56 และ 224.54 นาโนเมตร ตามลำดับ และสารแขวนลอยมีความเสถียรสูง ไม่เกิดการตกตะกอนได้ถึง 28 วัน อย่างไรก็ตาม PAA(450k) และ PAA(3000k) สามารถใช้เป็นสารช่วยกระจายตัวที่มีประสิทธิภาพได้เช่นกันเมื่อใช้ในปริมาณที่สูงกว่า จากการคำนวณปริมาณการดูดซับของ PAA บนพื้นผิวอนุภาค ZnO พบว่าข้อมูลมีรูปแบบ Langmuir isotherm เมื่อคำนวณพื้นที่ผิว ZnO ที่ถูกครอบคลุมต่อหนึ่งโมเลกุลของ PAA บนอนุภาค ZnO ขนาดต่างกัน ผลที่ได้แสดงให้เห็นว่า PAA น้ำหนักโมเลกุลต่ำจะดูดซับบนพื้นผิวอนุภาคแบบ loops และ tails ในขณะที่ PAA น้ำหนักโมเลกุลสูง จะดูดซับแบบ tails เป็นส่วนใหญ่ และ PAA จะดูดซับบนอนุภาคขนาดใหญ่แบบ loops และ tails ในขณะที่บนอนุภาคขนาดเล็กจะเป็นแบบ tails ความแตกต่างของรูปร่าง PAA ที่ดูดซับบนผิว ZnO เกี่ยวข้องโดยตรงกับประสิทธิภาพการทำหน้าที่เป็นสารช่วยกระจายตัวของ PAA นอกจากผลของ PAA ต่อการเตรียมสารแขวนลอยอนุภาค ZnO ระดับนาโนเมตรแล้ว ในงานวิจัยนี้ยังศึกษาถึงอิทธิพลของ PAA ต่อลักษณะสมบัติของอนุภาค ZnO ระดับนาโนเมตรซึ่งสังเคราะห์ด้วยวิธีการตกตะกอนอีกด้วย โดยพบว่าขนาดอนุภาคเดี่ยวของ ZnO ที่สังเคราะห์ได้ถูกควบคุมโดยความเข้มข้นของ PAA ที่ใช้ เมื่อเพิ่มความเข้มข้นของ PAA ในกระบวนการสังเคราะห์ ทำให้อนุภาคมีขนาดเล็กลงและการกระจายขนาดอนุภาคแคบลง โดยสามารถสังเคราะห์อนุภาคเดี่ยวที่มีขนาดเฉลี่ยประมาณ 20 นาโนเมตรได้ เมื่อใช้ PAA ประมาณร้อยละ 1 โดยน้ำหนัก นอกจากนี้ยังพบว่า อนุภาค ZnO ที่สังเคราะห์โดยใช้ PAA มีค่าศักย์ซีต้าสูงกว่าอนุภาคที่สังเคราะห์โดยไม่ใช้ PAA และ ค่าศักย์ซีต้าของอนุภาคเพิ่มขึ้นเมื่อเพิ่มปริมาณ PAA ที่ใช้ในกระบวนการสังเคราะห์ ดังนั้นจากผลการทดลอง อนุภาค ZnO ที่สังเคราะห์โดยใช้ PAA ที่ปริมาณร้อยละ 0.5-1 โดยน้ำหนักมีแนวโน้มที่จะกระจายตัวได้ดีในน้ำ และสารแขวนลอยที่ได้มีความเสถียรสูง ซึ่งเป็นที่ต้องการสำหรับการใช้งานด้านต่างๆ

ภาควิชา วัสดุศาสตร์ ลายมือชื่อนิสิต .....

สาขาวิชา วัสดุศาสตร์ ลายมือชื่อ อ.ที่ปรึกษาวิทยานิพนธ์หลัก .....

ปีการศึกษา 2555 ลายมือชื่อ อ.ที่ปรึกษาวิทยานิพนธ์ร่วม .....

5073938123 : MAJOR MATERIALS SCIENCE
KEYWORDS : ZINC OXIDE / NANOPARTICLES / AQUEOUS SUSPENSION / MOLECULAR WEIGHT

RUDEERAT SUNTAKO : EFFECTS OF DISPERSANT MOLECULAR WEIGHT ON DISPERSION AND STABILITY OF ZINC OXIDE NANOPARTICLE AQUEOUS SUSPENSION. ADVISOR : : ASST. PROF. NISANART TRAIPHOL, Ph.D, CO-ADVISOR : ASST. PROF. RAKCHART TRAIPHOL, Ph.D., 129 pp.

Aqueous suspensions of zinc oxide (ZnO) nanoparticles are prepared at 0.5 wt% solids content using polyacrylic acid (PAA) as a dispersant. Average primary particle sizes of ZnO powder are 65.31, 174.56 and 224.54 nm and PAA molecular weights are 1.8k, 450k and 3000k g/mol. Particle dispersion and stability of the suspensions are investigated. It is found that PAA(1.8k) exhibits the highest dispersant efficiency for all ZnO sizes. Well-dispersed and highly stable suspensions can be obtained at 0.5 wt% PAA(1.8k). Median agglomerate sizes are 0.18, 0.37 and 1.02 μm for suspensions prepared with ZnO powder of sizes 65.31, 174.56 and 224.54 nm, respectively. The highly stable suspensions are not completely precipitate up to 28 days. However, PAA(450k) and PAA(3000k) are also effective as dispersants when using at higher concentrations. Adsorption amounts of PAAs on ZnO surface are determined and the data exhibits Langmuir isotherm. Evaluated area occupied per molecule of PAAs on various ZnO sizes suggests that low molecular weight PAA adsorbed on particles as loops and tails while high molecular weight PAA mostly adsorbed as tails. Also, PAAs adsorbed as loops and tails on large particles while frequently tails on small particles. These differences in adsorption conformation could directly relate to dispersant efficiency of PAAs. In addition to the effects of PAAs on preparation of ZnO nanoparticle suspensions, its influence on characteristics of ZnO nanoparticles synthesized by precipitation method is also investigated. It is found that primary size of synthesized ZnO nanoparticles can be controlled by PAA concentrations. Increasing of PAA concentration narrow the distribution and shift the size to smaller particles. Average primary particle size of around 20 nm can be obtained with 1 wt% PAAs. Moreover, ZnO particles synthesized using PAAs exhibits higher zeta potential than the one without PAA, and the zeta potential values increase with increasing PAA concentration. It suggests that ZnO particles synthesized using 0.5-1 wt% PAAs should be well-dispersed in aqueous medium and provide a highly stable suspension, which is desired for most applications.

Department : Materials Science Student's Signature .....
Field of Study : Materials Science Advisor's Signature .....
Academic Year : 2012 Co-advisor's Signature .....

ACKNOWLEDGEMENTS

I could not have reached this education point without the encouragement of many people who have given me assistance and guidance during my study. I would like to express my gratitude and thanks to the following persons.

Firstly, I would like to thank my dissertation advisor, Asst. Prof. Dr. Nisanart Traiphol, who has kindly given me opportunity and inspiration for Ph.D. study and supported all the research necessities. Next, I wish to thank my co-advisor, Asst. Prof. Dr. Rakchart Traiphol, who has kindly given me very useful suggestions in my research.

I would like to acknowledge Program Strategic Scholarships for Frontier Research Network for the Join Ph.D. Program Thai Doctoral Degree, the Office of the Higher Education Commission, the 90th Anniversary of Chulalongkorn University Fund (Ratchadaphiseksomphot Endowment Fund), and Center of Excellence on Petrochemical and Materials Technology, Chulalongkorn University for my Ph.D. scholarship and research funding. The scholarship and funding have made it possible for me to fulfill my research work.

I would like to thank all my colleagues and staff members in the Department of Materials Science, Chulalongkorn University for their friendship. I am happy to be among them.

Finally, I wish to dedicate this dissertation to my mother and family, who have given me the lasting encouragement and support to make this dissertation possible.

CONTENTS

Page

Page

Page

LIST OF TABLES

Page

LIST OF FIGURES

Page

Page

Page

Page

Page

CHAPTER 1
INTRODUCTION

Zinc oxide (ZnO) is extensively used in many applications such as cosmetics, paints, ceramics and electronics [1]. In these applications, a well-dispersed suspension and a highly stable suspension are required. With increasing attention in nanoparticles, the dispersion and stability of the suspension become a challenge. Due to high surface area (>10-300 m^2/g) and surface energy, nanoparticles tend to agglomerate in the suspension [2]. The nanoparticle agglomerates are often 10-20 times larger than their primary sizes [3]. Particle agglomeration is caused by Van der Waals attractive interactions between particles. To separate particles in a medium, the Van der Waals force must be overcome by repulsive interactions [4]. The main purpose of dispersion in a liquid medium is to break down agglomerates into primary particles, which can be achieved by mechanical action and/or chemical additives [5]. Once the particles are separated, stabilization mechanisms are required to control the dispersion and stability of the particles in a suspension. In general, particles in suspensions can be stabilized by electrostatic, steric, or electrosteric stabilizations [6]. The most effective stabilization mechanism is electrosteric stabilization, which involves electrostatic mechanism from polymer dissociation and steric mechanism from polymer chain conformation. One of the most popular polyelectrolytes used in aqueous suspensions is polyacrylic acid (PAA). It has been reported to promote dispersion and stability of ZnO, Al_2O_3, Si_2N_4, TiO_2, Fe_2O_3, ZrO_2 and $BaTiO_3$ aqueous suspensions [7-15].

Among several factors controlling dispersion of particles in a suspension, properties of a polymeric dispersant including concentration, conformation and molecular weight are ones of the most important. The optimum dispersant concentration suggests that there is an adequate amount of dispersant to cover the particle surface. Therefore, particles can be separated from other particles and stabilized in a medium. Conformation of polymer chains in the suspension also affects the dispersant efficiency. The coiled polymers decrease interparticle distance and cause agglomeration. On the other hand, the extend polymer chains adsorb on particle surface and provided

electrosteric stabilization [16]. The effects of molecular weight are also reported that the optimum polymer length is required for well-dispersed and highly stable suspensions Excessively long polymer chain can cause agglomeration of small particles [17]. In addition, size of particles is found to have effects on adsorption conformation of polymer, which directly influence dispersant efficiency [18]. Therefore, compatibility between particle size and dispersant molecular weight at optimum concentration yields a well-dispersed and highly stable suspension. In this study, influences of PAA dispersant molecular weights on dispersion and stability of ZnO nanoparticle aqueous suspension are investigated. Molecular weights of the PAA used as dispersants are 1.8k, 450k and 3000k g/mol. Particle dispersion is investigated by means of laser light scattering technique, optical microscopy and scanning electron microscopy. Stability of suspensions is studied through sedimentation experiment. Zeta potential is measured to study the net surface charge of particles. Adsorption of PAA on ZnO nanoparticle surface is investigated by FTIR and titration method. Area occupied per molecule of PAA is determined from Langmuir equation. Molecular structure of the polymer additives also plays an important role on synthesis of nanoparticles. Particles with desired characteristics can be achieved by using polymer additives to control size, morphology and surface properties. In this research, effects of PAA molecular weight on ZnO nanoparticles synthesized by precipitation method are investigated. Powder X-ray diffraction (XRD) patterns are measured by X-ray diffractometer. Particle size and morphology are investigated by TEM. Specific surface area is measured by BET technique. Zeta potential is measured in aqueous medium to study surface charge. Optical microscope and light scattering techniques are used to study particle dispersion in aqueous suspension.

The objectives of this study are as follows;

- To study the effects of PAA molecular weight on dispersion and stability of ZnO nanoparticle aqueous suspension and adsorption behavior of PAA on ZnO nanoparticle surface.

- To study the relationship of ZnO particle size and PAA molecular weight in aqueous suspension.
- To study the effects of PAA as an additive on synthesis of ZnO nanoparticles by precipitation method

CHAPTER 2
THEORY AND LITERATURE REVIEWS

This chapter consists of theory on surface properties, dispersion and stabilization of particles in media. Techniques used in this research are reviewed. Literature reviews on dispersion and stability of ZnO particles in suspension using polyelectrolyte and synthesis of ZnO nanoparticles using polymeric additive in process for controlling shape, size and morphology are included.

2.1. Zinc Oxide (ZnO)

2.1.1. ZnO structure

Zinc oxide is an inorganic compound with ZnO formula and white powder appearance. ZnO is widely used as a main material and additive in products including ceramics, glass, cement, plastics, rubber, lubricants, paints, ointments, etc. Additionally, ZnO is a stable material for inorganic anti-bacterial. Zinc oxide nanoparticles have ability in UVA and UVB protection, anti-bacteria and fungal, which are suitable for product improvement in many industries [19].

ZnO crystals have two main forms as hexagonal wurtzite and cubic zinc blende. The hexagonal wurtzite structure consists of a hexagonal close-packed (HCP) lattice as shown in Fig. 2.1 (a). The zinc blende structure has a face-centered cubic (FCC) lattice. The four cations (Zn^{2+}) are at corners of a tetrahedral and it is surrounded by anion (O^{2-}) as shown in Fig.2.1(b) [19].

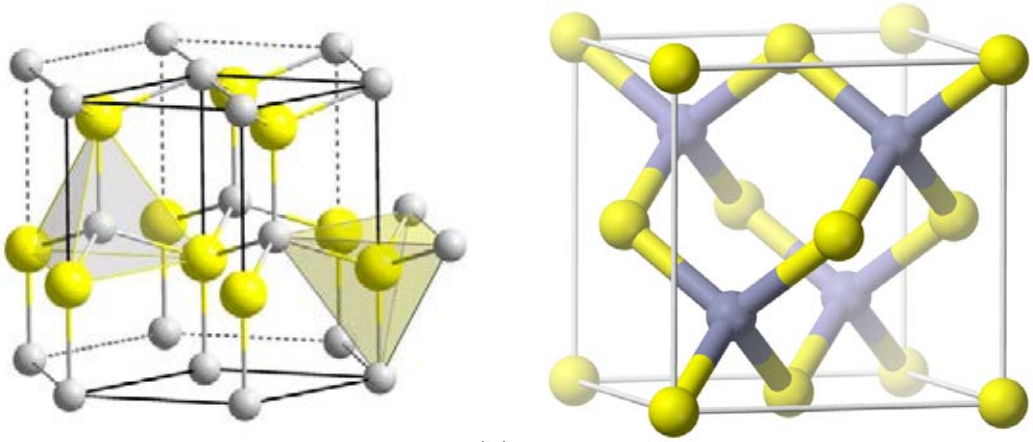

(a) (b)

Fig. 2.1 ZnO crystal structure (yellow=Zn, white/gray=O);
(a) wurtzite structure and (b) cubic zinc blende [19].

2.1.2. Synthesis routes for ZnO powders

ZnO is used in many applications such as cosmetics, paints, ceramics and electronics. Recently, ZnO nanoparticles have attractted researcher's interest for electronic devices such as light-emitting diodes, varistors and electrochemical cells [20]. These applications need nanomaterials with high density and quality of products is controlled through processing starting from synthesis of raw materials, forming and sintering. Many methods for ZnO nanoparticles synthesis have been reported in wet chemistry such as thermal decomposition, sol-gel techniques, precipitation and colloidal synthesis. These processes have succeeded in controlling of shape, size and morphology at low temperature. Advantages of aqueous precipitation use in this research are low cost, simplicity and non-toxic. Mechanisms begin from precursors dissolved in a solution. Precipitate can be formed as nuclei and then growth of nuclei becomes particles. Nuclei formation state and growth of nuclei depend on concentration of precursor solution and reactive time. Additionally, the use of polymeric additive can be used to control size, shape and chemical composition of the precipitate. The

polymeric additive changes the surface charge of particles or modifies crystal growth [20].

2.1.3. Application of ZnO

ZnO is extensively used in many applications such as ceramics, cement, glass, plastics, rubber cosmetics, paints and electronics. ZnO has high refractive index, high thermal conductivity, antibacterial and UV protection properties [1, 21].

2.1.3.1. Cosmetics aspect

ZnO nanoparticles shows excellent ability in protecting UVA and UVB. Its safety for human makes it suitable to be used in sunscreen products for physically blocking the UVA and UVB.

2.1.3.2. Industrial aspect

In rubber industry, ZnO nanoparticles are used as an effective inorganic surfactant for an efficient production of anti-abration rubber. Ceramics industry is widely use ZnO as a white color pigment. Added ZnO nanoparticles can decrease sintering temperature of ceramic products for 400 – 600 °C. For painting industry, ZnO nanoparticles are semiconductive, which can be used to improve UV shielding, and self-cleaning properties of paints.

2.2. Polyacrylic acid (PAA)

Dispersant is a chemical substance which is added to suspensions. It can provide particle dispersion in suspension and control precipitation. Generally, particles in suspension tend to agglomerate. Therefore, we need dispersant for a well-dispersed

suspension [5] There are several factors controlling dispersion of particles in suspensions, properties of a polymeric dispersant including concentration, conformation and molecular weight are ones of the most important factor [8-11, 22]. The optimum dispersant concentration suggests that there is an adequate amount of dispersant to cover the particle surface [16, 23]. Therefore, particles can be separated from other particles and stabilized in a medium. Conformation of polymer chains in the suspension also affects the dispersant efficiency and adsorption behavior of polymer on particle surface. To acquire electrosteric stabilization in aqueous suspensions, polyelectrolytes are often the choice of dispersants. The polymer chains provide steric stabilization and dissociation of the polymer in water provides repulsive charges between particles. Polyelectrolytes at optimum concentration and conformation have been reported to enhance electrosteric stabilization in aqueous suspensions [5].

Polyacrylic acid (PAA) is an anionic polyelectrolyte used in aqueous suspensions, which has COOH group as a major composition. PAA structural formula is shown in Fig.2.2. Dissociation of PAA in water provides COO^- group and H^+ shown in equation (1). In colloidal ceramic processing, PAA is an effective dispersant in many industry both of conventional and advanced ceramics [6,8,14,24]. PAA has been reported to promote dispersion and stability of ZnO, Al_2O_3, Si_2N_4, TiO_2, Fe_2O_3, ZrO_2 and $BaTiO_3$ aqueous suspensions [6-14].

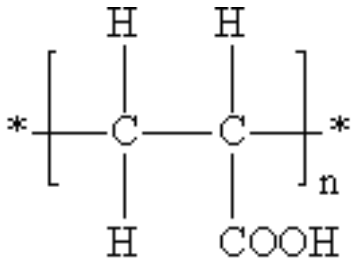

Fig. 2.2 Structural formula of polyacrylic acid (PAA).

$$[CH_2CHCOOH]_n \rightarrow [CH_2CHCOO^-]_n + nH^+ \quad (1)$$

Important factors in dispersant efficiency of polyelectrolytes are dissociation, adsorption behavior and conformation of polyelectrolytes. These can be changed depending on pH and concentration of ionic strength in suspension [25]. For example, polyelectrolytes poorly dissociate, and exhibit compact coil conformation at low pH and high ionic strength as shown in Fig.2.3(a). However, at high pH ~ 8.5 and low ionic strength, polyelectrolytes highly dissociate and in stretch form as shown in Fig.2.3(b). This highly affects charge and thickness of polymer layer adsorbed on particle surface. Therefore, at low pH, anionic polyelectrolytes are inefficient for stabilizing suspensions. For high pH, anionic polyelectrolytes are effective in stabilization of particles in suspensions.

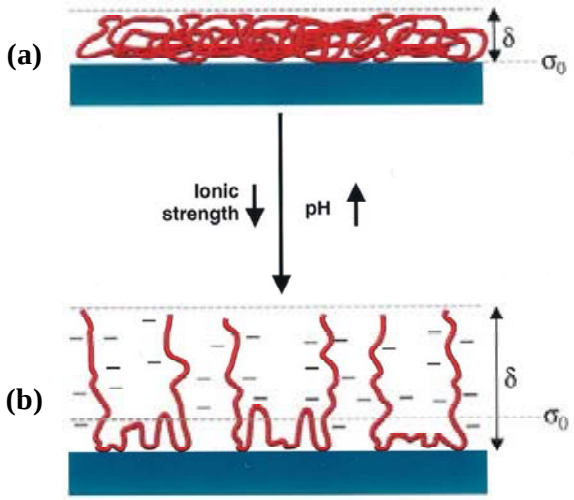

Fig. 2.3 Adsorption of an anionic polyelectrolyte on particle surface as a function of pH and ionic strength (δ is adlayer thickness and σ_0 the plane of charge [4].

2.3. DLVO theory and repulsive potential energy

DLVO theory is an important theory which describes stability of colloid system by the scientists Derjaguin, Verwey, Landau and Overbeek in 1940s. This theory describes

that stability of particle in suspension depend on the total potential energy (V_T) as shown in equation (2) [5,26].

$$V_T = V_A + V_R + V_S \quad (2)$$

V_T = Total potential energy (Joule)

V_A = Van der Waals attractive potential energy (Joule)

V_R = Repulsive potential energy (Joule)

V_S = Potential energy due to solvent (Joule)

Potential energy (V_S) due to solvent has value less than other potential energies. Therefore, we care for V_A and V_R, which are the attractive and repulsive energy. V_A and V_R can be obtained as shown in equations (3) and (4), respectively.

$$V_A = \frac{-A}{12\pi D^2} \quad (3)$$

A = the Hamaker constant (Joule$\cdot$m^2)

D = the interparticle separation

$$V_R = 2\pi\varepsilon_r\varepsilon_0\psi_0^2 \ln\left[1+\exp(-\kappa D)\right] \quad (4)$$

ε_0 = relative dielectric constant of mudium

ε_r = relative dielectric constant of water at 25 $^\circ$C = 80

ψ_0 = surface potential (Volt)

κ = reverse of κ^{-1}

κ^{-1} = thickness of double layer or Debye-Huckel screening length (m)

Relationship of equations (3) and (4) are shown in Fig.2.4. DLVO theory describes that particles have Brownian motion and kinetic energy leads to collision of particles and then agglomeration occurs. However, efficient particle stabilization can prevent agglomeration of particles and lead to a system of dispersed and stabilized particles in a medium.

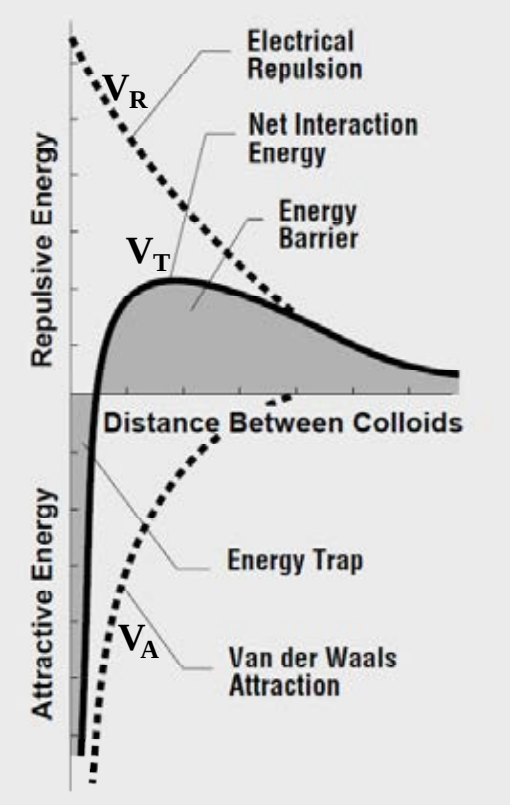

Fig. 2.4 The total interaction potential (V_T) shown the Van der Waals attractive potential (V_A) and DLVO repulsive potential (V_R) curves [46].

2.4. Dispersion and stabilization of suspension

In various applications of ZnO nanoparticles, a well-dispersed and highly stable suspension is required. It is very difficult to disperse nanoparticles in a suspension due to agglomeration of particles and precipitation under gravity force. With increasing attention in nanoparticles, the dispersion and stability of the suspension become a challenge. Due to high surface area (>10-300 m^2/g) and surface energy, nanoparticles tend to agglomerates in the suspension [2]. The nanoparticle agglomerates are often 10-20 times larger than their primary sizes [2, 3]. Particle agglomeration is caused by Van der Waals attractive interactions between particles. To separate particles in a medium, the Van der Waals force must be overcome by repulsive interactions. The main purpose of dispersion in a liquid medium is to break agglomerates into primary particles, which can be achieved by mechanical action and/or chemical additives [28]. Once the particles are separated, stabilization mechanisms are required to control the dispersion and stability of the particles in a suspension. Typically, when ceramic powders are added to a suspending medium such as water, the presence of attractive Van der Waals forces results in particle agglomeration. To produce particles that suspend in a medium without agglomeration and precipitation, stabilization mechanisms are needed [5]. The stabilization mechanisms can be divided into three forms. Electrostatic stabilization produces the repulsive coulomb forces between charged particles. Steric stabilization is achieved by polymer coating on the particle surface, which creates a repulsive force and separates the particle from another particle. Finally, electrosteric stabilization, which is a combination of electrostatic and steric stabilization. Three forms of particle stabilization are shown in Fig.2.5 [5]. The most effective stabilization mechanism is electrosteric stabilization. To acquire electrosteric stabilization in aqueous suspensions, polyelectrolytes are often the choice of dispersants. The polymer chains of polyelectrolyte provide steric stabilization and dissociation of the polymer in water provides repulsive charges between particles [5, 28]. One of the most popular polyelectrolytes used in aqueous suspensions is polyacrylic acid (PAA). It has been

reported to promote dispersion and stability of ZnO, Al_2O_3, Si_2N_4, TiO_2, Fe_2O_3, ZrO_2 and $BaTiO_3$ aqueous suspensions [7-15, 29].

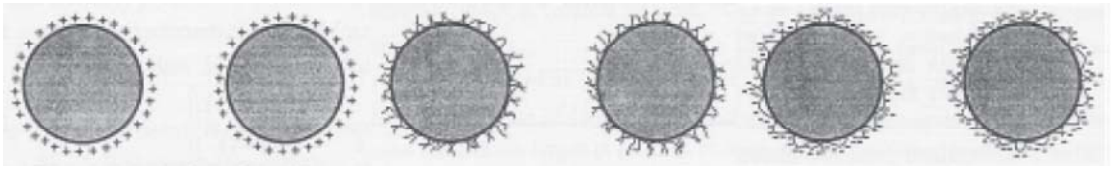

(a) (b) (c)

Fig. 2.5 Three forms of stabilization for particles; (a) Electrostatic stabilization, (b) Steric stabilization and (c) Electrosteric stabilization [30].

2.4.1. Origin of surface charge

Surface charge depend on types of particle and medium in suspension. Origins of the surface charge can be classified in the followings [5].

2.4.1.1. Ionisation of surface groups

Dissociation of acidic particle surface causes negatively charge on surface of particle as shown in Fig.2.6(a). Conversly, dissociation of basic particle surface causes positively charge in Fig.2.6(b). Therefore, amounts of charge on particle surface can be controlled by adjusting pH of suspensions in order to control dissociation. The magnitude of surface charge depends on the acidic and basic strength of particle surface and pH of the solution.

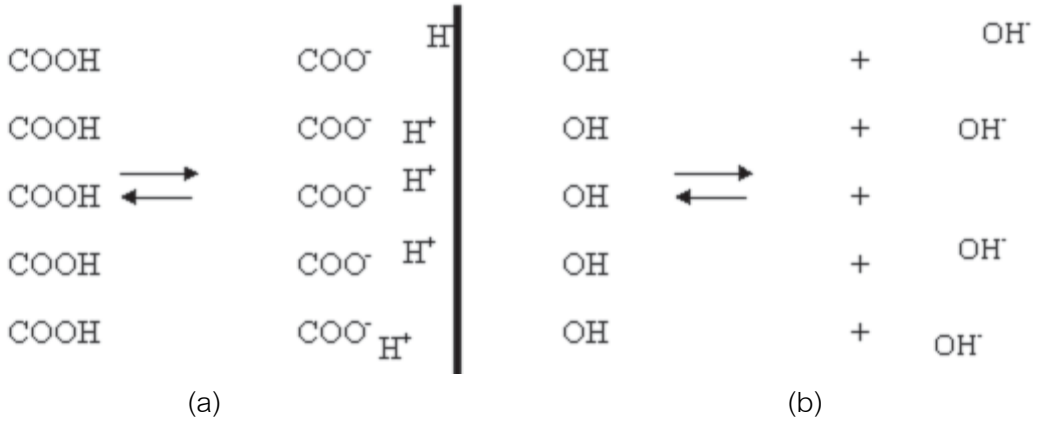

Fig. 2.6 Origin of surface charge by; (a) Ionization of acidic particle surface to negatively charged surface and (b) Ionization of basic particle surface to positively charged surface [26].

2.4.1.2. Differential loss of ions from the crystal lattice

AgI crystal suspended in water is an example. It was found that Ag^+ ions dissolve from crystal structure more than I^- ions as shown in Fig.2.7. Therefore, surface of AgI suspended in water is positively charged.

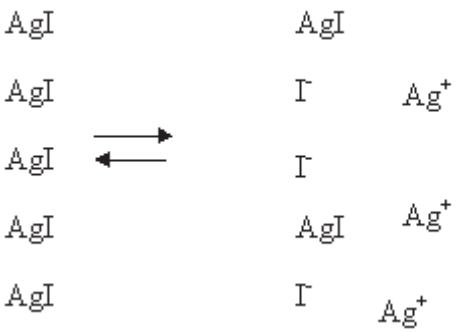

Fig. 2.7 Origin of surface charge by differential loss of ions from AgI crystal lattice [26].

2.4.1.3. Adsorption of charged species

Adsorption of charged species occurs by electrolyte addition to suspension. The electrolyte can be classified into 2 types; (1) cationic electrolyte, dissociating to provide positive charge and (2) anionic electrolyte dissociating to provide negative charge as shown in Fig.2.8.

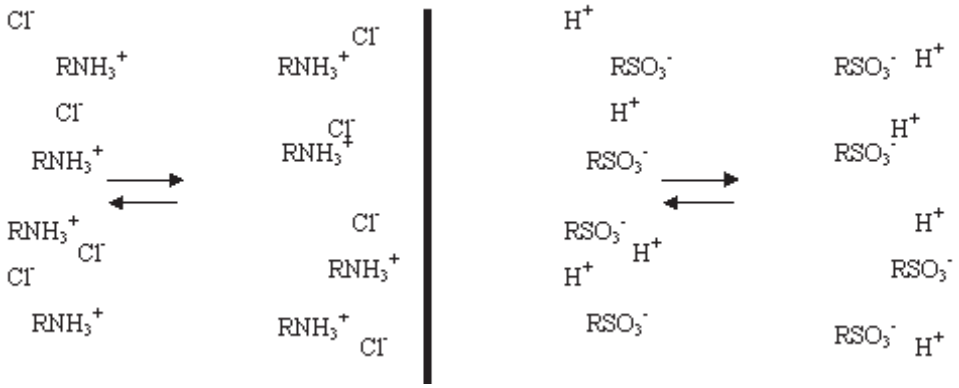

(a) (b)

Fig. 2.8 Origin of surface charge by; (a) adsorption of cationic electrolyte and (b) adsorption of anionic electrolyte. R = hydrocarbon chain [26].

2.4.2. The electrical double layer

Particles attract to opposite charge molecules or counter ions to balance their surface charge. Then, an electrical double layer occurs around the particle, which is a basic of electrostatic stabilization of suspension. the electrical double layer surrounds a particle and ions adsorbed on particle surface as shown in Fig.2.9. It consists of two layers [5]:

(1) Stern layer is an inner region that contacts with particle surface. Charge of this layer is opposite to the surface charge of particle. This layer occurs by attractive force between particle surface and counter ions with opposite charge.

(2) Diffuse layer is an outer region next to stern layer. This layer consists of counter ions that still attracted by surface charge of particle, but they are pushed by counter ions in the stern layer. The region between stern layer and diffuse layer is called shear plane.

From Fig.2.9, stern layer has the maximum electrical potential value. With increasing distance from particle surface, electrical potential decreases to zero. The electrical potential at shear plane is called zeta potential, which indicates potential stability of suspension and magnitude of negative or positive zeta potential.

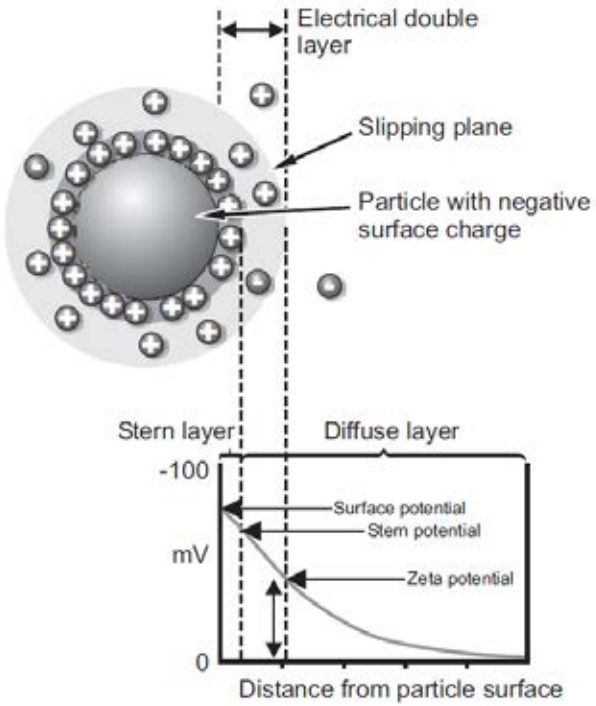

Fig. 2.9 Illustration of electrical double layer, shear plane and zeta potential value [47].

2.4.3. Zeta potential

Zeta potential is the electrical potential at the shear plane of electrical double layer. Since zeta potential directly relates to repulsive potential energy (V_R), zeta potential measurement can be used to indicate stability of particles in suspension. Particles with high zeta potential value possess high V_R, leading to high repulsive force between particles. This leads to a well-dispersed, high stability suspension and the minimum precipitation [5].

The important factors affecting zeta potential value are pH of suspension and concentration of electrolyte in suspension. K-L Ying et al. studied the zeta potentials of ZnO suspensions without dispersant as a function of pH as shown in Fig.2.10 [31]. It can be seen that zeta potential values range from large positive to negative depending on pH of suspension. At zero zeta potential, it is called isoelectric point (IEP). For ZnO particles in suspension, IEP occurs at pH 8.6 as shown in Fig.2.10. At pH lower than pH_{IEP}, zeta potential values are positive, indicating positive surface charge of ZnO particles. Therefore, the particles at this pH ranges possess counter ions as anion more than cation. On the other hand, at pH higer than pH_{IEP}, zeta potential values are negative. Then, surface charge of particle is negative, which mean there are more cation than anion as counter ions. pH_{IEP} of common ceramics is listed in Table 1.

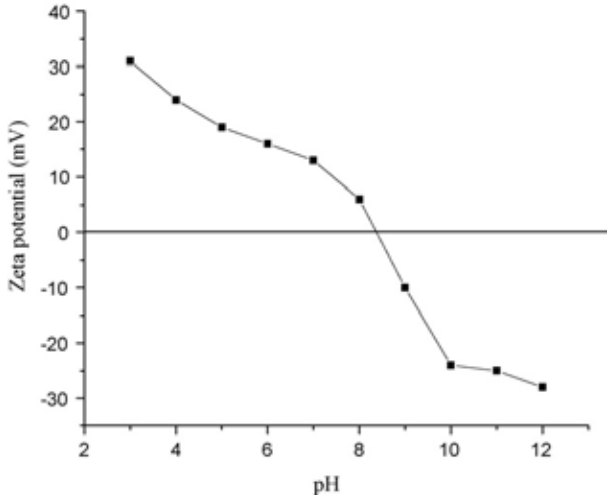

Fig. 2.10 Zeta potential of ZnO suspensions without dispersant as a function of pH [31].

Table 2.1 Isoelectric point (IEP) of ceramic materials [4].

Material	pH_{IEP}
α-Al_2O_3	8-9
$3Al_2O_3 \cdot 2SiO_2$	6-8
$BaTiO_3$	5-6
CeO_2	6.7
Cr_2O_3	7
CuO	9.5
Fe_2O_4	6.5
La_2O_3	10.4
MgO	12.4
MnO_2	4-4.5
NiO	10-11
SiO_2 (amorphous)	2-3
Si_2N_4	9
SnO_2	7.3
TiO_2	4-6
ZnO	9
ZrO_2	4-6

Fig.2.11 shows effects of electrolyte concentration on zeta potential of alumina aqueous suspension [32]. Addition of ammonium polyacrylate increases negative zeta potential value and decrease viscosity of the suspension. It is shown that zeta potential is changed by variation in ions adsorbed on particle surface.

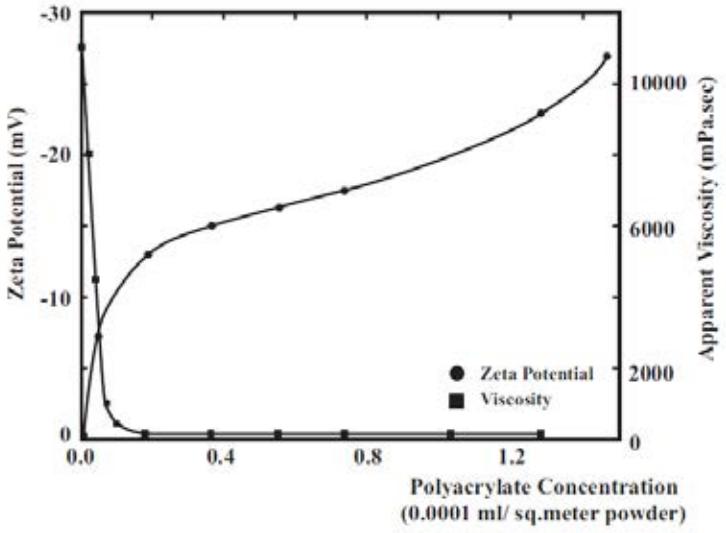

Fig. 2.11 Zeta potential and deflocculation curve of calcined alumina aqueous suspension 50 vol% using ammonium polyacrylate as dispersant [32].

2.4.4. Electrosteric stabilization

Electrosteric stabilization is the most effective particle stabilization. Electrosteric stabilization is combination of electrostatic and steric stabilization, which can be achieved by addition of polyelectrolyte to coat on the particle surface. Polyelectrolyte dissociates in medium and provide charged ions and/or molecules [25]. For example, Na^+ and COO^- groups dissociate from sodium polyacrylate (Fig.2.12) as shown in equation (5)

$$[CH_2CHCOONa]_n \rightarrow [CH_2CHCOO^-]_n + nNa^+ \qquad (5)$$

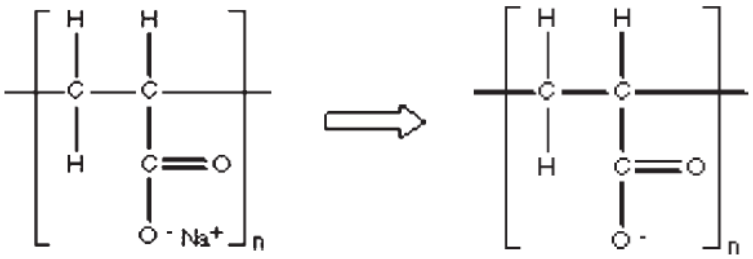

Fig. 2.12 Dissociation of sodium polyacrylate [25].

Polyelectrolyte can be classified into two types according to type of charge on polymer chain.

(1) Anionic polyelectrolyte: polymer chain with negative charges and cations dissociated from anionic polyelectrolyte. For example, sodium polyacrylate, ammonium polyacrylate(APA), polyacrylic acid(PAA) sodium dodecyl sulphate (SDS) phosphate ester and ammonium polycarboxylate [2, 16, 20, 33, 34]. In Fig.2.13 shown polymer chain dissociated from sodium polyacrylate.

(2) Cationic polyelectrolyte: polymer chain with positive charges and anions dissociated from cationic polyelectrolyte. For example, quaternary ammonium, imidazoline and ethoxylated amine complex [34].

Electrosteric stabilization of particles with positive charge such as Al_2O_3 and ZnO at pH 7 can be obtained using anionic polyelectrolyte. For particle with negative charge such as SiO_2 at pH 7, cationic polyelectrolyte should be used as a dispersant [25]. Anionic polyelectrolyte is usually lower cost and easier process compared to cationic polyelectrolyte. Therefore, anionic polyelectrolyte is typically used for stabilization more than cationic polyelectrolyte. Major anionic polyelectrolyte used as dispersant in commercial is composed of carboxyl group (COOH).

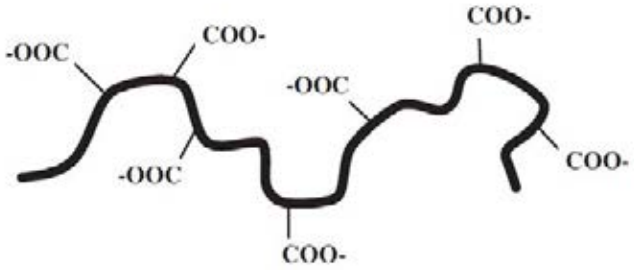

Fig. 2.13 Anionic polyelectrolyte chain dissociated from sodium polyacrylate [35].

2.5. Langmuir Adsorption Isotherm

Adsorption is capability of adsorbent (particle) to attract adsorbate (PAA) on its surface. Surface adsorption of solid is divided into two categories; physical adsorption and chemical adsorption.

1. Physical adsorption

Physical adsorption can be occurred as multilayers on surface of adsorbent (particle). The adsorption occurs mildly and no bonding chemically but the adsorbate (PAA) adsorbed on surface of adsorbent by Van der Waals attractive force. It can occur easily as multilayered adsorption in low temperature and adsorption energy.

2. Chemical adsorption

Chemical adsorption is adsorption involving chemical bonding between adsorbent and adsorbate. Molecules of adsorbate can adsorbed on adsorbent as only monolayer.

The chemical adsorption process can be described by Langmuir adsorption isotherm. Assumptions of Langmuir adsorption isotherm are (a) only one layer of molecule adsorption on surface of adsorbent (b) adsorption is specific and (c) adsorbate is strongly attracted on surface of adsorbent. From assumptions, Langmuir

equation which shows the fraction of the adsorption sites occupied by solute can be written in equation (6) [36].

$$\theta_2 = \frac{Ka_2^b}{Ka_2^b + 1} \tag{6}$$

θ_2 = surface adsorption

K = equilibrium constant

a_2^b = activity of the species

If $a_2^b \rightarrow 0$; $\theta = Ka_2^b$ (7)

If $Ka_2^b \geq 1$; $\theta = 1$ (8)

Equation (7) shows that θ_2 increases linearly with slope equals K constant. Equation (8) exhibits that saturation on surface of adsorbed solute occurs at higher concentrations. Fig.2.14(a) shows two conditions of equations (7) and (8). The fraction of the adsorption sites occupied by solute can not be measured directly. Therefore, the number of moles of solute adsorbed per weight of adsorbent (n_2^s / W) is measured.

$$\frac{n_2^s}{W} = \frac{n}{A} A_{sp} \tag{9}$$

n_2^s = the number of moles of solute adsorbed

W = weight of adsorbent

A = area of adsorbent

A_{sp} = the specific surface area of the adsorbent

It can be expressed as:

$$\theta = \frac{n_2^s}{A} N_A \sigma^0 = \frac{n_2^s N_A \sigma^0}{W A_{sp}} \tag{10}$$

N_A = Avogadro's number

σ^0 = the area occupied per molecule

The saturation adsorption occurs at θ = 1. Therefore, equation (10) can be written as followed:

$$\left(\frac{n_2^s}{W}\right)_{sat} = \frac{A_{sp}}{N_A\sigma^0} \tag{11}$$

data achieved from experiment are shown in Fig.2.14 (b).

In the case of adsorption of polymer on particle surface, Langmuir isotherm in equation (6) can be written as equation (12).

$$m\left(\frac{n_2^s}{W}\right) = \frac{(m/b)C}{(m/b)C+1} \tag{12}$$

Where m, m/b = empirical constants

We can rewrite equation (12) as:

$$\frac{C}{n_2^s/W} = mC + b \tag{13}$$

and plot $\frac{C}{n_2^s/W}$ versus C as straight line as shown in Fig.2.15 where m is slope and b is a constant. Values of m and b in equation (12) can be compared with (6) and (10) as

$$m = \frac{N_A\sigma^0}{A_{sp}} \tag{14}$$

and $$m/b = K \tag{15}$$

Therefore, if A_{sp} is known, we can find the area occupied per molecule (σ^0) (14).

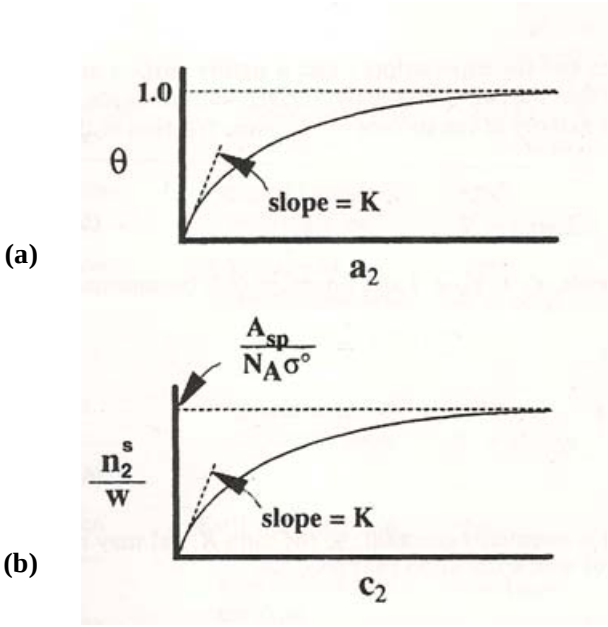

Fig. 2.14 Langmuir isotherm; (a) relationship of the adsorption sites occupied versus solute activity and (b) the number of moles of solute adsorbed per weight of adsorbent versus equilibrium concentration of polymer [36].

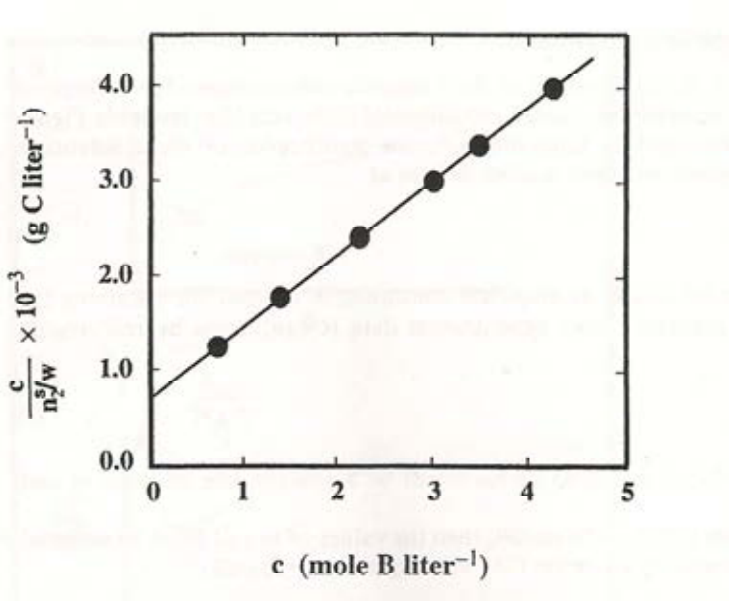

Fig. 2.15 Plot of the Langmuir equation expressed by equation (12) [36].

2.6. Characterization techniques

2.6.1. Particle size distribution measurement

Measurement of particle size distributions is done by light scattering technique. Laser light scattering is a widely used particle size measurement for particle in range of 0.01μm -3500μm [37]. Laser light scattering measures particle size distributions by measuring angle variation in intensity of light scattering as a laser beam passes through particle. Large particles scatter light at small angle and small particles scatter light at large angle as shown in Fig.2.16. The angle of light scatter is analyzed to calculate size of particle by the Mie theory of light scattering.

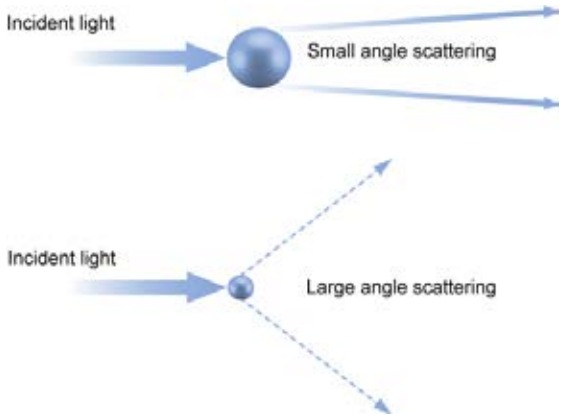

Fig. 2.16 Scattering of light from small and large particles [37].

2.6.2. Zeta potential measurement

Zeta potential value is the electrical potential at shear plane. The zeta potential value indicates potential stability of the suspension. If the particles in suspension have a large negative or positive zeta potential, there is high repulsive force between particles. If the particles have low zeta potential values, there is low repulsive force between particles and then flocculation can be occurred. Normally, particles with zeta potential more than +30 or -30 mV are considered stable [26].

Zeta potential can be measured based on electrophoresis effects, which is the movement of charge particle relative to the liquid which it is suspended under the influence of an applied electric field. When an electric field is applied, charged particles are attracted to the electrode of the opposite charge as shown in Fig.2.17. Viscous force acting on particle leads to moving of particles with constant velocity. The velocity depends on the strength of electric field, the dielectric constant of medium, the viscosity of medium and the zeta potential. The velocity of a particle referred to its electrophoretic mobility. Zeta potential is related to the electrophoretic mobility by the Henry equation (16).

$$U_E = \frac{2\varepsilon z f(\kappa a)}{3\eta} \tag{16}$$

where U_E = electrophoretic mobility, ε = dielectric constant, z = zeta potential, f(κa) = Henry's function. κ is in term of the Debye length come from κ^{-1} that is taken as a measure of thickness of the electrical double layer. Parameter a is a radius of the particle. Therefore, κa is a ratio of particle radius to electrical double layer thickness. Electrophoretic determinations of zeta potential are the most commonly made in aqueous media, which f(κa) is 1.5. The velocity of particles are measured and expressed in field strength as their mobility.

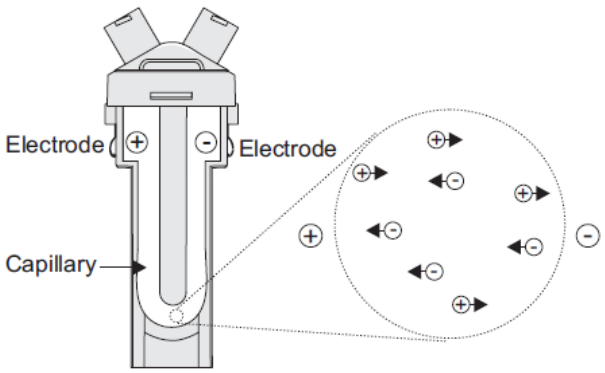

Fig. 2.17 Movement of particles toward the electrode of opposite charge [38].

The equipment used for Zeta potential measurement consists of laser as a light source. The light source provides an incident and reference beam. The incident laser beam pass through the sample cell and the scattering light is detected. When an electric field applied to cell, particles moving through the measurement volume will cause the intensity of light detected to fluctuate with a frequency proportional to the particle speed. Then, a frequency spectrum which is the electrophoretic mobility and zeta potential is calculated [26].

2.6.3. Fourier Transform Infrared Spectroscopy (FTIR)

FTIR is a technique which is used to obtain an infrared spectrum of absorption, emission, photoconductivity or Raman scattering of a solid, liquid or gas. In infrared spectroscopy, IR radiation is passed through a sample. Some of the infrared radiation is absorbed by the sample and some of it is transmitted. The result of spectrum shows the molecular absorption and transmission, creating a molecular fingerprint of the sample. An infrared spectrum represents absorption peaks which correspond to the frequencies of vibrations between the bonds of the atoms. [39].

IR radiation and Raman scattering will consider the electric field and neglect the magnetic field component. The important parameters are the wavelength (λ), frequency (ν), and wavenumbers ($\bar{\nu}$, number of waves per unit length) and all of them are related to one another by the following equation (17) [40].

$$\bar{\nu}(cm^{-1}) = \frac{10^4}{\lambda(\mu m)} \qquad (17)$$

Where $\nu = c\lambda$; c is speed of light.

IR lights are electromagnetic radiation with the wavelength longer than visible lights, measuring from the nominal edge of visible red light at 0.74 μm and extending to 300 μm. Group frequency analysis is used to determine various functional

groups in molecules as followed. The spectrum can be divided into regions shown in Fig.2.18.

(1) X-Y stretching is the highest frequency (3700-2500 cm^{-1})

(2) X≡Y stretching and cumulated double bonds X=Y=Z asymmetric stretching is in the frequency ranges 2500-2000 cm^{-1}

(3) X=Y stretching is in the frequency ranges 2000-1500 cm^{-1}

(4) X=H deformation is in the frequency ranges 1500-1000 cm^{-1}

(5) X=Y stretching is in the frequency ranges 1300-600 cm^{-1}

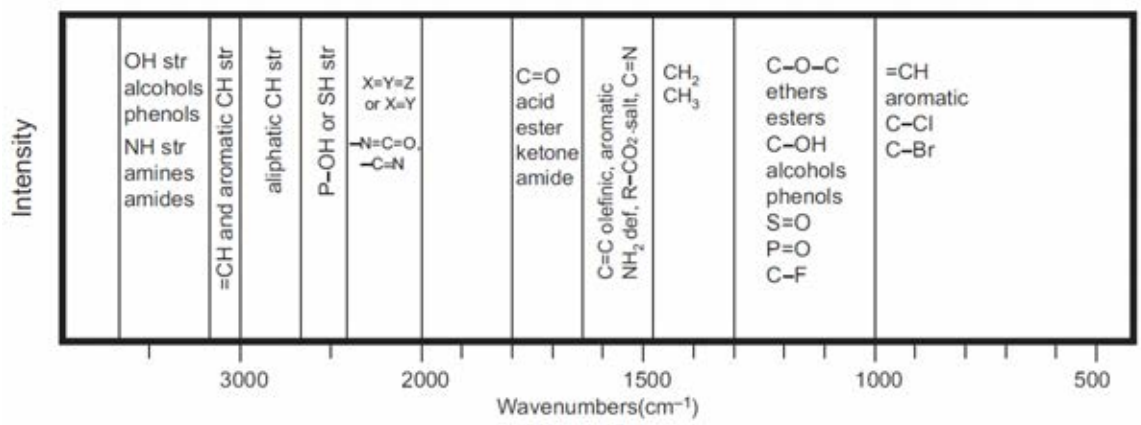

Fig. 2.18 Regions of the spectrum with some group frequency [40].

The vibration within a molecule causes a net change in the dipole moment of the molecule. The electrical field of the radiation interacts with fluctuations in the dipole moment of the molecule. If the frequency of the radiation matches with frequency of the molecule, radiation will be absorbed, leading to changes in the amplitude of molecular vibration. Vibrations are classified into two main categories of stretching and bending.

(1) Stretching: changes in inter-atomic distance along bond axis as shown in Fig.2.19.

(2) Bending: changes in angle between two bonds. There are four types of bending: rocking, scissoring, wagging and twisting as shown in Fig.2.19 [40].

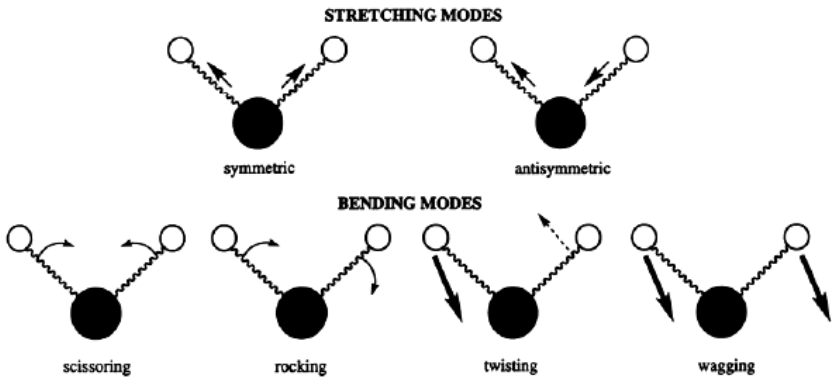

Fig. 2.19 Vibration characteristic of bonding [41].

Components of Fourier Transform Infrared (FT-IR) spectrometer are as followed and sample analysis process is describes in Fig.2.20 [40].

(1) Light source

Infrared energy is emitted from a source as continuous radiation. This beam passes through an aperture, which controls the amount of energy that goes into the sample.

(2) Interferometer

Beam from the light source enters the interferometer, which produces a unique signal with encoded infrared frequency. Then, the interferogram signal exits the interferometer.

(3) Sample

The beam enters the sample and then transmits through or reflects from the sample, depending on the method of measurement. Specific frequency of energy that is absorbed by the sample indicates characteristics of the sample.

(4) Detector

Finally, the beam goes to the detector. The detector is specially designed to detect the interferogram signal.

(5) Computer

The signal is digitized and sent to the computer. The final infrared spectrum is presented to the user for interpretation and any further manipulation.

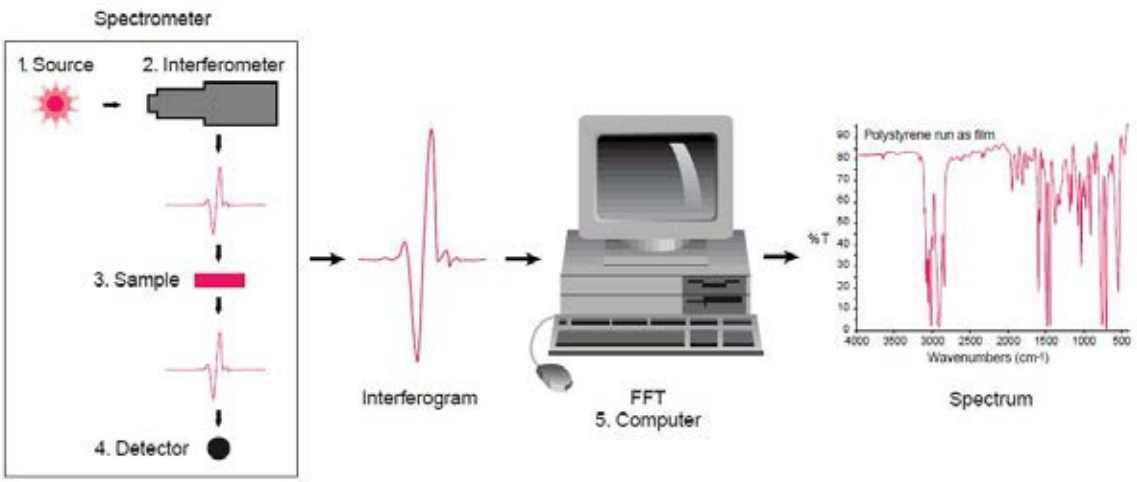

Fig. 2.20 The analysis process of Fourier Transform Infrared (FT-IR) spectrometer [39].

2.6.4. Microscopy

Microscopy is the technique of using microscope to view samples and objects that cannot be seen with naked eyes. Optical and electron microscopy involve the diffraction, reflection, or refraction of electromagnetic radiation/electron beams when interacting with a specimen, and the subsequent collection of this scattered radiation or another signals in order to create an image. This process may be carried out by wide-field irradiation of the sample (for example standard light microscopy and transmission electron microscopy) or by scanning of a fine beam over the sample (for example scanning electron microscopy) [42].

2.6.4.1. Optical microscopy (OM)

Optical microscope involves passing visible light transmitted through or reflected from the sample through a single or multiple lenses to allow a magnified view of the sample. The image can be detected by the eye. The resolution limit was around 0.2 μm. In this work, it is used to investigate particle dispersion [42].

2.6.4.2. Scanning electron microscopy (SEM) and Transmission electron microscopy (TEM)

Both SEM and TEM are the methods used in electron microscopy. Both also use electrons as electron beam which scan and transmit it through the sample. Images produced from these instruments are highly magnified and have a high resolution. SEM is based on scattered electrons while TEM is based on transmitted electrons. The scattered electrons in SEM are classified as backscattered or secondary electrons. The scattered electrons in SEM produced the image of the sample after the microscope collects and counts the scattered electrons. In TEM, electrons are directly pointed toward the sample. The electrons that pass through the sample are the parts that are illuminated in the image. The focus of analysis is also different. SEM focuses on the sample's surface and its composition. On the other hand, TEM seeks to

see what is inside or beyond the surface. SEM also provides a three-dimensional image while TEM delivers a two-dimensional picture. In terms of magnification and resolution, TEM has an advantage compared to SEM. TEM has up to a 50 million magnification level while SEM only offers 2 million as a maximum level of magnification. The resolution of TEM is 0.5 Å while SEM has 0.4 nm [42].

2.7. Literature reviews

Among several factors controlling dispersion of particles in suspension, properties of dispersant including concentration, conformation and molecular weight are ones of the most important.

R. Suntako et al. [16] investigated the effects of ammonium polyacrylate as dispersant concentration and pH on properties of lead zirconate titanate aqueous suspension. At the optimum dispersant concentration, there was an adequate amount of dispersant to cover the particle surface. As a result, particles were separated from other particles by electrosteric stabilization. The effects of pH on particle dispersion could be explained based on the dissociation of polyelectrolyte in water and the adsorption of the polymer chain on the particle surface as shown in Fig.2.21. At pH 3.2, the suspension produced COOH functional groups, which rollup on itself caused a decrease in electrostatic repulsive force between particles. At pH 10.1, high concentration of hydroxide ions resulted in the dissociation of the polyelectrolyte to produce COO^- functional groups. The stretch polymer chains covered the particle surface, providing electrosteric stabilization. At pH 11.9, although negative charges from the polyelectrolyte dissociation, the net particle surface charge was highly negative. Therefore, most of the stretch polymer chains were dispersed in the suspension with only small amounts adsorbed on the particle surface. Particle stabilization mechanism at pH 11.9 was mainly electrostatic, which was insufficient to separate particles apart, leading to flocculation. Adsorption models of polymer adsorption on particle surface with

various pH shown in Fig.2.21. This suggests that in acidic pH suspensions rolled up on itself. The coiled polymers decreased interparticle distance and caused agglomeration. On the other hand, in alkaline pH suspensions, the extend polymer chains adsorbed on particle surface and provided electrosteric stabilization [16].

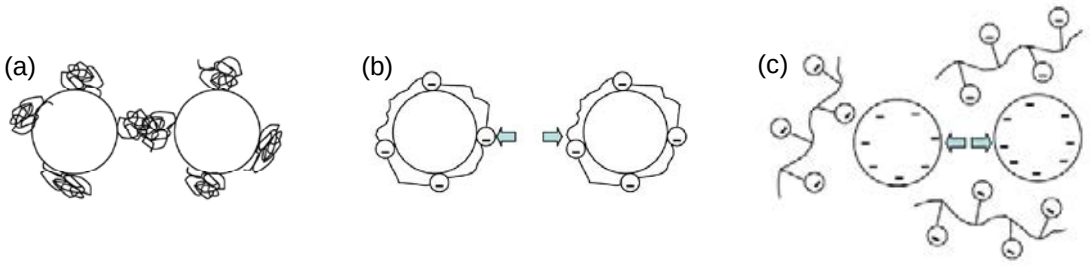

Fig. 2.21 Adsorption models of the polymer chain on PZT particle surface in suspensions with various pH (a) pH 3.2, (b) pH 10.1 and (c) pH 11.9 [16].

A. Degen et. al. [29] studied the properties of aqueous suspensions of ZnO powders with different purities using poly(acrylic) ammonium as a dispersant. The sedimentation and adsorption studies showed that the as-received ZnO powders required different optimum concentrations of the dispersant to prepare stable aqueous suspensions. At the optimum concentrations of the dispersant, the particles were completely covered with dispersant molecules. The suspensions exhibited the highest values of zeta potential and the lowest sediment heights. The maximum amount of negatively charged dispersant molecules that adsorbed onto the oxide surface was dependent on the positive surface charge of ZnO powders.

V.A. Hackley investigated the role of PAA in the dispersion of silicon nitride (Si_3N_4) suspensions [6]. It was found that degree of ionization increased as the pH increased for all molecular weights, and PAA changed from a compact coiled conformation to a stretched one. Adsorption isotherms of PAA interacted with Si_3N_4 increased as PAA concentration and molecular weight increased. The amount of

adsorption was low in alkaline pH suspension as a result of repulsive electrostatic forces.

Differences in molecular weight of a dispersant also affect particle dispersion and suspension stability. D. Santhiya et al. [11] investigated effects of PAA molecular weight as a dispersant on adsorption density in alumina aqueous suspension. The specific surface area (BET method) of alumina was 8.76 m^2/g and PAA molecular weight were 2000, 5000, 50000 and 90000. It was found that the adsorption of PAA on the particle surface increased with increasing molecular weight. This is due to an increase in numbers of polymer segments that adsorb on particle surface and provide better particle stabilization. Effects of pH on adsorption density showed that high adsorption density occurred at acidic pH. The adsorption amounts decreased with increasing pH due to electrostatic forces of repulsion between negatively charged PAA and alumina surface in alkaline pH ranges. Effects of PAA molecular weight showed that high molecular weight PAA exhibited higher adsorption density more than low molecular weight PAA.

N. Traiphol et al. [43] studied effects of molecular structure of dispersant on particle stabilization in PZT aqueous suspension. Poly(acrylic acid-co-maleic acid) (PACM) and PAA were used as dispersants. Molecular structures of the dispersants were in Fig.2.22. It was found that PACM promoted particle stabilization better than PAA. This is due to higher density of COO^- groups along the backbone of PACM, which is adsorbed on particle surface. The effects of pH indicated that dissociation of PACM and PAA increased with increasing pH. The COO^- concentration of PACM increased more than that of PAA at the same pH as shown in Fig.2.23. The results suggested that PACM was more efficient as a dispersant than PAA in dispersion and stability of PZT aqueous suspension.

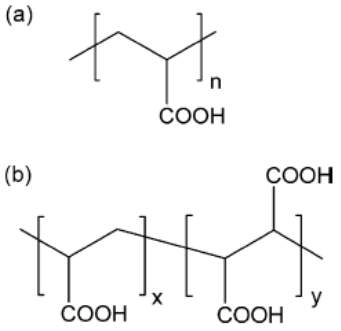

Fig. 2.22 Molecular structure of (a) PAA and (b) PACM [43].

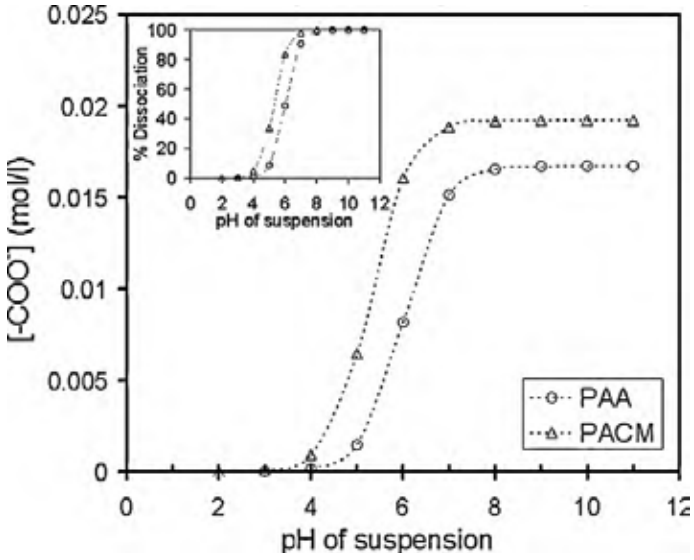

Fig. 2.23 The COO^- concentration as a function of pH in PZT aqueous suspensions prepared with dispersants [43].

V.N. Kislenko and R.M. Verlinskaya [44] studied adsorption of PAA and its copolymer with acrylonitrile, containing different quantities of carboxyl groups, on ZnO particles of micron size. This work focused on the kinetics of polymer desorption.

H. Liu et. al. [19] investigated adsorption of poly(ethylene oxide) with different molecular weights on the surface of silica nanoparticles and the suspension stability. It was found that the adsorbed amount of PEO increased with increasing polymer

concentrations until reaching a plateau. The saturated adsorbed amounts depended on the molecular weight. The change of the molecular weight or the conformation of polymer chain adsorbed at particle surface contributes to the zeta potential, which decreased with increasing molecular weight. The decrease in the adsorbed amount with increasing molecular weight can be explained that the segments in the polymer structures tend to change from trains to tails, resulting in low PEO density on the particle surface. The mechanism of the dispersion was electrostatic repulsion for low molecular weight PEO. On the other hand, the mechanism was steric interaction for the high molecular weight one. Using the suitable molecular weight PEO, the highly stable suspension can be achieved as a result of the electrostatic and steric combination.

K.K. Das et. al. [9] investigated flocculation/dispersion characteristics of alumina using a wide molecular weight ranges of polyacrylic acids. The PAA of molecular weight 50k g/mol showed higher adsorption than the 5k g/mol under the alkaline pH condition. PAA was held to the particle by hydrogen bonding with electrostatic repulsion displace the chain from the particles to dangle into the aqueous phase. Since larger molecular weight showed greater adhesion to the particle, therefore 50k g/mol can be adsorbed to the particle surface more than 5k g/mol PAA at alkaline pH. Comparison between a low and a high molecular weight PAA on alumina flocculation found that with PAA(1,000k), a small number of polymer molecules per alumina particle can cause flocculation while with PAA(5k), the corresponding number is very high as shown in Fig.2.24(a). Fig.2.24(b) suggested that flocculation occurred by polymer bridging in the case of PAA(1,000k) while charge neutralization was the case for PAA(5k). The bridging is easy when the polymer size is large and it can overcome the interparticle electrostatic forces. Fig.2.25 showed that number of polymer molecules per particle required to obtain 80% flocculation drastically decreased with the rms length of polymer. Therefore, flocculation was enhanced by an increase of polymer molecular weights.

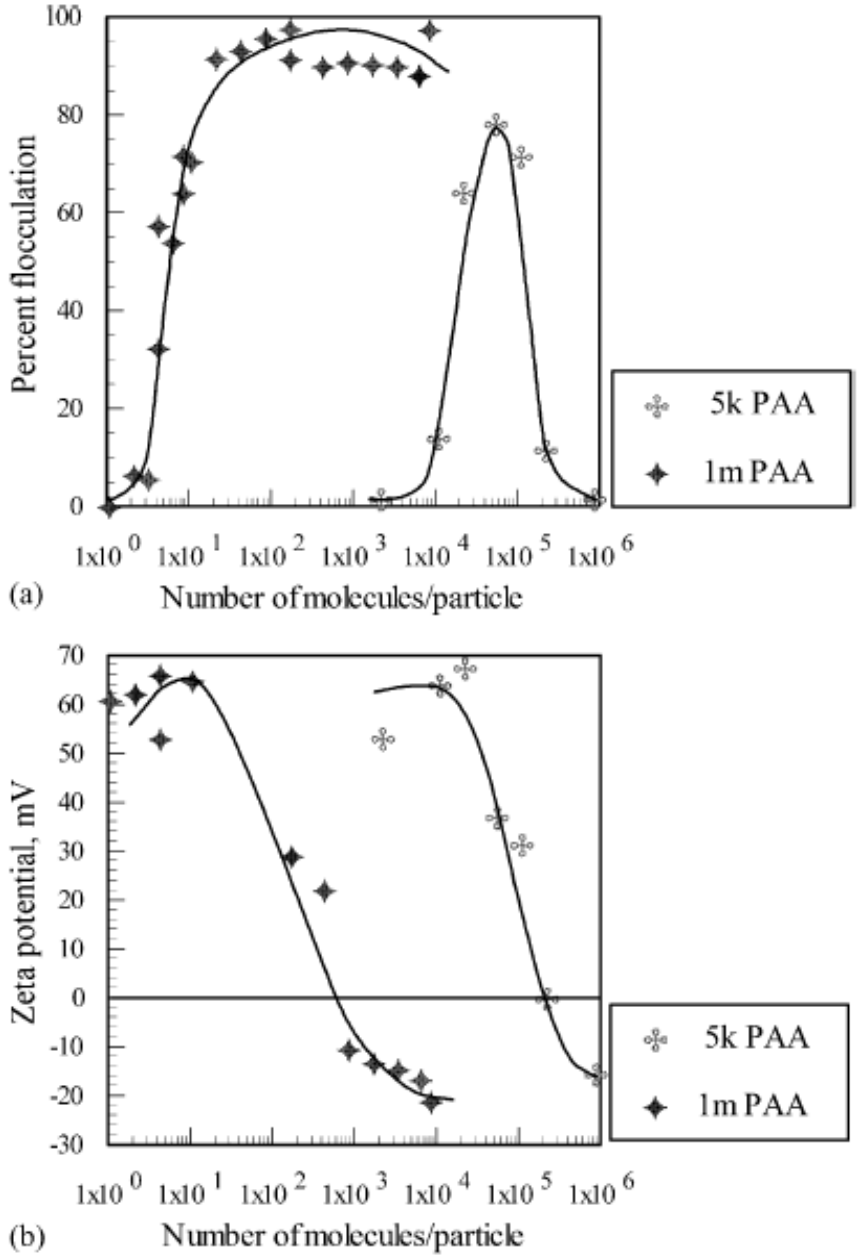

Fig. 2.24 (a) Comparison of flocculation response of alumina as a function of the number of molecules/particle for 5k and 1,000k g/mol PAA and (b) Zeta potential of polymer coated particles at various number of molecules/particle [9].

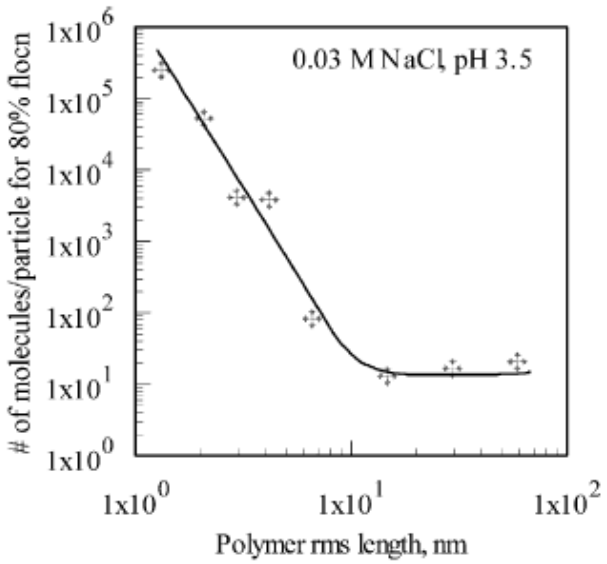

Fig. 2.25 Number of polymer molecules per particle required to obtain 80% flocculation as a function of the polymer size [9].

For nanoparticles dispersion, S. Luifu et. al. [10] studied adsorption of PAA in aqueous suspension onto the surface of TiO_2 nanoparticles. The average diameter of synthesized TiO_2 were 20 nm and PAA molecular weight were 2000, 10000 and 120000 g/mol. Adsorption isotherms indicated that the adsorption density and layer thickness of PAA on TiO_2 particles were found to increase with the increasing of PAA concentration and molecular weight. At higher molecular weight PAA reduced the zeta potential to negative value. PAA of molecular weight 10,000 g/mol was found to provide better particle dispersion through electrosteric repulsion than that of molecular weight 2,000 g/mol. With increasing molecular weight of PAA up to 120,000, the polymer was found to flocculate due to bridging of the long macromolecular chains.

S. Fazio et al. [17] studied the colloidal behavior of three different titania nanopowders aqueous suspension using Duramax and citric acid as dispersants. A commercial powder of anatase (34 nm) and rutile (55 nm) with a synthesised anatase (11 nm) were compared. It was found that stable suspensions of commercial nanopowders were obtained with Duramax polyelectrolyte of 1.0 – 1.5 wt%. The stability

of the suspensions was confirmed by a maximum zeta potential of commercial nanopowders in Fig.2.26. Long chain polyelectrolyte provided well-dispersed suspensions of commercial nanoparticles. Conversely, the cryogel can be effectively dispersed using the short chain molecules of citric acid. Fig.2.27 showed that, for synthesized nanopowder suspension, the zeta potential changed from the positive values to the negative values as the citric acid increased

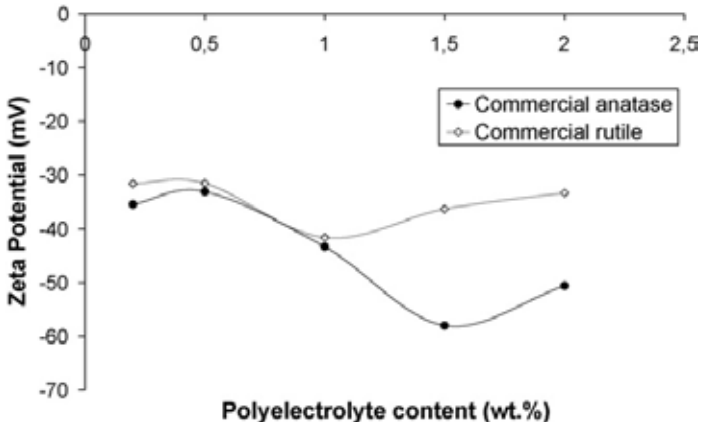

Fig. 2.26 Zeta potential versus polyelectrolyte concentration for commercial anatase and rutile [17].

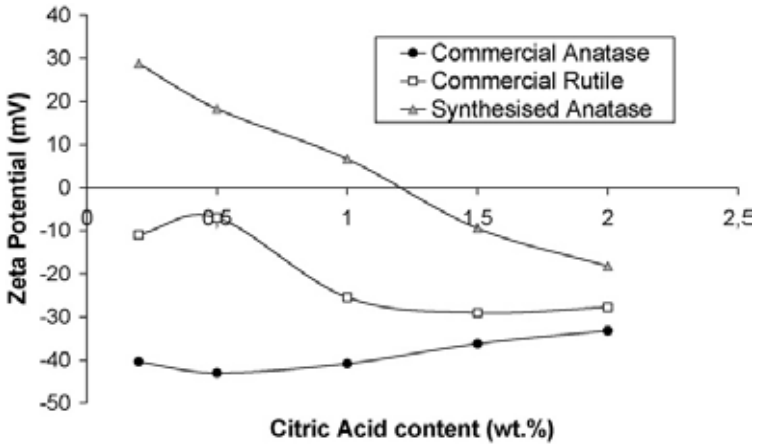

Fig. 2.27 Zeta potential versus citric acid concentration for the three powders [17].

S. Yang and D. Yan [18] studied structure of polymer adsorbed on particle of various sizes. In general, polymer adsorption was loop and tail characteristics. It was suggested that entanglements between particles occurred between tails of polymer. For nanoparticles, entanglements were occurred due to short loops and long tails. Therefore, particle size afftected conformation of polymer adsorbed. Well-dispersed suspension as tail are suitable length. The average tail length of the polymer adsorbed decreased with increasing particle size and chain entanglements occurred. This suggested that agglomeration of particles caused entanglement of polymer chains.

It is clearly showed that compatibility between particle size and dispersant molecular structure is one of the most important factors in order to obtain a well-dispersed and highly stable suspension. From literature review of the previous works, further study with a well-defined system is essential in order to verify the relationship of particle size and dispersant structure. Therefore, our work aims to study dispersion of ZnO nanoparticles using PAA dispersant by systematically varying ZnO size and PAA molecular weight.

For synthesis of ZnO nanoparticles by precipitation method, previous researches are reviewed as followed. Precipitation method is ones of the synthesize methods, which can control size, shape and morphology of particles. Additionally, precipitation of nanoparticles can be controlled from precursor dissolved in solution. E. Tang et al. [44] studied synthesis of ZnO nanoparticles by precipitation method. Urea was used as precipitant by mixing into zinc nitrate solution. Sodium dedecyl sulfonate (SDS), an anionic polyelectrolyte was added into solution to block ZnO crystal growth and particle agglomeration. Synthesized ZnO nanoparticles exhibited nearly spherical shape with particle size of 10-40 nm.

R. Hong et al. [45] synthesized ZnO nanoparticles by precipitation method from zinc acetate and ammonium carbonate using polyethyleneglycol (PEG) as additive. Synthesized particles are spherical and average particle size about 30 nm with narrow size distribution.

A. Aimable et al. [20] studied ZnO nanoparticles by aqueous precipitation in mild hydrothermal condition (90°C). The influence of PAA(M_w = 2000) and Dispex A40 (commercial PAA, M_w = 10000) on controlling particle size was investigated. Small and homogeneous roundish particles around 100-135 nm with narrow size distribution can be obtained. Roles of PAA on controlling the particle size were suggested as followed. PAA dissociated around 35% at pH 5.6, providing COO^- group. The COO^- groups adsorbed on ZnO surface and inhibited the crystal growth, controlling the particle size to be in nanometer ranges. Differences in particle size of ZnO prepared from PAA and Dispex A40 were not obvious.

From literature review of the previous works, it is believed that precipitation method is an effective and simplify method to produce ZnO particles with particle size <50 nm and narrow size distribution. In this study, PAA is used as an additive to control ZnO particle size. Effects of PAA molecular weight and concentration on characteristics of ZnO particles synthesized by precipitation method are focused.

CHAPTER 3
EXPERIMENTAL PROCEDURES

The experimental procedure is divided into two parts. The first part is preparation and characterization of ZnO aqueous suspensions to study effects of dispersant concentration and molecular weight on dispersion and stability of the suspensions. Polyacrylic acid (PAA) with molecular weights of 1.8k, 450k and 3000k g/mol are used as dispersants. ZnO particle sizes were 65.31, 174.56 and 224.54 nm. In the second part, synthesis of ZnO nanoparticles by precipitation method using various PAA concentrations and molecular weights are presented.

3.1. Materials

This study used ZnO powder (Nano Materials Technology, Ltd.) with particle sizes of 65.31, 174.56 and 224.54 nm determined from TEM images. The details of ZnO powder were shown in Appendix A. The purity of ZnO powder is 99.5%. The specific surface areas (BET method) of ZnO were 24.22, 11.93 and 8.35 m^2/g for sizes of 65.31, 174.56 and 224.54 nm, respectively. The dispersant was polyacrylic acid (PAA, Sigma-Aldrich, Inc.) with molecular weights 1.8k, 450k and 3000k g/mol. PAA dissociation in water to produce COO^- group and H^+. Double distilled water was used throughout the experiment. For adsorption experiment, NaOH (Suntaichemicals Co., Ltd) was used as a titrant and phenolphthalein (Asia Pacific Speciality Chemicals, Ltd.) was used as an indicator. For ZnO nanoparticles synthesis, Zinc nitrate tetrahydrate ($Zn(NO_3)_2 \cdot 4H_2O$, Science Diagnostic Materials Co., Ltd.) and sodium hydroxide (NaOH, Suntaichemicals Co., Ltd) were used as starting materials. PAAs (1.8k, 450k and 3000k) were used as the additives at concentrations of 0, 0.05, 0.5 and 1 wt%.

3.2. Characterization of as-received ZnO powder

The phase identification of all ZnO powders was conducted by X-ray diffraction (XRD, D8-Advance, Bruker, CuK_{α} radiation, λ = 1.54 angstrom). This technique was based on the scattered intensity of X-ray beam hitting a sample as a function of incident and scattered angle. Data was collected at 2θ from 5° to 75°. XRD pattern reveals information about the crystal structure, chemical composition and physical properties of powder. Morphologies and primary sizes of synthesized ZnO were analyzed by transmission electron microscopy (TEM, JEM-2100, JEOL). Brunauer-Emmett-Teller (BET) specific surface areas (S_{BET}, m^2/g) were estimated from N_2 adsorption isotherms (SA 3100, Beckman Coulter, Ltd).

3.3. Preparation and characterization of ZnO nanoparticle aqueous suspensions using various ZnO particle sizes and PAA molecular weights

3.3.1. Preparation of ZnO aqueous suspensions

ZnO aqueous suspensions of 0.5 wt% solids content were prepared by mixing ZnO powder, double-distilled water and PAAs using ultrasonic probe (High Intensity Ultrasonic Processor VC/VCX, Sonics & Materials, Inc.) at 75 W energy for 4 min. Concentrations of PAA were varied from 0-5 wt% base on solid loadings.

3.3.2. Particle dispersion

Laser light scattering technique (Mastersizer 2000, Malvern Instruments, Ltd.) was used to measure median diameter and particle size distribution of ZnO particles dispersed in the suspensions. Optical microscopy (OM, BX60M, Olympus Optical Co., Ltd) and scanning electron microscopy (SEM, JSM-6480 LV, JEOL Co,. Ltd) were used to study particle dispersion.

3.3.3. Sedimentation behavior

Stability of ZnO particles in the suspensions was studied via sedimentation experiment. The suspensions prepared with various ZnO sizes, PAA concentrations and molecular weights were filled in sealed graduate test tubes and initial suspension heights (h_0) were measured. Sedimentation heights (h) were measured at the complete precipitation. Results were expressed as the h/h_0 ratios and the characteristics of sediment.

3.3.4. ZnO surface charge

Surface charges of ZnO particles in suspensions prepared with various PAA concentrations and molecular weights were determined by zeta potential measurement (ZetaPaLs, Brookhaven Instruments Corporation, Ltd.). The results verify types and quantities of net charges on the surface of ZnO and ZnO covered with dispersant.

3.3.5. Adsorption of PAA on ZnO surface

ZnO aqueous suspensions of 0.5 wt% solids content were prepared by ultrasonic probe at 75 W energy for 4 min using double-distilled water and PAA of molecular weights 1.8k, 450k and 3000k g/mol with various concentrations. The suspensions were stirred with magnetic stirrer for 24 h to reach equilibrium. Then, suspensions were centrifuged at 12,000 rpm for about 30 min in order to achieve the precipitatate for FTIR and clear supernatant for titration experiment.

3.3.5.1. Determination of Functional groups

The sediment particles were dried at 100°C for 24 h and mixed with potassium bromide (KBr) to form pellets for IR study. In order to prepare a KBr pellet, sample/KBr ratio must be considered in sample preparation. The concentration of the sample in KBr should be in the range of 0.2-1%. Too high concentration caused difficulty in obtaining clear pellet. Thus, IR beam was absorbed completely or scattered from the sample, which resulted in very noisy spectra. Fine powder mixed with KBr was placed in a mold, and a pellet is formed by the hydraulic press. The sample pellet is now ready to be inserted into the IR sample holder for obtaining the spectrum. Fourier transform infrared spectroscopy (FTIR, Nicolet 6700 FT-IR spectrometer, Thermo Scientific) was employed to record the IR spectra in the ranges of 4000-400 cm^{-1}. The spectrum showed the molecular absorption and transmission, creating a molecular fingerprint of the sample. Absorption peaks corresponded to the frequencies of vibrations between bonded atoms.

3.3.5.2. Determination of amounts of adsorbed PAA

The clear supernatant solution was analysed for the amounts of PAA adsorbed on ZnO particle surface by titration method. First, PAA solutions of known concentrations were titrated in order to obtain standard plots. Then, supernatants were titrated to determine unadsorbed PAA amounts. After subtracting these values from PAA amounts used to prepare the suspensions, amounts of PAA adsorbed on ZnO surface can be determined. Using theory of Langmuir adsorption isotherm which reported in details in chapter 2 (page 20), area occupied per molecule of PAA with different molecular weights can be evaluated. Details of the experiment and calculation are as followed.

Titration is a method of analysis that will determine the end point of a reaction and the quantity of reactant in the titration flask. A burette was used to

deliver the reactant to the flask and Phenolphthalein was used as indicator to detect the end point of the reaction.

1) Amount of 100% PAA adsorption on ZnO surface

First step, titrant solution of 0.01 mol/l NaOH was filled in a burette. Air bubbles and leaks were checked before proceeding with the titration and an initial volume was recorded. Second step, PAA solutions of 0.5, 1, 3 and 5 wt% were prepared by mixing PAA and double-distilled water in flasks. Magnetic stirrers were put in the flasks and Phenolphthalein was added as an indicator for 2-3 drops. Titration began by using the burette to deliver NaOH solution to PAA solution. At the end point, the PAA solution changed from colorless to pale pink and the final volume in the burette was recorded. The initial volume is subtracted with the final volume to obtain the amount the amount of delivered titrant. Finally, the used amount of the titrant was used to calculate amount of PAA in mg/m^2 by the following equation (18).

$$C_1V_1 = C_2V_2 \quad (18)$$

C_1 = concentration of NaOH (mol/l)

C_2 = concentration of PAA (mol/l)

V_1 = volume of NaOH at the end point (ml)

V_2 = volume of PAA (ml)

2) Amount of PAA adsorbed on ZnO surface

First step, titrant solution of 0.01 mol/l NaOH was filled in a burette. Air bubbles and leaks were checked before proceeding with the titration and an initial volume was recorded. Second step, filled a flask with clear supernatant obtained from centrifuging of suspension, put a magnetic stirrer in the flask and added Phenolphthalein as an indicator for 2-3 drops. Third step, NaOH solution was delivered to supernatant using burette. At the end point, the supernatant change from colorless to pale pink and the final volume in the burette was recorded. The initial volume is subtracted with the final volume to obtain the amount of delivered titrant. Finally, the

used amount of the titrant was used to calculate amount of PAA in supernatant by the equation (18). The amount of PAA adsorbed on ZnO surface (mg/m^2) was calculated from the difference between amount of 100% PAA adsorption (from 1)) and amount of PAA in supernatant. Relationships between amount of PAA concentration and amounts of PAA adsorbed on ZnO surface were plotted to obtain Langmuir isotherm (Fig.2.14). Base on Langmuir equation for the case of PAA adsorption, $\left(\frac{n_2^s}{W}\right)$ is plotted as a function of C to obtain a straight line of slope m and intercept b (Fig.2.15). Then, area occupied per molecule of PAA can be evaluated using known specific surface area (A_{sp}) of ZnO particle of various sizes followed in equation (14).

The flow chart of preparation and characterization of ZnO nanoparticle aqueous suspensions using various ZnO particle sizes and PAA molecular weights was shown in Fig.3.1. Characterization included particle size distribution, optical microscopy, sedimentation experiments, zeta potential measurement and adsorption experiments.

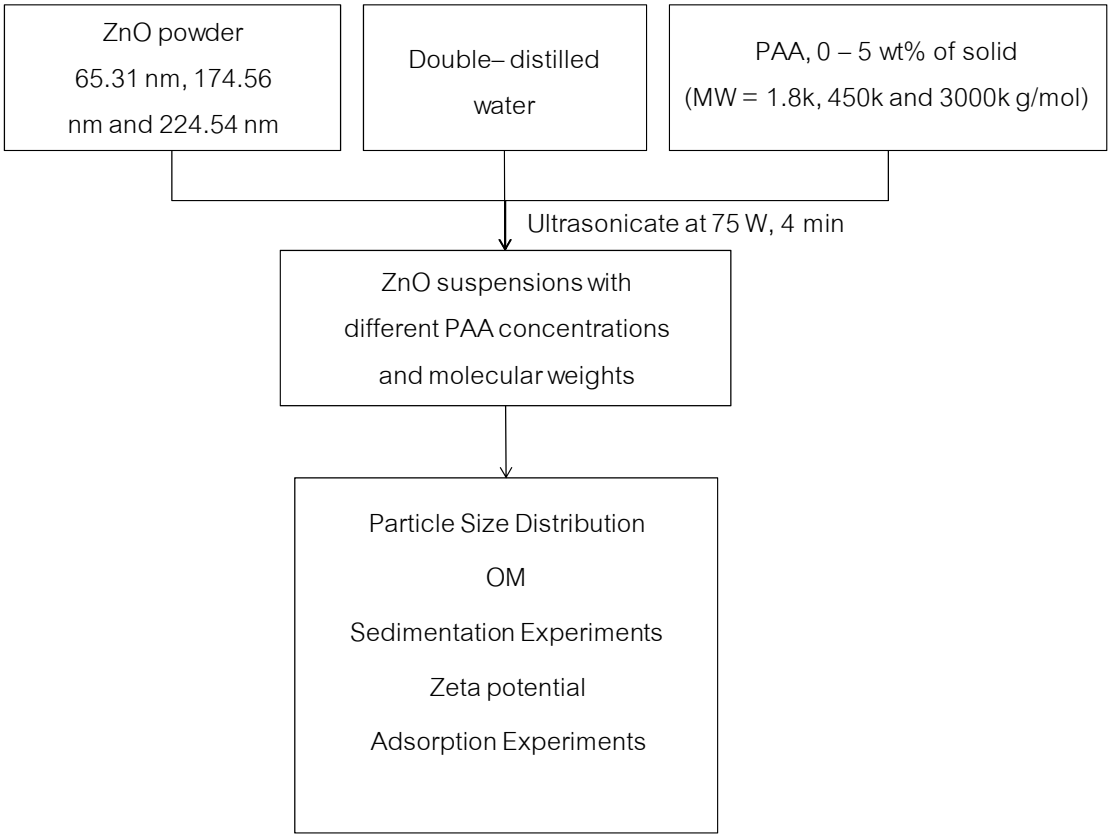

Fig. 3.1 Flow chart of preparation and characterization of ZnO nanoparticle aqueous suspensions using various ZnO particle sizes and PAA molecular weights.

3.4. Synthesis and characterization of ZnO nanoparticles using various PAAs

3.4.1. Synthesis of ZnO nanoparticles by precipitation method

ZnO was produced by mixing zinc nitrate and sodium hydroxide aqueous solutions as shown in equation (19).

$$Zn^{2+}_{(aq)} + 2HO^{-}_{(aq)} \rightarrow ZnO_{(s)} + H_2O \qquad (19)$$

The Zn^{2+} reactant solution of 0.1 mol/l was prepared by dissolving $Zn(NO_3)_2 \cdot 4H_2O$ in pure water. The NaOH solution of 0.1 mol/l was prepared by dissolving NaOH in pure water. Polyacrylic acid (PAA) was prepared by dissolving 0-1 wt% in the NaOH reaction solution. PAA molecular weights were 1.8k, 450k and 3000k.

Precipitation reactions occurred by mixing of two reactants. The NaOH solution of 0.1 mol/l was added into zinc nitrate solution, stirred, heated at 95°C and then placed in a bath of cold water for cooling. Synthesized ZnO was collected by washing with double-distilled water and ethanol, then filtered and dried at 200 °C for 3 h.

3.4.2. Characterization of synthesized ZnO nanoparticles

The phase identification of the precipitates was conducted by X-ray diffraction (XRD, D8-Advance, Bruker, CuK_α radiation, λ = 1.54 angstrom). This technique was based on the scattered intensity of X-ray beam hitting a sample as a function of incident and scattered angle. Data was collected at 2θ from 5° to 75°. XRD pattern reveals information about the crystal structure, chemical composition and physical properties of powder. FTIR spectra were recorded on FTIR spectrometer in a KBr matrix in the range from 400 to 4000 cm^{-1} to study functional groups. Synthesized ZnO was mixed with potassium bromide (KBr) and formed pellets using hydraulic press. The sample pellet was insert into the IR sample holder and the spectrum was obtained. The result of spectrum shows the molecular absorption and transmission, creating a molecular fingerprint of the sample. Optical microscopy (OM, BX60M, Olympus Optical Co., Ltd) was used to study particle dispersion. Morphologies and primary sizes of synthesized ZnO were analyzed by transmission electron microscopy (TEM, JEM-2100, JEOL). The particle size distribution was measured by laser light scattering technique (Mastersizer 2000, Malvern Instruments, Ltd.). Brunauer-Emmett-Teller (BET) specific surface areas S_{BET} (m^2/g) were estimated from N_2 adsorption isotherms (SA 3100, Beckman Coulter, Ltd). Surface charge of synthesized ZnO was determined by zeta potential measurement (ZetaPaLs, Brookhaven Instruments Corporation, Ltd.).

The flow chart of synthesis and and characterization of ZnO nanoparticles using PAA dispersant of various molecular weights was shown in Fig.3.2. Characterization techniques included XRD, FTIR, OM, TEM, light scattering and BET.

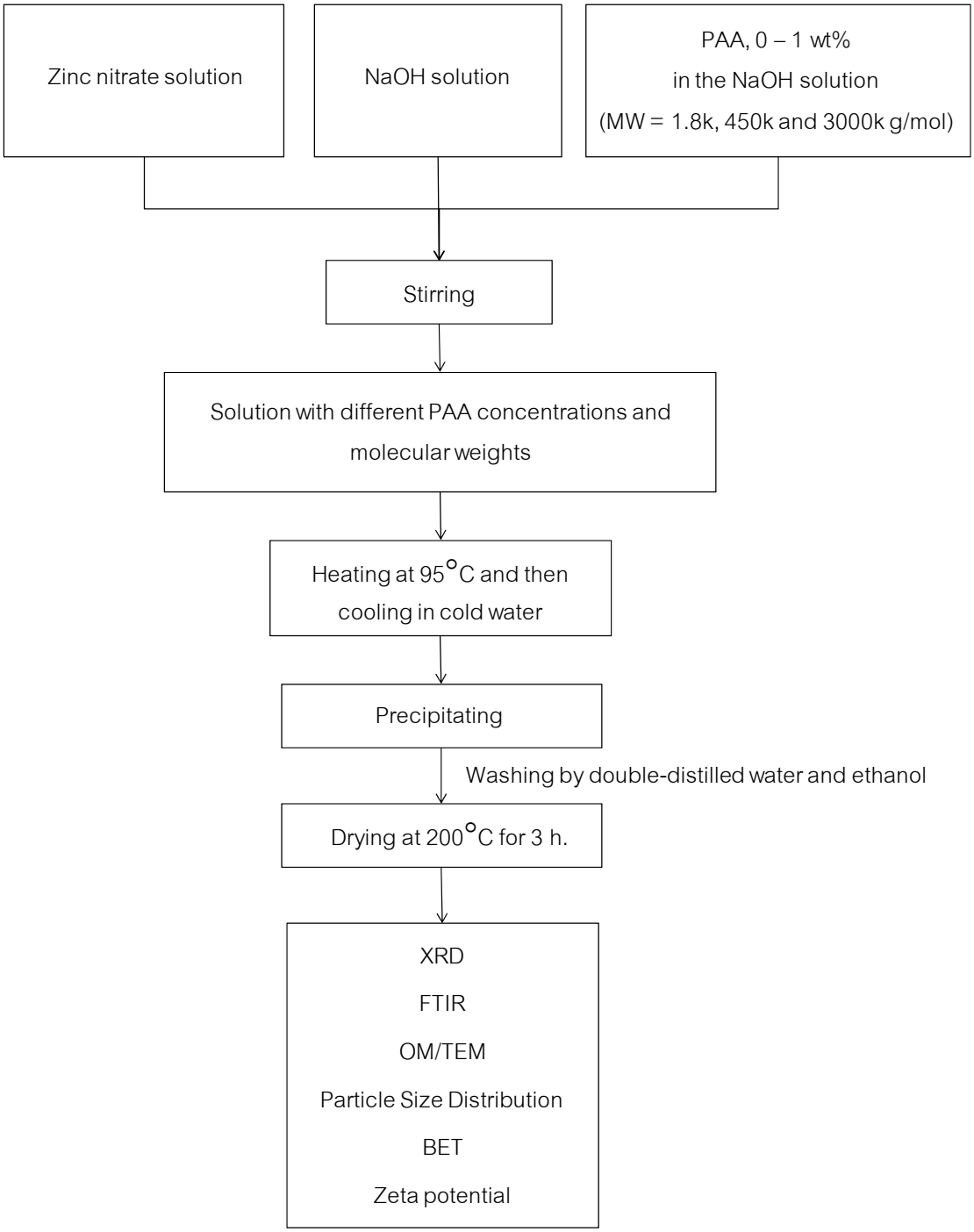

Fig. 3.2 Flow chart of synthesis and characterization of ZnO nanoparticles using PAA dispersant of various molecular weights.

CHAPTER 4
RESULTS AND DISCUSSIONS

4.1. Characterization of raw materials

4.1.1. XRD patterns of as-recieved ZnO powder

XRD patterns of ZnO powder size of 65.31 nm are similar for different particle sizes and shown in Fig.4.1. All diffraction peaks of ZnO powder are confirmed to be a crystalline material with hexagonal structure of the wurtzite. These peaks correspond to the crystal planes of (100), (002), (101), (102), (110), (103), (200), (112), (201) and (004), respectively [46]. Miller indices (h k l) to each peak reported in JCPDS card (No.00-036-1451) is shown in Appendix B.

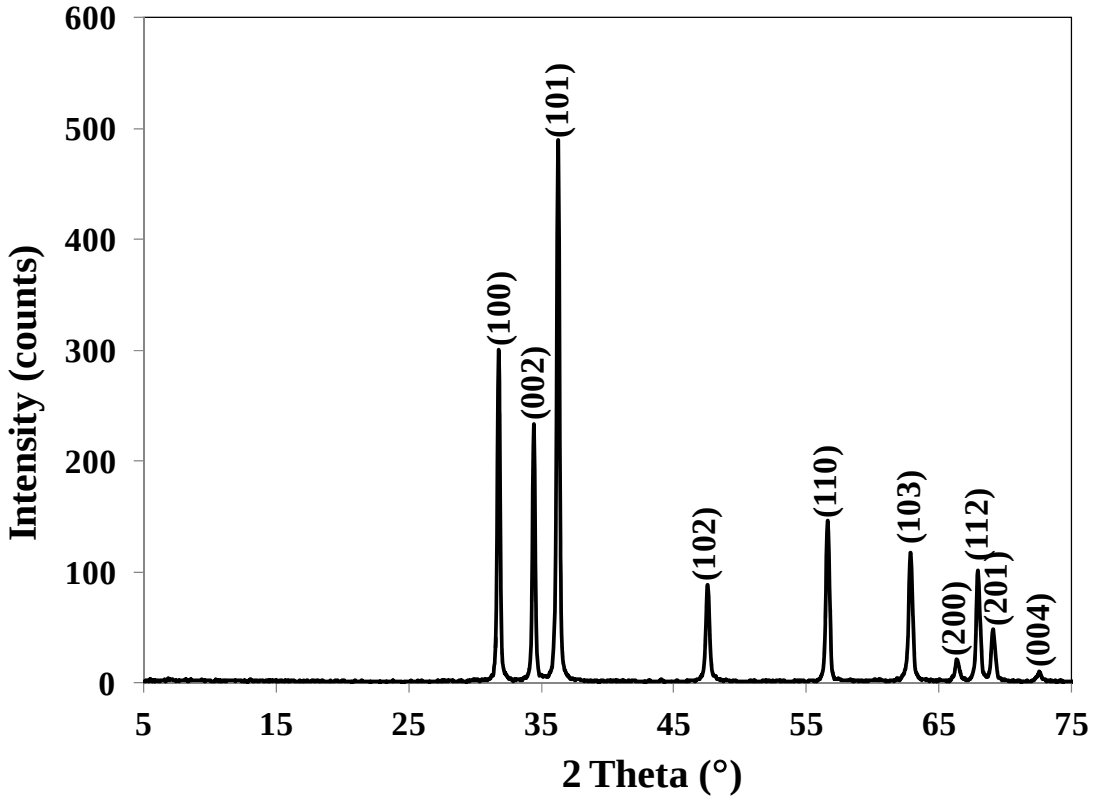

Fig. 4.1 XRD pattern of as –received ZnO powder size of 65.31 nm.

4.1.2. Transmission electron microscopy (TEM) of as-received ZnO powder

The morphology and primary size of ZnO powder can be observed in the TEM micrographs in Fig.4.2. Smaller particle is nearly spherical while larger particle are more elongated, rod-like particles. Average primary sizes are evaluated from TEM images by equivalent spherical diameter calculation as shown in equation (20) [47]. Average ZnO primary sizes are 65.31, 174.56 and 224.54 nm with standard deviations of 27.39, 74.75 and 96.95, respectively.

$$X = \sqrt[3]{\frac{3V}{4\pi}} \tag{20}$$

X = equivalent volume radius

V = volume of sphere = $\frac{4}{3}\pi r^3$

r = radius

V = volume of cylinder = $\pi r^2 h$

h = height

Particle size distribution of ZnO powder is shown in Fig.4.3. The smallest ZnO powders of average size 65.31nm show narrow distribution with most of the particles are smaller than 100 nm (Fig.4.3(a)). Larger ZnO of sizes 174.56 and 224.54 nm show wider distributions (Fig.4.3(b, c)) with size ranges between 50 to 380 nm and 90 to 460 nm, respectively.

(a)

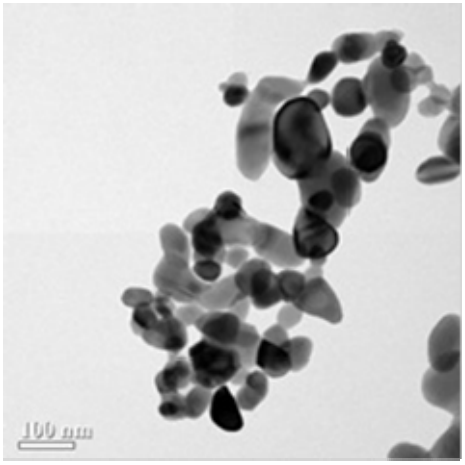

(b)

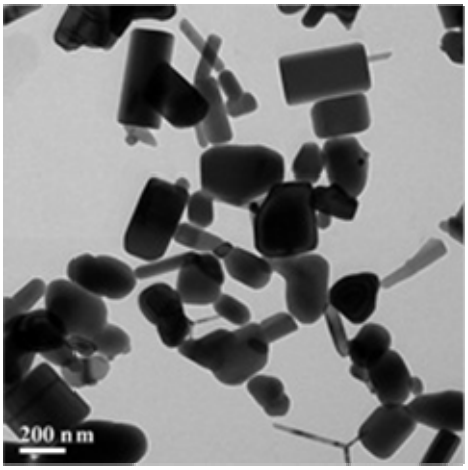

(c)

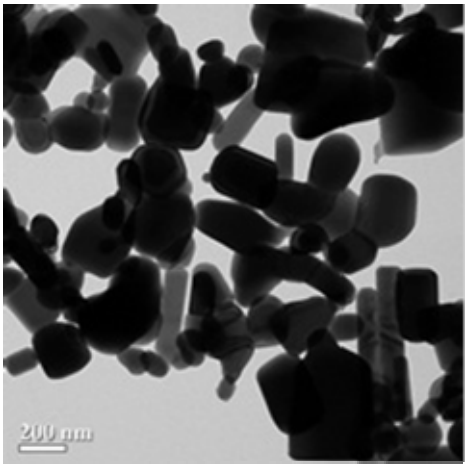

Fig. 4.2 TEM micrographs of ZnO powder; (a) ZnO 65.31 nm, (b) ZnO 174.56 nm and (c) ZnO 224.54 nm.

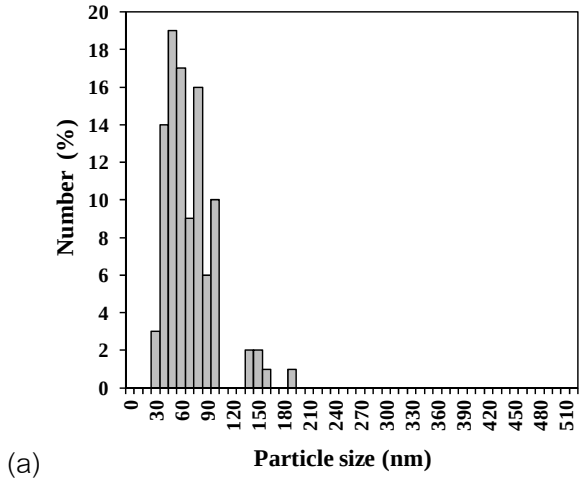

(a)

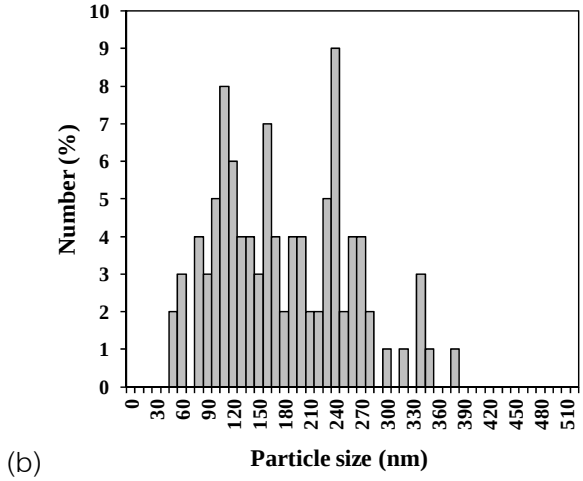

(b)

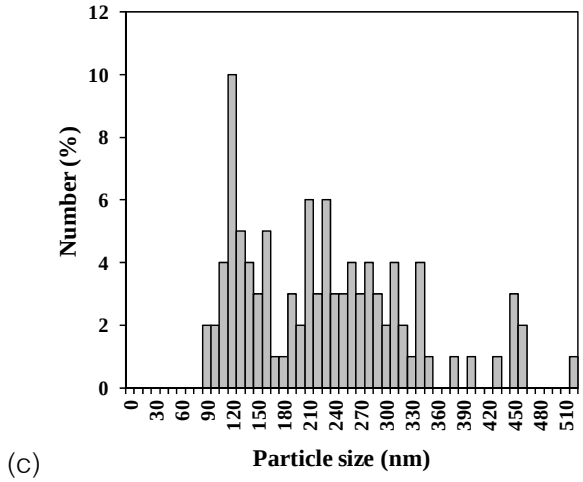

(c)

Fig. 4.3 Particle size distribution of ZnO powders; (a) ZnO 65.31 nm, (b) ZnO 174.56 nm and (c) ZnO 224.54 nm.

4.1.3. Specific surface area (BET) of as-received ZnO powder

The specific surface area of ZnO powders with different sizes was investigated by BET technique and shown in Table 4.1. It can be seen that specific surface area decreases with the increasing particle size as expected. The specific surface area is used for evaluation of area occupied per molecule of PAA on ZnO surface in the following adsorption part.

Table 4.1 The specific surface area of ZnO powders by BET technique.

ZnO powder (nm)	Specific surface area (m^2/g)
65.31	24.22
174.56	11.93
224.54	8.35

4.2. Preparation and characterization of ZnO nanoparticle aqueous suspensions using various ZnO particle sizes and PAA molecular weights

4.2.1. Particle dispersion

4.2.1.1. Particle size distribution

Particle size distribution of suspensions using ZnO with primary size of 65.31 nm and PAA of various concentrations and molecular weights are shown in Fig.4.4. Without PAA, particles are highly agglomerated. The agglomerate sizes are in the range of 1–100 μm. With 0.5 wt% PAA(1.8k), agglomerate size decreased drastically. All agglomerates are smaller than 10 μm and particles smaller than 100 nm can be found as shown in Fig.4.4(a). Increasing PAA(1.8k) concentrations to 1, 3 and 5 wt% slightly improves particle dispersion. Well-dispersed particles can also be achieved with PAA(450k) at 5 wt% as shown in Fig.4.4(b). However, PAA(3000k) slightly aided

particle dispersion. With 5 wt% PAA(3000k), most particles are still highly agglomerated. Particle sizes are in the 10 μm ranges with very few particles smaller than 1 μm as shown in Fig.4.4(c). It is obvious that PAA(1.8k) can greatly improve particle dispersion when using at low concentration PAA(450k) can also be an effective dispersant but high concentration is required. However, PAA(3000k) are inefficient as a dispersant for 65.31-nm ZnO suspension. Particle dispersion is only slightly improved when adding PAA(3000k) up to 5 wt%. Therefore, for 65.31-nm ZnO suspensions, the effective dispersants are PAA(1.8k) and PAA(450k) at high concentration.

Fig.4.5 shows particle size distribution of suspensions prepared with ZnO of primary size 174.56 nm. Particles are highly agglomerated in suspension without PAA. Most of the agglomerate sizes are in the range of 1 – 50 μm with small amounts of agglomerate sizes smaller than 1 μm. With addition of PAA(1.8k), agglomerate sizes decrease. Amounts of small particles of around 0.1 μm (100 nm) increase with increasing PAA(1.8k) concentrations (Fig.4.5(a)).PAA(450k) and PAA(3000k) at low concentrations (0.5-1 wt%) slightly improve particle dispersion as amounts of particles smaller than 1 μm slightly increase (Fig.4.5(b, c)). When using at high concentration of 3 and 5 wt%, PAA(450k) and PAA(3000k) significantly promote particle dispersion. All agglomerates are smaller than 10 μm. Thus, for 174.56 nm-ZnO suspensions, all PAAs are effective dispersants with a condition that high molecular weight PAA(450k) and PAA(3000k) must be used at high concentration.

Fig.4.6 shows particle size distribution of suspensions prepared from ZnO of primary size 224.54 nm. Similar to the other suspensions, PAA(1.8k) is an effective dispersant at low concentration. Agglomerate sizes decrease significantly with 0.5 wt% PAA(1.8k) and amounts of small particles increase with increasing concentration. PAA(450k) and PAA(3000k) improve particle dispersion at high concentration. Slightly boarder distribution with particle size in the ranges of 0.5-10 μm is observed for suspension using PAA(3000k) at 5 wt% comparing to that using PAA(450k) at the same concentration. Similar to 174.56 nm-ZnO suspension, PAA(1.8k)

is the most effective dispersant and PAA(450k) and PAA(3000k) can be used at high concentration.

Fig.4.7(a-c) shows particle size distribution of ZnO aqueous suspensions prepared with 5 wt% PAAs and ZnO primary sizes of 65.31, 174.56 and 224.54 nm, respectively. Results show that the best particle dispersion for 65.31 nm-ZnO can be achieved using PAA(1.8k) due to higher amounts of small agglomerates with <1 μm in size. However, PAA(450k) is slightly more effective for preparation of suspensions using ZnO with larger primary sizes of 174.56 and 224.54 nm. As can be seen in Fig. 4.7 (b,c) that 5 wt% PAA(450k) provides more small agglomerates than the other dispersants.

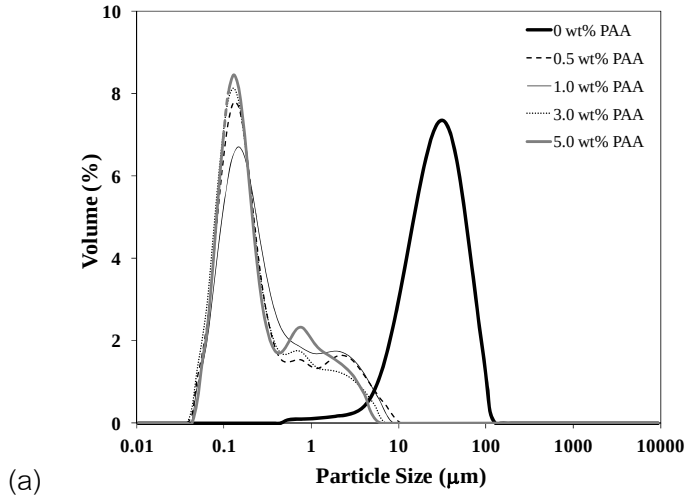

(a)

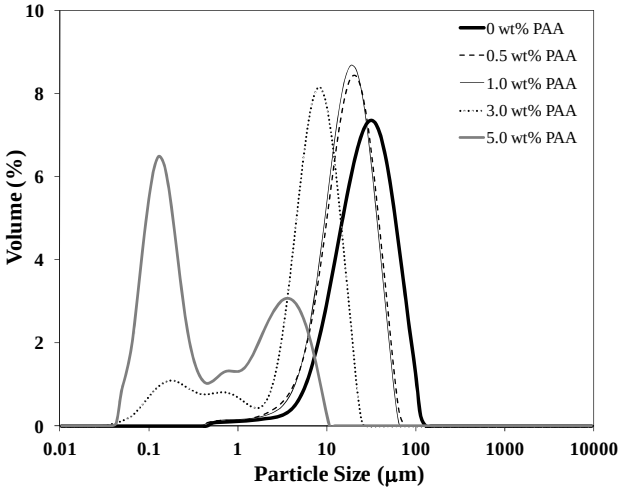

(b)

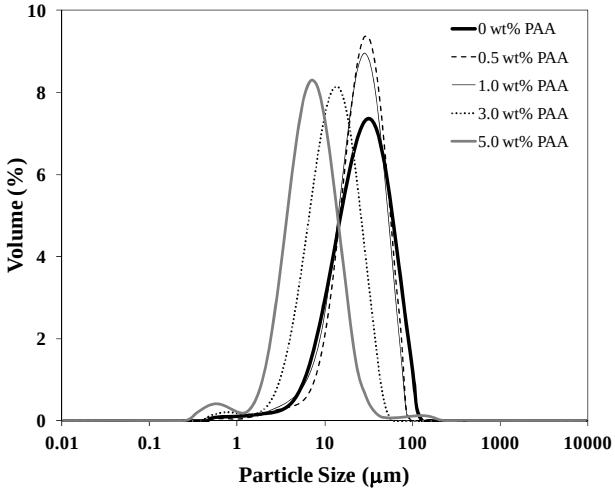

(c)

Fig. 4.4 Particle size distribution of suspension using ZnO primary size of 65.31 nm with various PAA concentrations and molecular weights
(a) PAA(1.8k), (b) PAA(450k) and (c) PAA(3000k).

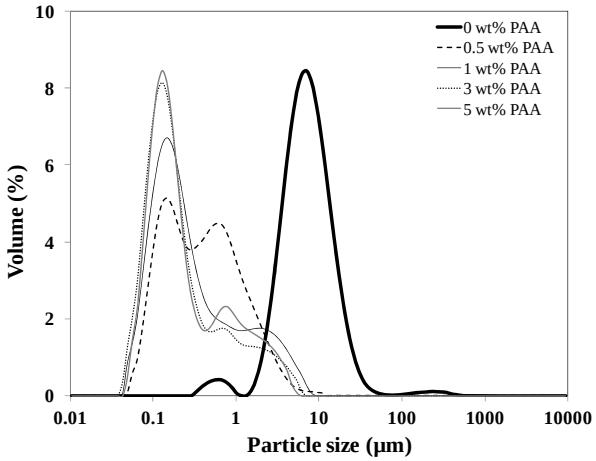

(a)

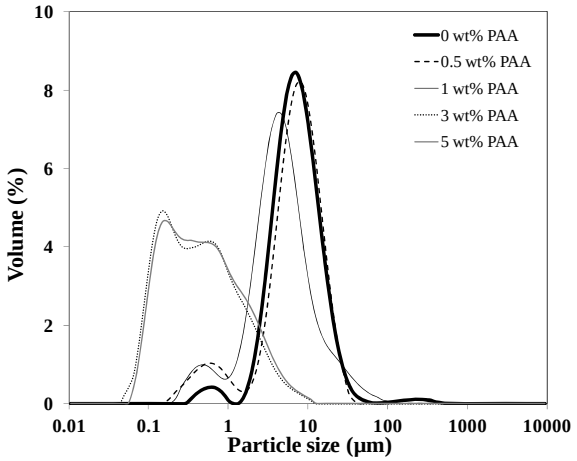

(b)

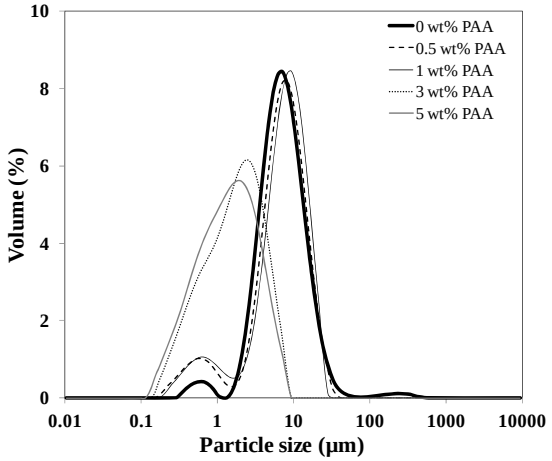

(c)

Fig. 4.5 Particle size distribution of suspension using ZnO primary size of 174.56 nm with various PAA concentrations and molecular weights
(a) PAA(1.8k), (b) PAA(450k) and (c) PAA(3000k).

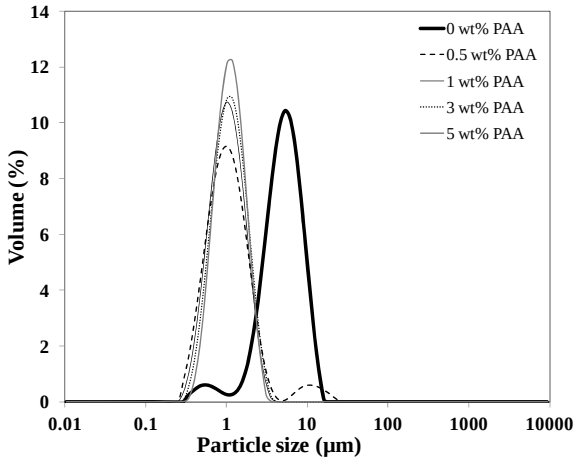

(a)

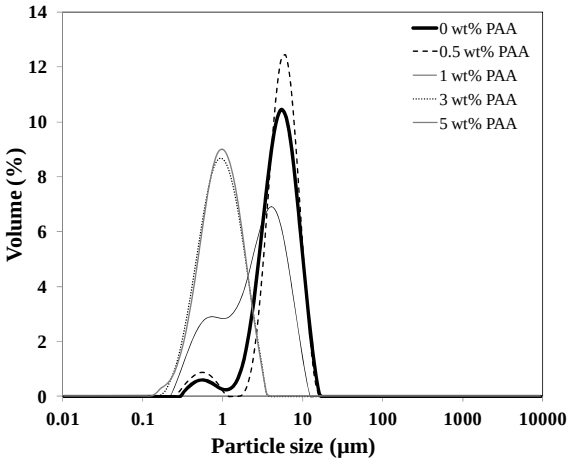

(b)

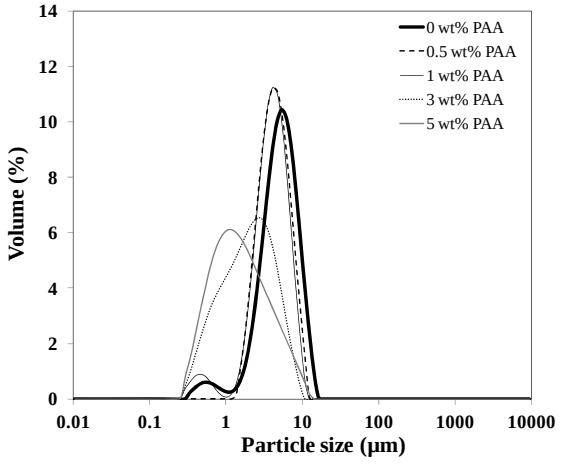

(c)

Fig. 4.6 Particle size distribution of suspension using ZnO primary size of 224.54 nm with various PAA concentrations and molecular weights

(a) PAA(1.8k), (b) PAA(450k) and (c) PAA(3000k).

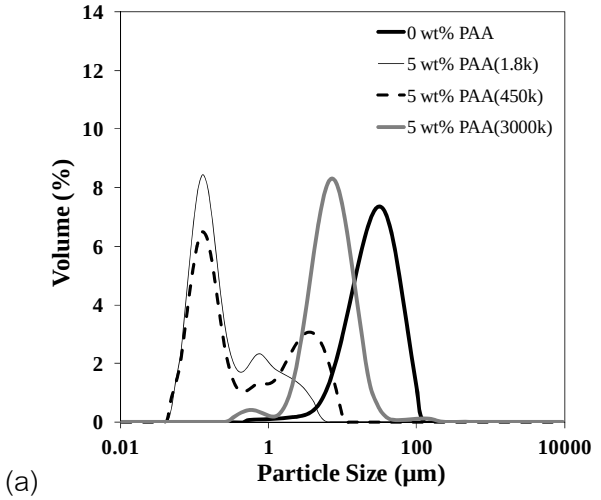

(a)

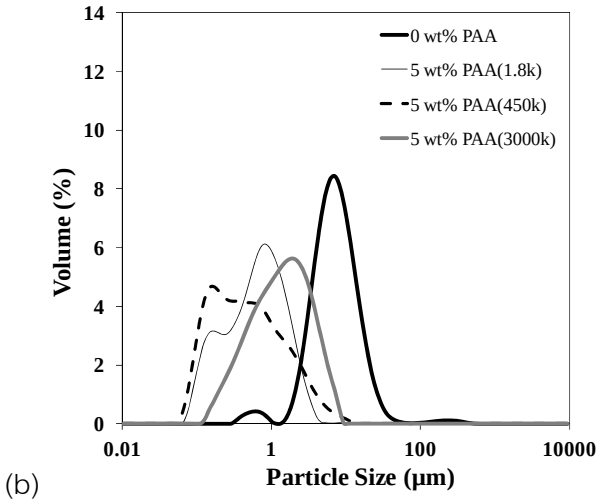

(b)

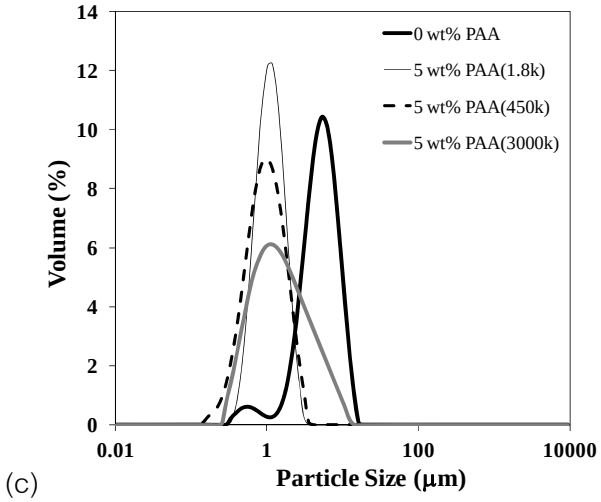

(c)

Fig. 4.7 Particle size distribution of ZnO suspensions prepared with 5 wt% PAAs. Average primary size of ZnO powders are (a) 65.31 nm, (b) 174.56 nm and (c) 224.54 nm.

The median size of agglomerates in suspensions using various ZnO primary particle sizes and PAA(1.8k), PAA(450k) and PAA(3000k) at various concentrations are shown in Fig.4.8. The median particle sizes in the suspension without PAA are 27, 7 and 5.1 μm for ZnO primary size of 65.31 nm, 174.56 nm and 224.54 nm, respectively. It is obviously shown that, when dispersed in aqueous medium, ZnO with smaller primary size agglomerates more than the ones with larger primary size. This is due to high specific surface area and attractive force between particles of small size. When PAAs are added to the suspensions, dispersion of ZnO in suspensions is improved. Agglomerate size decreases with the increasing PAA concentrations for all molecular weights. For ZnO primary size of 65.31 nm, the minimum aglgomerate sizes of 0.18 and 0.25 μm can be obtained with 0.5 wt% PAA(1.8k) and 5 wt% PAA(450k), respectively (Fig.4.8(a)). However, PAA(3000k) is not as effective in this case. Agglomerates with a median size of 7.02 μm are observed. ZnO primary sizes of 174.56 and 224.54 nm show similar trends in Fig.4.8(b, c). PAA(1.8k) provides particle dispersion at low concentration of 0.5 wt% while PAA(450k and PAA(3000k) improve particle dispersion at higher concentrations. It is noted that, for ZnO primary sizes of 174.56 an 224.54 nm, PAA(450k) at high concentrations of 3 and 5 wt% produce suspensions with slightly better dispersion than PAA(1.8k). For ZnO primary size of 174.56 nm, the minimum particle sizes of 0.65, 0.43 and 1.68 μm can be obtained with 5 wt% PAA(1.8k), PAA(450k) and PAA(3000k), respectively (Fig.4.8(b)). For ZnO primary size of 224.54 nm, the minimum particle sizes of 1.09, 0.96 and 1.41 μm can be obtained with 5 wt% PAA(1.8k), PAA(450k) and PAA(3000k), respectively (Fig.4.8(c)).

From the results, it can be suggested that PAA(1.8k) is an effective dispersant, which promotes excellent particle dispersion for all suspensions at low concentration (0.5 wt%). PAA(450k) can provide particle dispersion at higher concentrations (3, 5 wt%) with slightly better dispersant efficiency than PAA(1.8k) in the case of 174.58 and 224.54 nm-ZnO suspensions. On the other hand, the highest molecular weight, longest chain PAA(3000k) exhibits the lowest dispersant efficiency for the system. It is effective only at high concentration for a suspension of 224.54 nm-ZnO.

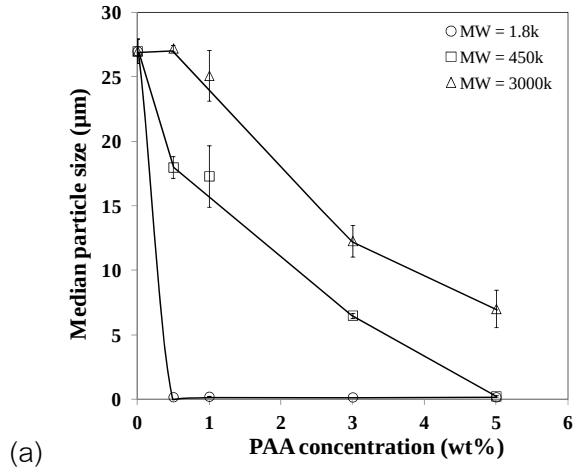

(a)

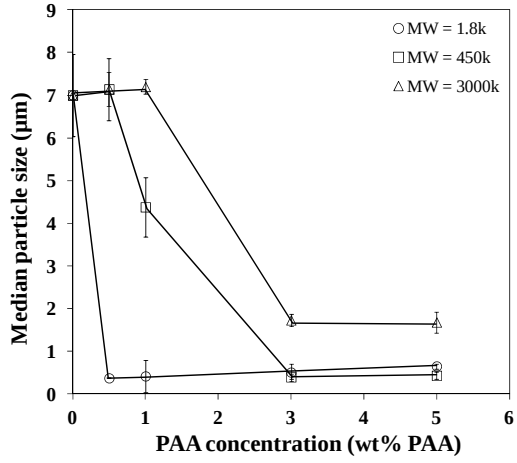

(b)

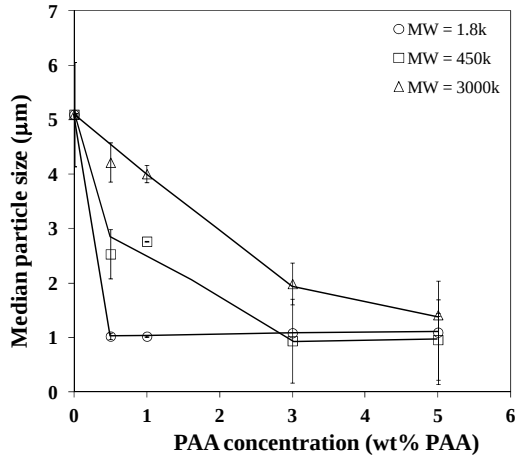

(c)

Fig. 4.8 The median particle size of suspensions prepared with various PAA concentrations and molecular weights. ZnO primary sizes are (a) 65.31 nm, (b) 174.56 nm and (c) 224.54 nm.

4.2.1.2. OM pictures

OM pictures in Fig.4.9 show particle dispersion of ZnO ((a)65.31, (b) 174.56 and (c) 224.54 nm) in suspensions prepared with various PAAs. The results are in agreement with particle size distribution reported above. For all suspensions without PAA, nanoparticles highly agglomerated with extremely large size. Additions of PAAs promoted particle dispersion in suspensions and agglomerate size decreased for all molecular weights. As an effective dispersant, PAA(1.8k) at 0.5 wt% promotes dispersion for all ZnO particle sizes. PAA(450k) is also a good dispersant at higher concentrations of 3 and 5 wt%. For PAA(3000k), high concentration is required to improve particle dispersion, however, this dispersant exhibits lower efficiency compare to the others. The results indicated that relatively short chain dispersant (PAA(1.8k)) is effective and provides well-dispersed suspension at low concentration of 0.5 wt%. Long chain dispersants can also be used to disperse particles in suspensions when using at high concentration. Our results are comparable to S. Liufu et al. [10], in a sense that higher molecular weight PAA is less effective as a dispersant comparing to the lower molecular weight ones. However, S. Liufu et al. reported flocculation of nanosized TiO_2 suspension with PAA(120k) while flocculation does not occur in our ZnO suspensions prepared with PAA of high molecular weight up to 3000k. This could be due to the difference in net surface charge of particles used in each research. The net surface charge of TiO_2 particle is negative while that of ZnO used in our study is positive.

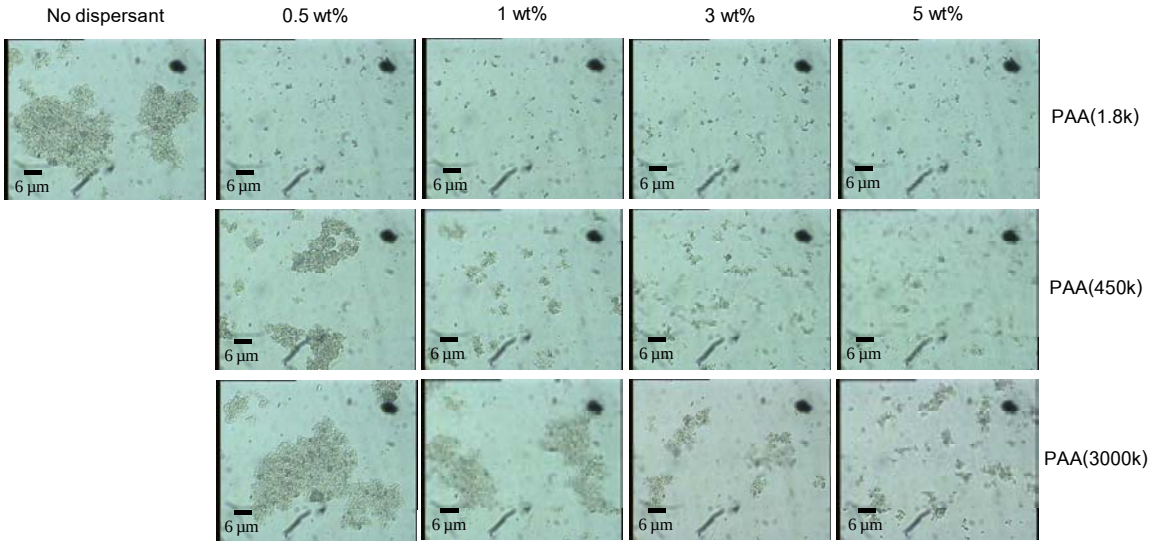
No dispersant
0.5 wt%
1 wt%
3 wt%
5 wt%
PAA(1.8k)
PAA(450k)
PAA(3000k)
6 µm

(a)

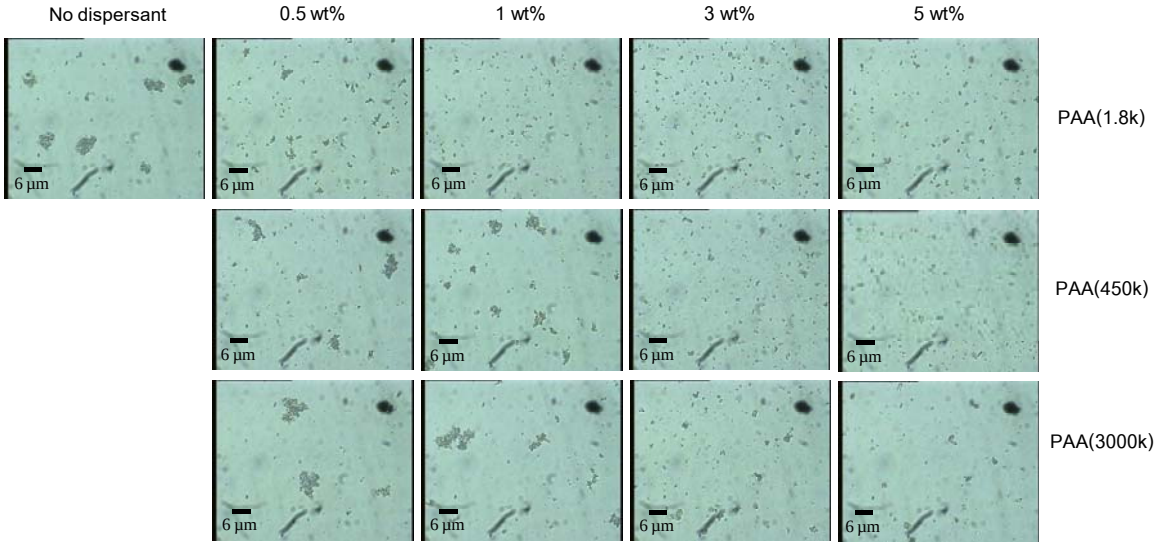
No dispersant
0.5 wt%
1 wt%
3 wt%
5 wt%
PAA(1.8k)
PAA(450k)
PAA(3000k)
6 µm

(b)

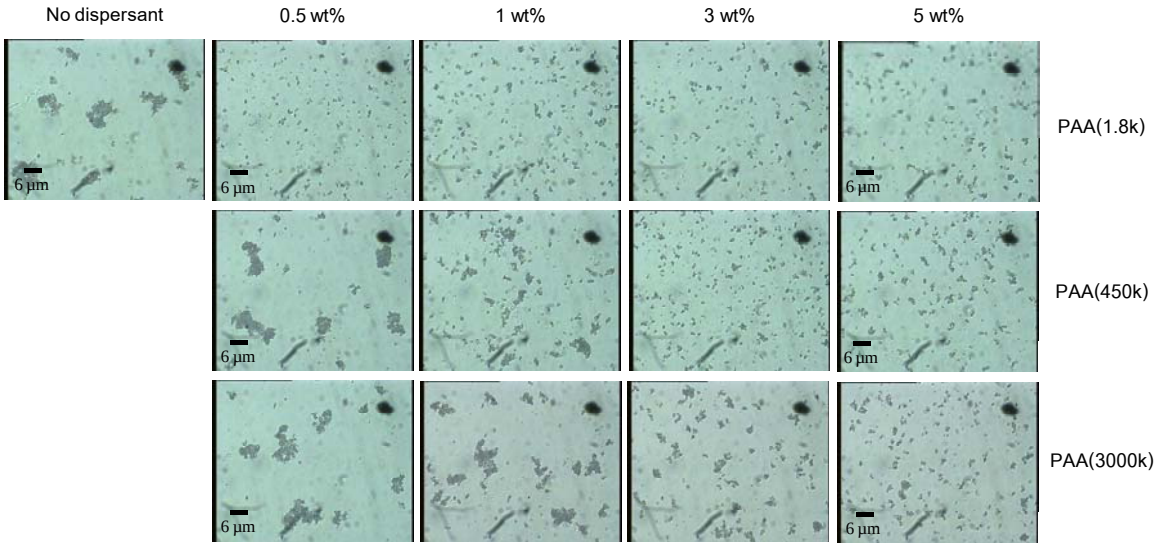

(c)

Fig. 4.9 OM pictures of ZnO particles in suspensions prepared with various concentrations and molecular weights of PAA;. ZnO primary sizes are (a) 65.31 nm, (b) 174.56 nm and (c) 224.54 nm.

4.2.2. Sedimentation behavior

Sedimentation experiments are conducted to study stability of suspensions. Results are shown in Fig.4.10. Cloudy supernatant showed particles suspended in media and clear supernatant indicated the complete precipitation. The suspensions of all ZnO sizes without PAA show clear supernatant, indicating complete precipitation within 1 day after mixing. Addition of PAAs promoted dispersion and stability of suspensions at different degrees. The 65.31 nm-ZnO suspension prepared with PAA(1.8k) exhibited well-dispersed and highly stable suspensions. The suspensions are stable up to 28 days then completely precipitated with h/h_0 ratios of 0.05. The 65.31 nm-ZnO suspension prepared with 0.5 wt%PAA(450k) is unstable and completely precipitates within 1 days. However, when increasing PAA(450k) to 5wt%, the suspension shows higher stabililty and completely precipitates at 28 days (Fig.4.10(a)). With PAA(3000k), the 65.31 nm-ZnO suspensions are unstable and

completely precipitated showing clear supernatant within 1 day for low concentration usages and within 2 days for 5 wt% PAA(3000k). The 174.56 nm-ZnO suspensions prepared with PAA(1.8k) and PAA(450k)are well-dispersed and highly stable . Stability of the suspension improves with increasing concentration of PAA(1.8k) and PAA(450k) dispersants and stable suspension up to 28 days can be achieved. When using PAA(3000k) as a dispersant at low concentration of 0.5 wt%, the 174.56 nm-ZnO suspensions completely precipitated within 1 days, however, suspension stability improves with increasing PAA(3000k) concentration. The 224.54 nm-ZnO suspensions show similar stability to the 174.56 nm-ZnO suspensions. Well-dispersed and highly stable suspensions can be obtained with PAA(1.8k) and PAA(450k) dispersants. The suspensions prepared with low concentration of PAA(3000k) are unstable, however, the suspension stability can be improved with higher concentration of PAA(3000k). Results of suspension stability are in agreement with the median agglomerate size of ZnO dispersed in aqueous medium as reported in the previous section. Well-disperse ZnO nanoparticles with small agglomerate sizes lead to highly stable suspensions desired for ceramic processing.

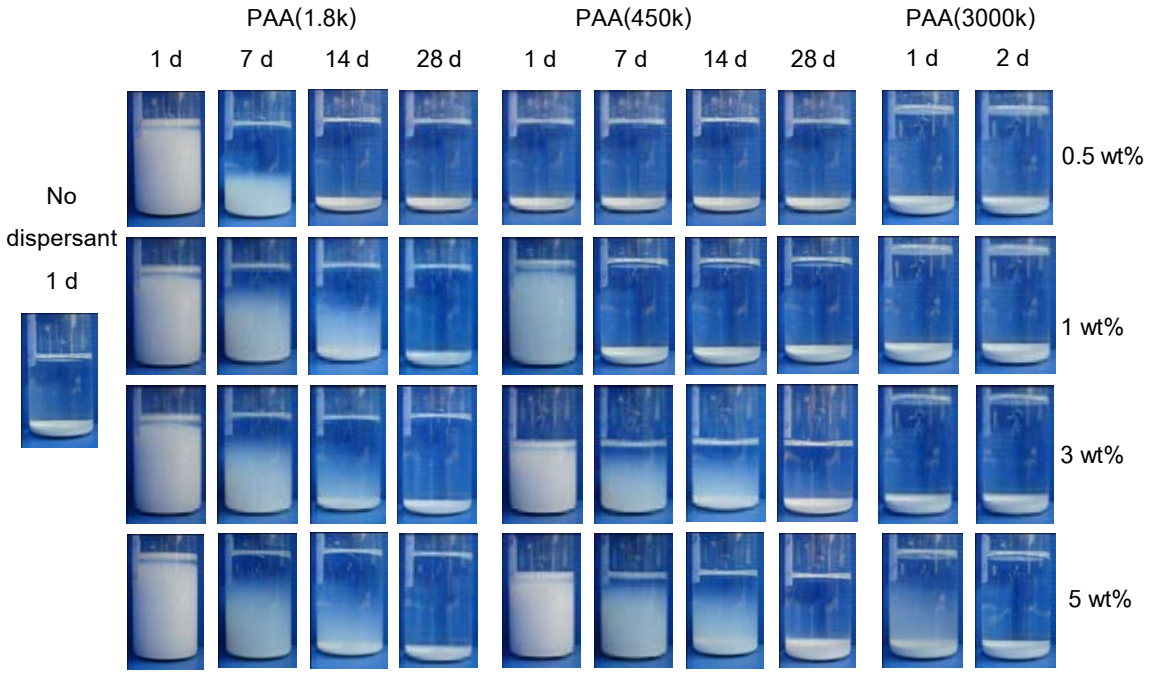

(a)

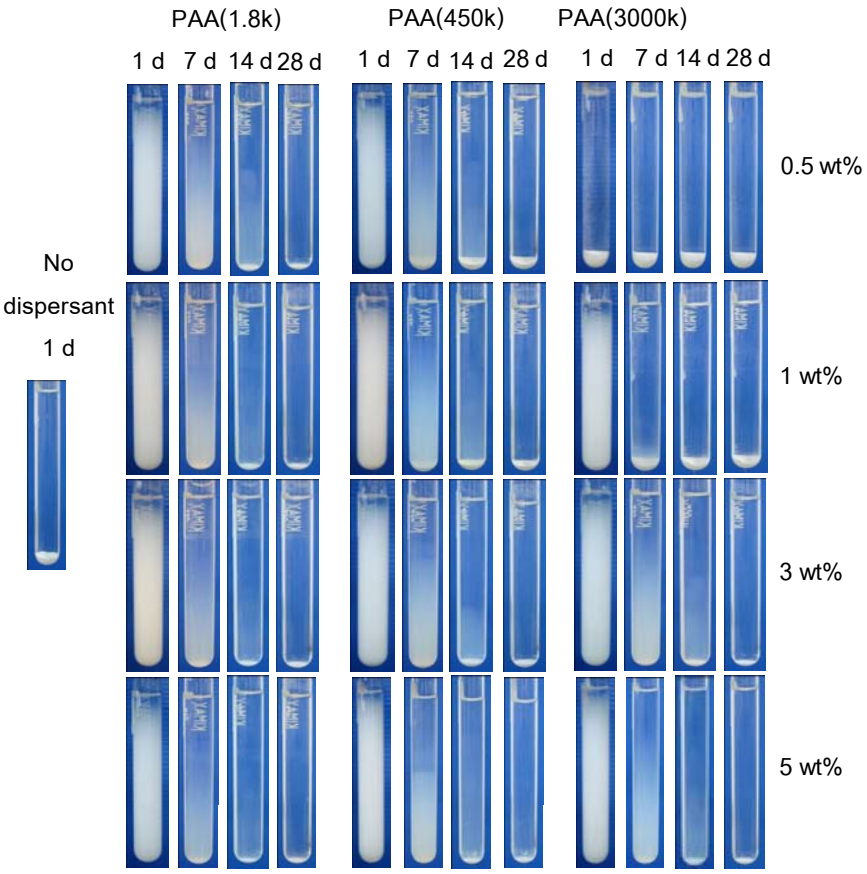
PAA(1.8k)
PAA(450k)
PAA(3000k)
1 d 7 d 14 d 28 d
1 d 7 d 14 d 28 d
1 d 7 d 14 d 28 d
No dispersant 1 d
0.5 wt%
1 wt%
3 wt%
5 wt%

(b)

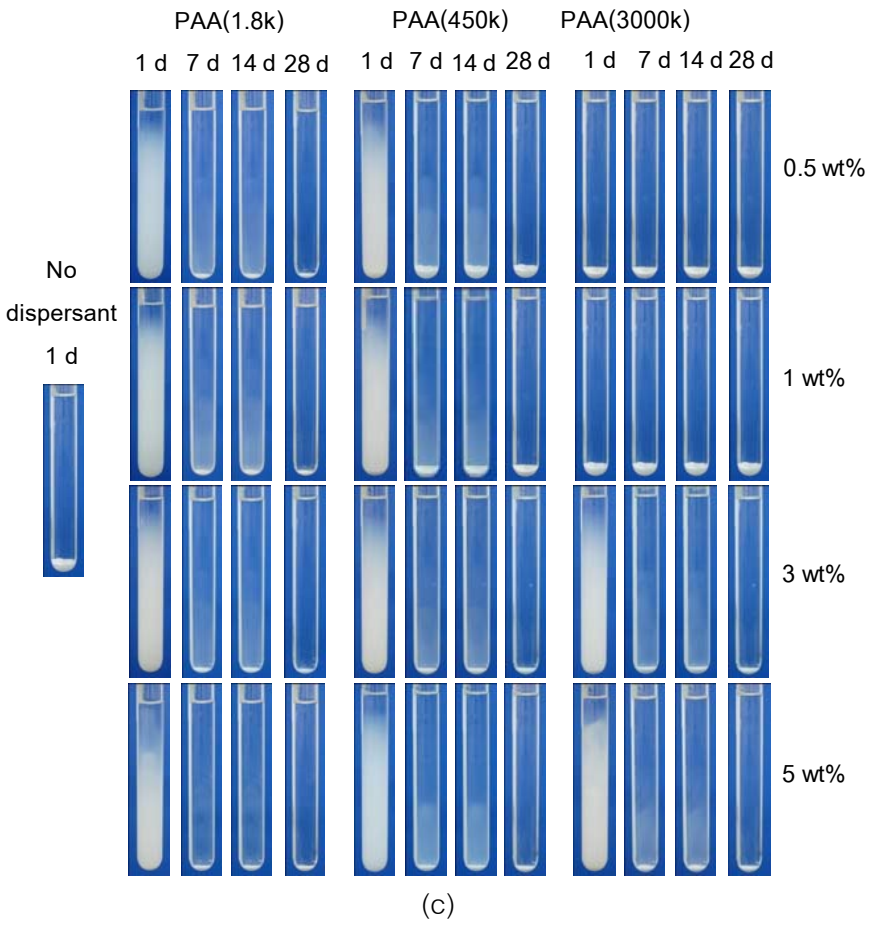

Fig. 4.10 Sedimentation experiments of suspension prepared with various PAAs and various ZnO primary sizes of; (a) 65.31, (b) 174.56 and (c) 224.54.nm.

Fig.4.11 showed the h/h_0 ratios measured at complete settling times of suspensions prepared with ZnO primary sizes 65.31, 174.56 and 224.54 nm using various PAAs. The lower h/h_0 ratios relate to slower precipitation of smaller particles or a well-dispersed and highly stable suspension. Results indicated that PAA(1.8k) provided the highest stable suspensions regardless of ZnO size. PAA(450k) and PAA(3000k) produced highly stable suspensions of 174.56 and 224.54 nm-ZnO at high concentration of 3 and 5 wt%. However, for 65.31 nm-ZnO suspension, the long chain polymers are inefficient. The h/h_0 ratios are in agreement with sedimentation behavior in Fig.4.10 and median particle size in Fig.4.8. A well-dispersed 65.31 nm-ZnO suspension

prepared with PAA(1.8k)with median agglomerate size of 0.18 μm is highly stable up to 28 days and completely precipitated with h/h_0 ratio of 0.05. The 65.31 nm- ZnO suspension prepared with PAA(450k) exhibits larger agglomerates, and thus, higher h/h_0 ratio compared to those prepared with PAA(1.8k). PAA(3000k), even at 5 wt%, produces an unstable 65.31 nm-ZnO suspension that completely precipitates within 2 days with the highest h/h_0 ratio of 0.1. For ZnO of primary size 174.56 nm in Fig.4.11(b), highly stable suspensions can be obtained with 0.5 wt% PAA(1800) and 3-5 wt% PAA(450k and 3000k). The suspensions completely precipitate with the minimum h/h_0 ratio of 0.02. For ZnO 224.54 nm in Fig.4.11(c), highly stable suspensions can be prepared with 0.5 wt% PAA(1.8k) and 5 wt% PAA(450k and 3000k). The suspensions completely precipitate with the minimum h/h_0 ratio of 0.02.

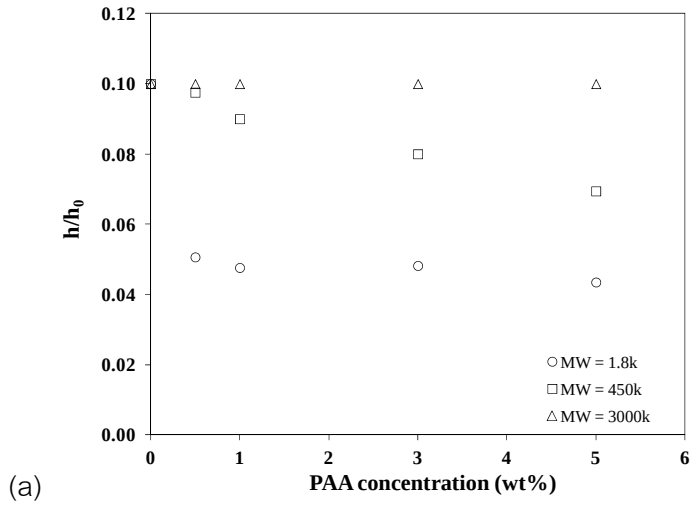

(a)

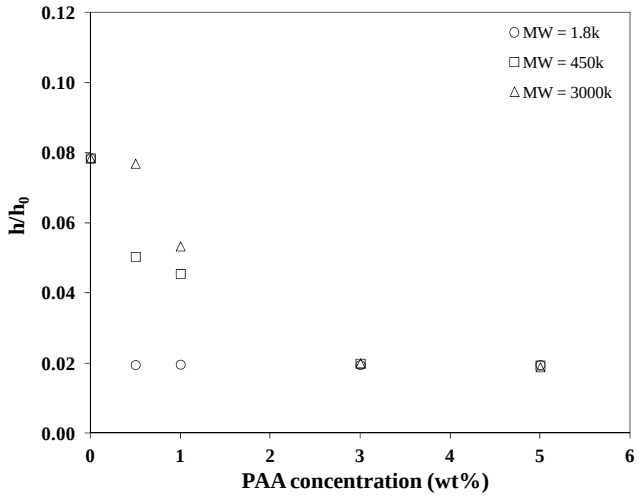

(b)

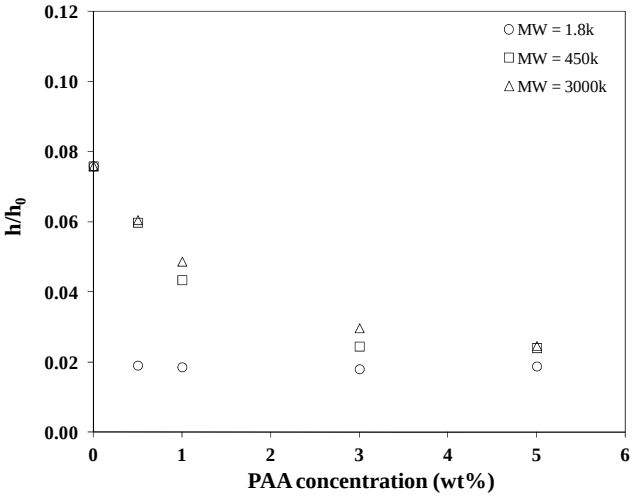

(c)

Fig. 4.11 The h/h_0 ratios at complete precipitation of suspensions prepared with various PAAs. Primary size of ZnO are(a) 65.31 nm, (b) 174.56 nm and (c) 224.54 nm.

4.2.3. Zeta potential

Theoretically, the high zeta potential or high surface charge results in high repulsive force and long distance between particles, which leads to a well-dispersed and high stable suspensions [5, 15-17]. The pH of suspensions prepared with PAAs at various concentrations is shown in Table 4.2. The effects of PAA concentration and its molecular weight on the zeta potential of suspensions prepared from ZnO of primary sizes 65.31, 174.56 and 224.54 nm are shown in Fig.4.12. Without PAA, the zeta potential are positive with values of 26.14, 23.57 and 16.57 mV for ZnO of primary sizes 65.31, 174.56 and 224.54 nm, respectively. Addition of PAAs shifts the zeta potential to negative side due to adsorption of COO^- groups on the ZnO particle surface from PAA dissociation. The values become more negative with increasing PAA concentrations because of an increase in COO^- group. Adsorption of PAA on ZnO particle surface leaded to electrosteric stabilization due to repulsive force between net surface charge on particle surface and steric hindrance from polymer chain. Addition of PAA(1.8k) provides higher zeta potential value than in the cases of PAA(450k) and PAA(3000k). It is suggested that low molecular weight PAA produces better particle dispersion and suspension stability than high molecular weight, which is confirmed by the above results. It is noted that zeta potential of the suspensions at the particular pH decrease with increasing PAA molecular weight, which is contrary to the previous work [10-11]. This might result from the differences in particle surface charge and PAA molecular weight used in each study. At pH of investigation, we study nanoparticles with positive surface charge and PAA of molecular weights 1.8k-3000k, whereas, negative-charged nanoparticles with 2k-120k PAAs, and micron-sized, positive-charged particles with 2k-90k PAAs [11] are examined in the other works. In addition, the colloidal system is extremely complex; therefore, comparison of the zeta potential can be applied only qualitatively [36].

Table 4.2 pH values of ZnO suspensions prepared with various ZnO sizes and PAAs.

ZnO size	M_W of PAA	0wt%	0.5wt%	1wt%	3wt%	5wt%
65.31nm	1.8k		7.66	7.50	7.33	7.25
	450k	8.12	7.67	7.67	7.53	7.63
	3000k		7.88	7.78	7.73	7.65
174.56 nm	1.8k		7.54	7.38	7.21	7.25
	450k	7.70	7.49	7.49	7.35	7.34
	3000k		7.35	7.32	7.40	7.43
224.54 nm	1.8k		7.40	7.24	7.07	7.04
	450k	7.91	7.64	7.64	7.55	7.54
	3000k		7.67	7.65	7.60	7.58

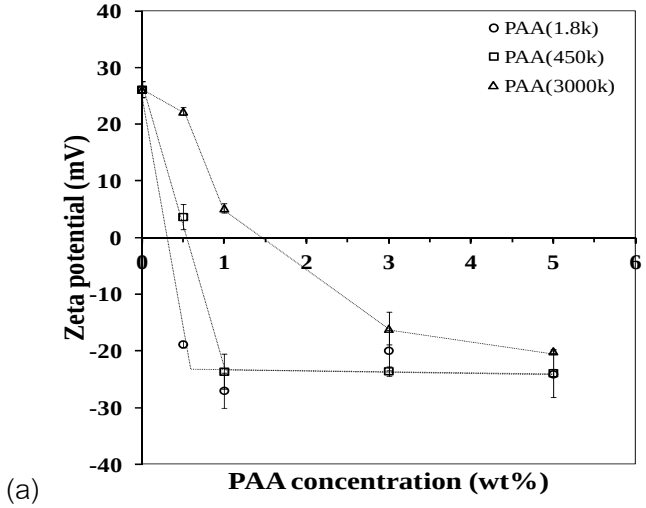

(a)

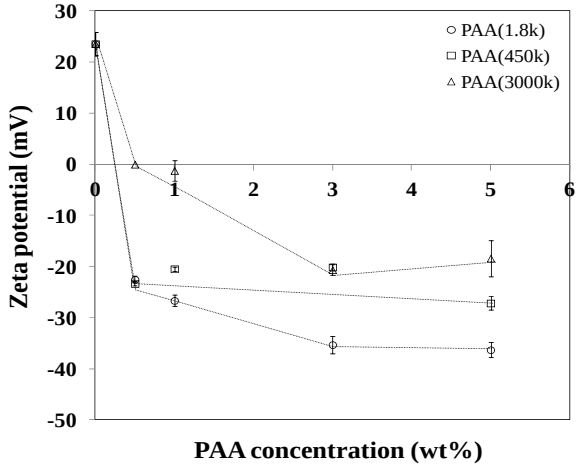

(b)

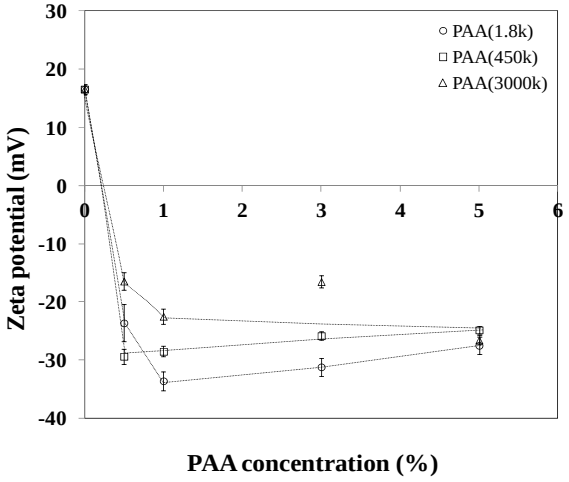

(c)

Fig. 4.12 Zeta potential values of suspensions prepared with various concentrations of PAAs. ZnO primary sizes are (a) 65.31 nm, (b) 174.56 nm and (c) 224.54 nm.

4.2.4. Adsorption experiment

4.2.4.1. FTIR spectra

Spectra from FTIR spectroscopy for PAA, ZnO and PAA adsorbed on ZnO particle surface are shown in Fig.4.13. Bands and peaks obtained in this study agree with previous reports for similar functional groups [10, 24, 48-49]. PAA spectrum in Fig.4.13(a) show broad band at 3485 cm^{-1} due to O-H stretching. The strong band at 1580 and 1380 cm^{-1} indicates COO^- stretching vibration. The FTIR spectrum of ZnO powder shown in Fig.4.13(e). A broad band at 3455 cm^{-1}, which may be attributed to hydroxyl groups on particle surface. A band at 1635 cm^{-1} is due to moisture and 478 cm^{-1} is due to Zn-O vibration. The FTIR spectrum of the ZnO interacting with 0.5 wt% PAA(1.8k), PAA(450k) and PAA(3000k) is shown in Fig.4.13(b-d). The broad band at 3455 cm^{-1} observed in the case of free ZnO shifts to lower wave numbers, indicating strong interaction of hydrogen bonding between OH group on ZnO surface and COOH group of PAA. In addition, COO^- stretching bands of PAA at 1580 and 1380 cm^{-1} shift to higher wavenumbers, corresponding to interaction of COO^- with ZnO surface[24, 46]. It is indicated that adsorption occurs between PAA on ZnO particle surface.

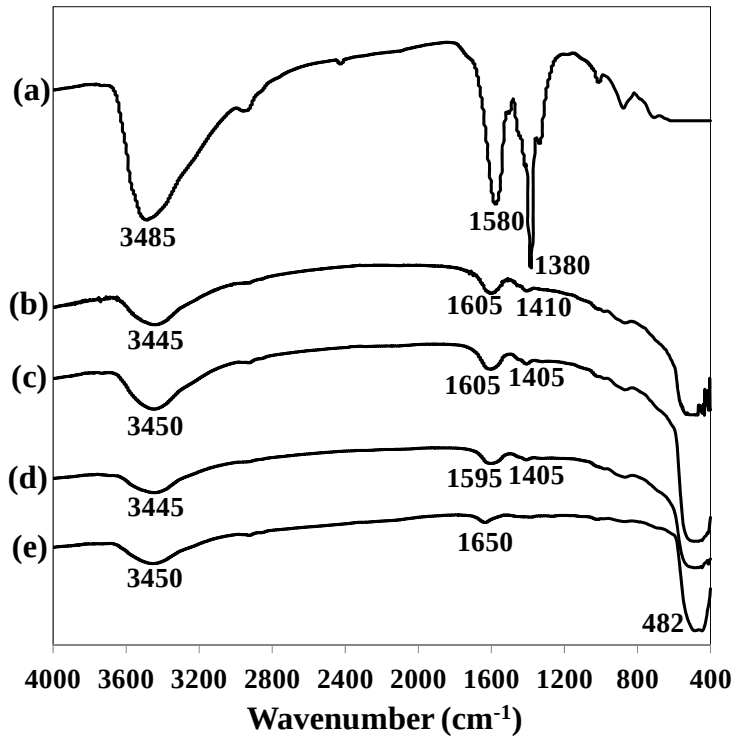

Fig. 4.13 FTIR spectra of (a) PAA, (b) ZnO with 0.5 wt% PAA(1.8k), (c) ZnO with 0.5 wt% PAA(450k), (d) ZnO with 0.5 wt% PAA(3000k) and (e) ZnO powder.

4.2.4.2. Adsorption amount of PAA on ZnO particles

Amounts of PAAs adsorbed on ZnO surface determined by titration method are shown in Fig.4.14. The 100% adsorption is shown as straight lines with no markers. Adsorption of PAA on the ZnO surface of various sizes exhibits Langmiur isotherm. It is found that the adsorbed amounts of PAA increase with the increasing PAA concentrations and molecular weights for all ZnO sizes, and then reach saturation. The adsorption takes place by hydrogen bonding between OH group on ZnO surface and COOH group of PAA [24, 50]. The increase of adsorption with the increasing PAA concentrations and molecular weights is similar to previous researches [9, 11]. K. K. Das et al [9] suggested that larger molecular weight polymer can adhere better on particle surface. Thus, PAA(3000k) shows higher adsorption than PAA(1.8k) and PAA(450k).

Fig.4.15 shows the monolayer coverage amount of PAA on ZnO particle surface. It is found that as PAA molecular weight increases, the monolayer coverage amount of PAA on ZnO surface increases for all ZnO sizes. The results agree with previous researches [9, 11] and can be explained based on conformation of polymer adsorbed on particle surface. It is suggested that higher molecular weight or longer chain length tend to form more loops and tails with longer loop and tail length compared to lower molecular weight polymer, leading to higher coverage amount [18, 51]. Effects of particle size on monolayer coverage of PAA(1.8k) and PAA(450k) can be clearly observed. The monolayer coverage amount of all PAAs is the highest for 65.31 nm-ZnO. With the increasing particle size, monolayer coverage decreased. For PAA(3000k), coverage amounts are similar on all ZnO sizes. This is reported by earlier research [18] that particle sizes determine the structure of polymer adsorbed on the surface. It is found that polymer adsorbed on various particle sizes with similar loop length. On the other hand, tail length decreases with the increasing particle size. Therefore, polymer adsorbed on small particles with more tails than loops. This is leaded to high amount of polymer adsorption per particle surface area. Initial concentrations of PAAs to be adsorbed as monolayer coverage on ZnO surface are shown in Fig.4.16. It can be seen that as particle size increases, the initial concentration of PAAs increases.

Adsorbed conformation of polymer could also be used to explain zeta potential values of particles prepared with PAA of various molecular weights. When adsorbing on particles of the same size. PAA(3000k) tends to exhibit longer tails than PAA(1.8k) and PAA(450k). Long dangling tails could wrap around particles, shielding the charge of COO^- group on the ZnO surface. Therefore, measured zeta potential values are lower for the system using higher molecular weight PAA.

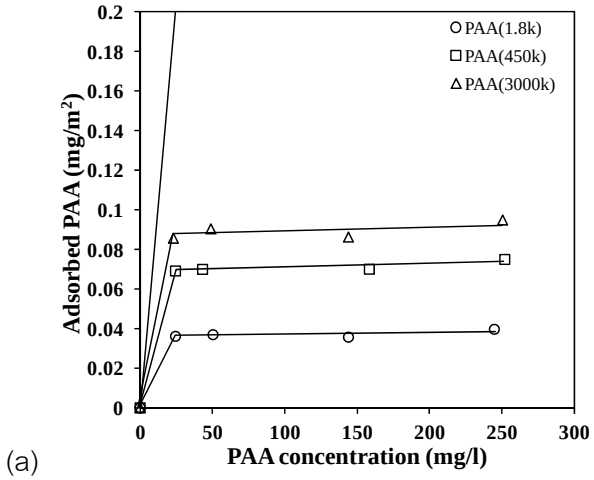

(a)

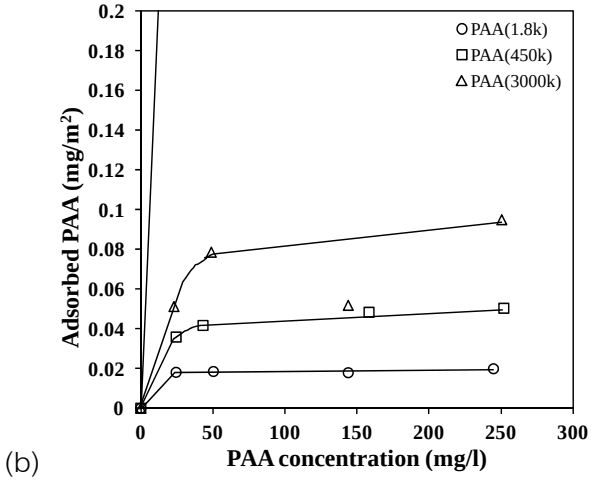

(b)

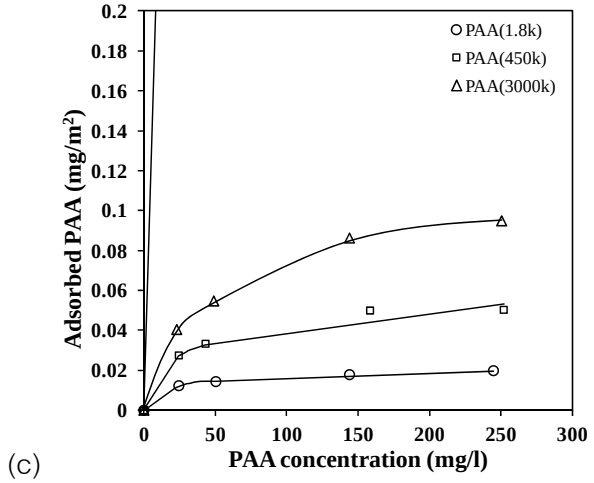

(c)

Fig. 4.14 Adsorption of PAA on the surface of ZnO primary sizes of;

(a) 65.31 nm, (b) 174.56 nm and (c) 224.54 nm.

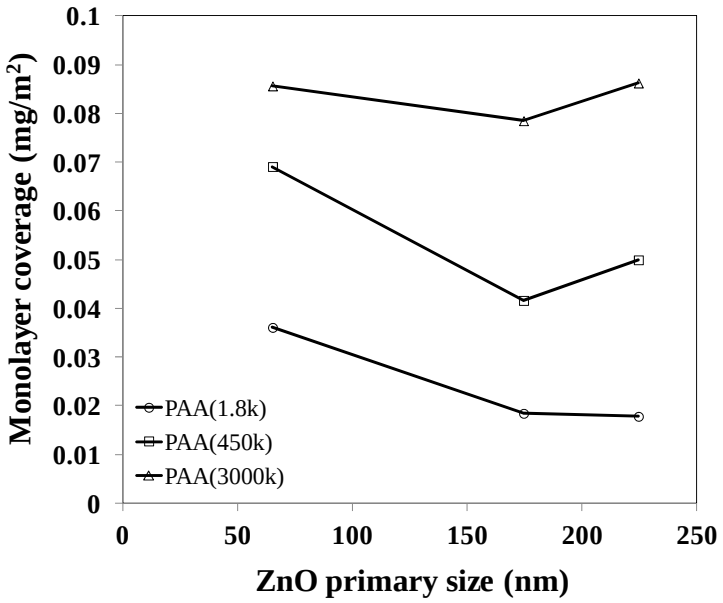

Fig. 4.15 The monolayer coverage of PAA adsorbed on ZnO primary sizes of;

(a) 65.31 nm, (b) 174.56 nm and (c) 224.54 nm.

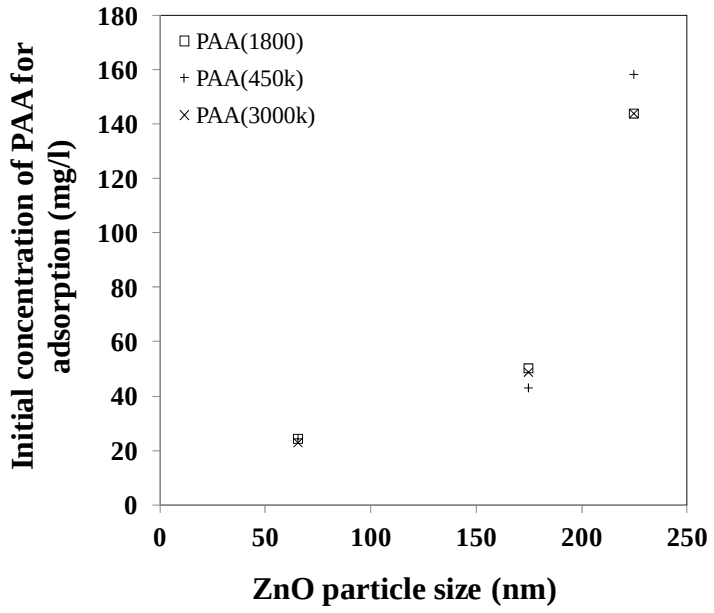

Fig. 4.16 The initial concentration of PAA for adsorption on ZnO primary sizes of;

(a) 65.31 nm, (b) 174.56 nm and (c) 224.54 nm.

Adsorption data are plotted in the form of equation (12) as shown in Fig.4.17(a,b,c) for suspensions of ZnO 65.31, 174.56 and 224.54 nm, respectively. Then, slopes and intercepts are evaluated. Since slope is determined as the area occupied per molecule of PAAs on various ZnO sizes can be calculated and shown in Table 4.3. It can be seen that area occupied per molecule of PAAs increases as ZnO size increases, especially for PAA(1.8k). The results suggest that PAA adsorbed on large particle surface as loops and tails. For small particle, PAA adsorbed with more tails. This result agrees with S. Yang et al. [18]. Adsorption of PAAs on the same particle size shown that area occupied per molecule of PAA on particle surface decreased with the increasing PAA molecular weight. It suggests that adsorbed polymer conformation turns to be more tails as molecular weight increases. The result is more pronounce with larger particle sizes due to considerable differences in adsorbed conformation of PAA with various molecular weights. The results suggest conformation of adsorbed polymer, which explain the difference in monolayer coverage density.

From the results, it is clearly shown that the conformation of adsorbed polymers is the main factor influencing dispersant efficiency. The results suggested that PAA(1.8k) adsorbed as loops and tails more than PAA(450k) and PAA(3000k). In addition, tail length is not too long due to low molecular weight. Thus, PAA(1.8k) provides electrosteric stabilization, separating particles from each others, and leading to highly stable suspension. On the other hand, high molecular weight, long chain PAA(450k) and PAA(3000k) mostly adsorb as tails. Extremely long tails of the polymers could lead to chain entanglement, bringing particles together and reducing dispersant efficiency of the polymers.

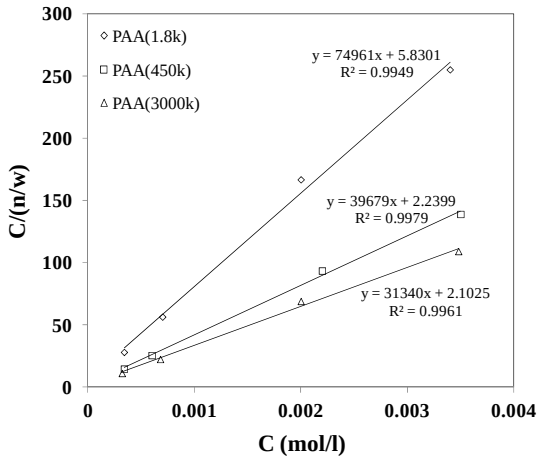

(a)

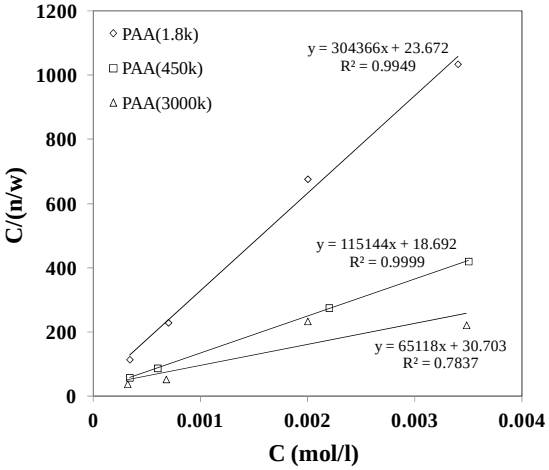

(b)

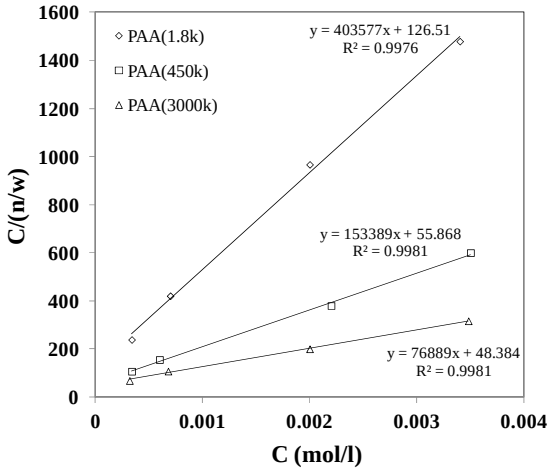

(c)

Fig. 4.17 Langmuir isotherm by equation (12) of suspensions prepared with ZnO primary sizes of; (a) 65.31 nm, (b) 174.56 nm and (c) 224.54 nm using PAAs of various molecular weights.

Table 4.3 Area occupied per molecule PAA on ZnO surface

Size / MW of PAA	Area occupied per molecule (nm^2/molecule)		
	ZnO 65.31 nm	ZnO 174.56 nm	ZnO 224.54 nm
PAA(1.8k)	3.02	12.25	16.24
PAA(450k)	1.60	4.63	6.17
PAA(3000k)	1.26	2.62	3.09

4.3. Synthesis and characterization of ZnO nanoparticles

4.3.1. XRD patterns

XRD patterns of ZnO synthesized by precipitation method are shown in Fig.4.18. Patterns of the batch using PAA and without PAA are similar. All diffraction peaks of ZnO are matched and confirmed to be a crystalline material with hexagonal structure of the wurtzite in all cases. These peaks correspond to the crystal planes of (100), (002), (101), (102), (110), (103), (200), (112), (201) and (004), respectively [46]. Miller indices (h k l) of each peak are reported in JCPDS card (No.00-036-1451) shown in Appendix B. The XRD patterns of other synthesized ZnO are shown in Appendix D.

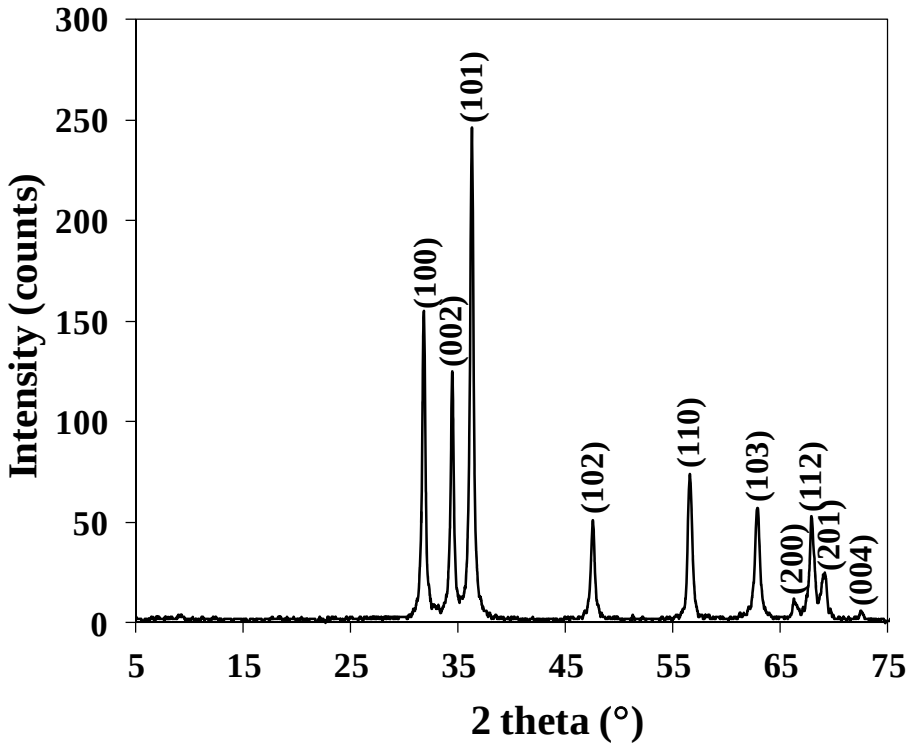

Fig. 4.18 XRD pattern of ZnO synthesized without PAA by precipitation method.

4.3.2. FTIR spectra

The FTIR spectra of PAA is shown in Fig.4.19(a). The broad band at 3485 cm^{-1} is due to stretching of OH groups. The strong band at 1580 cm^{-1} indicates –C=O vibration for carboxylic acids. The band at 1380 cm^{-1} is due to C-O stretching vibration for carboxylic acids. The FTIR spectrum of ZnO synthesized without using PAA is shown in Fig.4.19(b). A broad band is displayed at 3470 cm^{-1}, which may be attributed to OH groups on the surface. The adsorption band at 1600 cm^{-1} is due to the presence of moisture in the sample. The intense band in the vicinity of 400 – 600 cm^{-1} is due to Zn-O vibration. The spectra of ZnO synthesized using PAA is in Fig.4.19(c). The peak at 3470 cm^{-1} observed in free ZnO now appears at 3480 cm^{-1} with stronger and broader adsorption band, possibly indicating interaction through hydrogen bonding between the

hydroxylated ZnO surface and PAA [23, 52]. The bands at 1580 and 1380 cm^{-1} in free PAA due to COO^- stretching are slightly shifted to 1585 and 1380 cm^{-1} for ZnO with PAA, which might indicate chemical interaction between the ZnO surface and PAA.

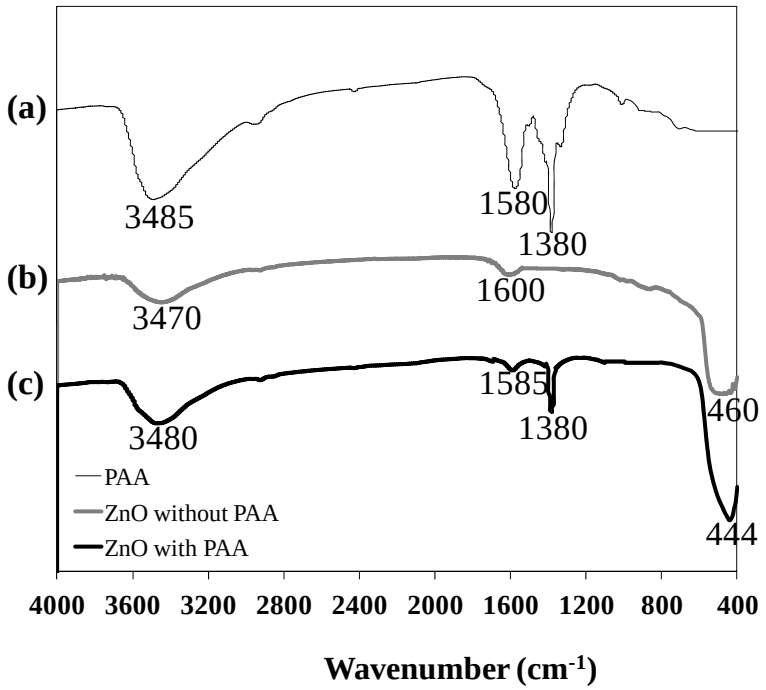

Fig. 4.19 FTIR spectra of; (a) PAA, (b) ZnO synthesized without PAA and (c) ZnO synthesized using 0.05 wt% PAA(1.8k).

4.3.3. Transmission electron microscopy (TEM)

The morphology and primary size of the synthesized ZnO nanoparticles can be observed in the TEM micrographs in Fig.4.20. The morphology of all synthesized ZnO nanoparticles is nearly spherical. ZnO synthesized without PAA exhibits large primary size with average particle size of 43.14 nm. With PAA addition as well as an increase in PAA concentration and molecular weight, the primary sizes of synthesized nanoparticles clearly decrease. Average primary sizes are evaluated from TEM images.

Particle size distributions of primary sizes are shown in Fig.4.21-4.24. It is clearly seen that synthesized ZnO nanoparticles without PAA show board distribution with sizes between 20-90 nm with average size of 43.14 nm as shown in Fig.4.21. Increasing of PAA concentration and molecular weight narrow the distribution and shift the size to smaller particles as shown in Fig.4.22-4.24. At 0.05, 0.5 and 1 wt% PAA(1.8k) (Fig.4.22), particles are in the ranges of 30-65 , 20-55 and 20-45 nm, with average particle sizes of 44.29, 30 and 22.71 nm, respectively. For PAA(450k), particles are in the range of 20-55 nm at 0.05 wt% dispersant and shifts to 15-25 nm at 1 wt% (Fig.4.23). Average particle sizes of 36.29, 20.43 and 24 nm can be obtained with 0.05, 0.5 and 1 wt% PAA(450k), respectively. With PAA(3000k), particles are in ranges of 20-45 nm and shift to 15-55 nm at 1 wt% (Fig.4.24). Average particle sizes of 30, 13 and 18.86 nm can be obtained with 0.05, 0.5 and 1 wt% PAA(3000k). It is note that the differences in average particle size are not obvious and the standard deviations are high. However, the particle size distributions clearly show the alteration in ZnO sizes, which can be controlled by using various PAAs in the synthesize process. It is clearly showed that the addition of polymer additive decreased particle size of synthesized powder in precipitation method. Moreover, size of nanoparticles with narrow particle size distribution can be controlled by concentration and molecular weight of the dispersant.

Comparing to ZnO particles synthesis from the same reactant solutions and PAA(M_W = 2000) and Dispex A40(commercial PAA, M_W = 10000) as dispersants, however, using hydrothermal process [46], our process provides smaller size ZnO particles. The previous report using hydrothermal process shows homogeneous, roundish ZnO particles around 100-135 nm while our particles are 10-40 nm. The obtained ZnO particles are comparable in size and shape to those synthesized by precipitation method using different reactants and surfactants including Sodium dedecyl soulfonate (SDS) [44] and polyethylene glycol (PEG) [41].

Effects of PAA on controlling of ZnO particle size can be explained as follow. The ZnO synthesis process by this precipitation method is slowly precipitating

from solution. The precipitation process starts from nuclei formation follows by nuclei growth [53]. At pH of investigation (around 7-8), PAA dissociates producing COO^- groups, which can adsorb on ZnO surface. Once the nuclei are formed, adsorbed PAA blocks crystalline growth and also prevents particle agglomeration [44]. From the results, it can be indicated that higher PAA concentration can block crystalline growth and prevent agglomeration better, which lead to small primary size and better particle dispersion. Comparing among PAA of various molecular weights, long chain PAA(3000k) with more COO^- groups could be adsorbed better than lower molecular weight PAA. Thus, longer chain length shows higher efficiency in blocking crystalline growth and provides better particle agglomeration, which leads to smaller particle size of synthesized ZnO.

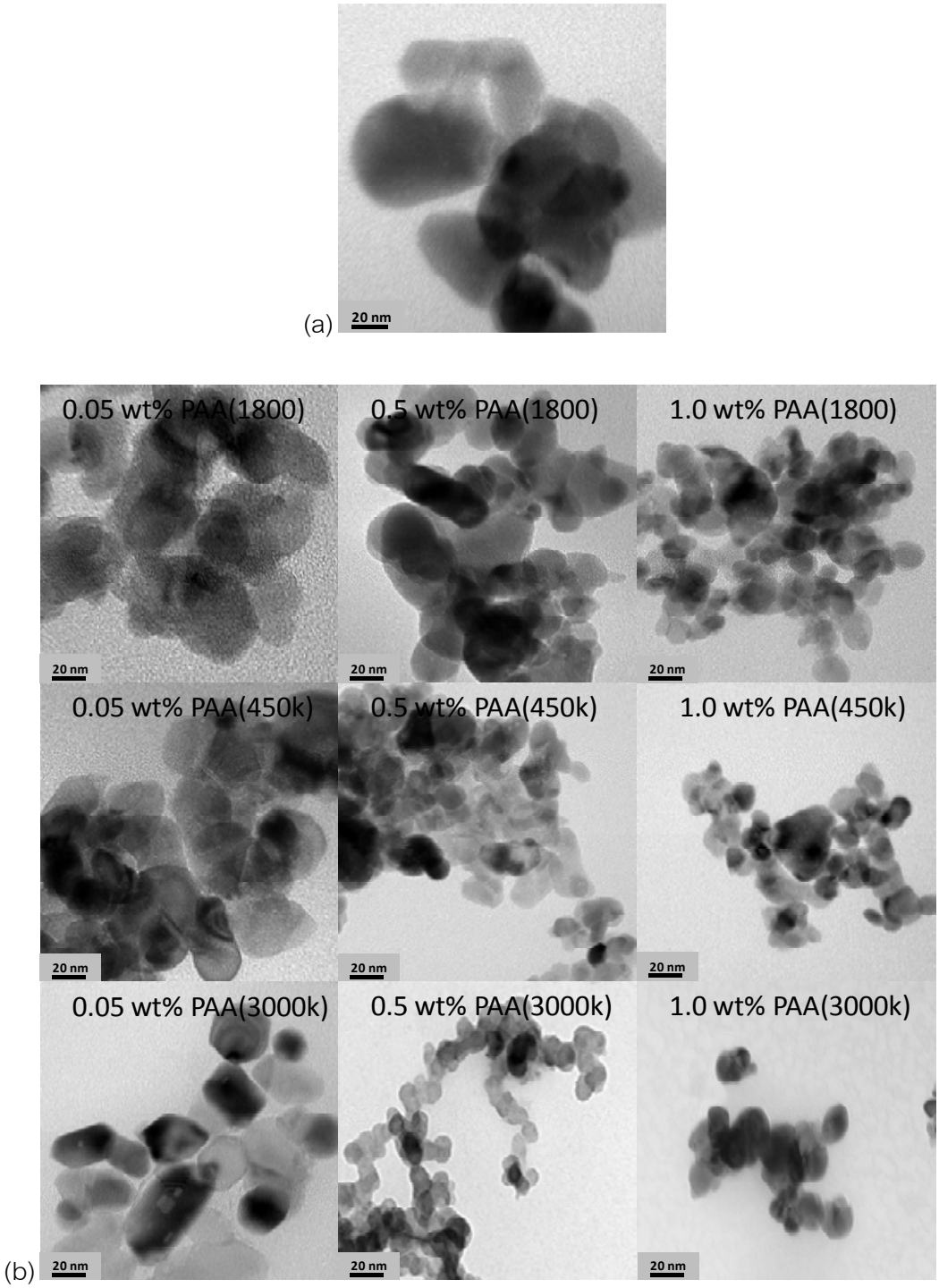

Fig. 4.20 TEM micrographs of ZnO synthesized using PAAs at various concentrations.

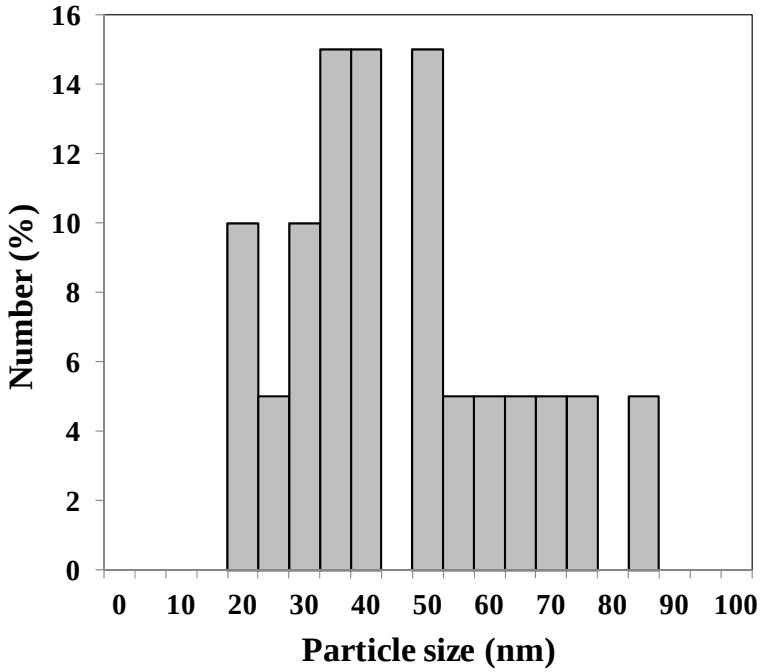

Fig. 4.21 Particle size distribution of ZnO synthesized without PAA.

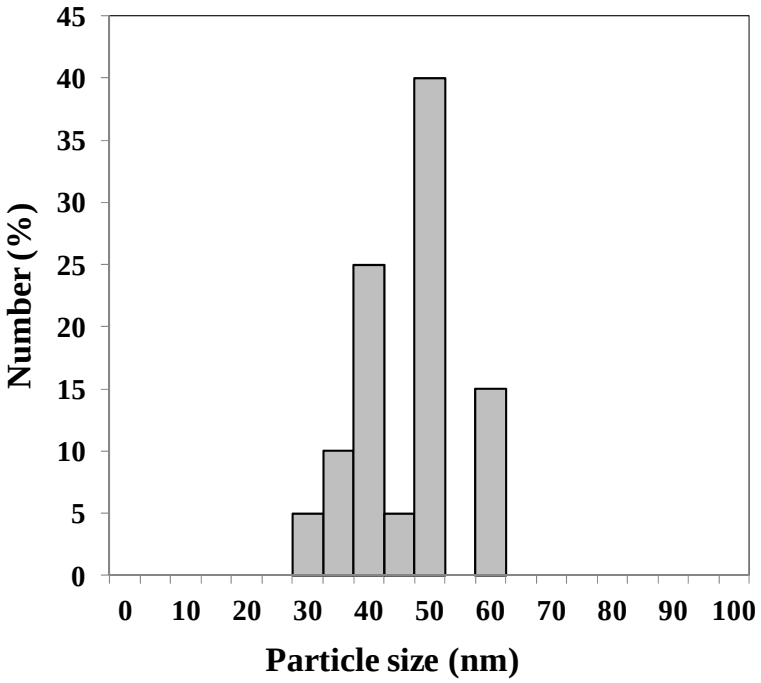

(a)

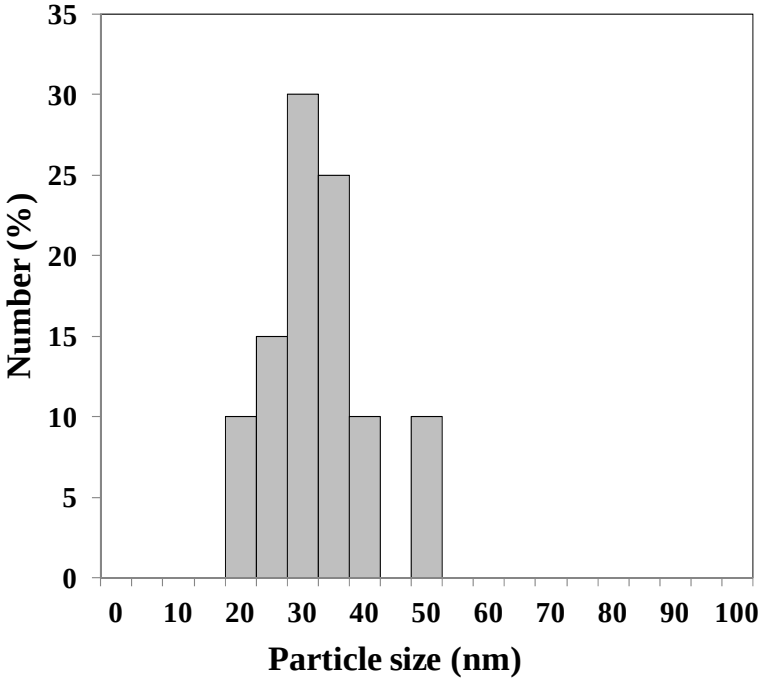

(b)

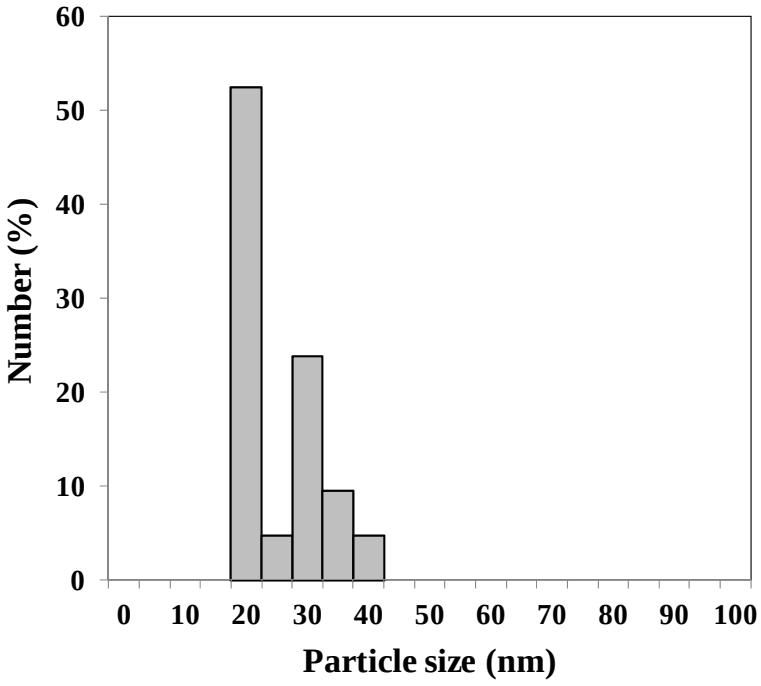

(c)

Fig. 4.22 Particle size distribution of ZnO synthesized using PAAs; (a) 0.05 wt% PAA(1.8k), (b) 0.5 wt% PAA(1.8k) and (c) 1 wt% PAA(1.8k).

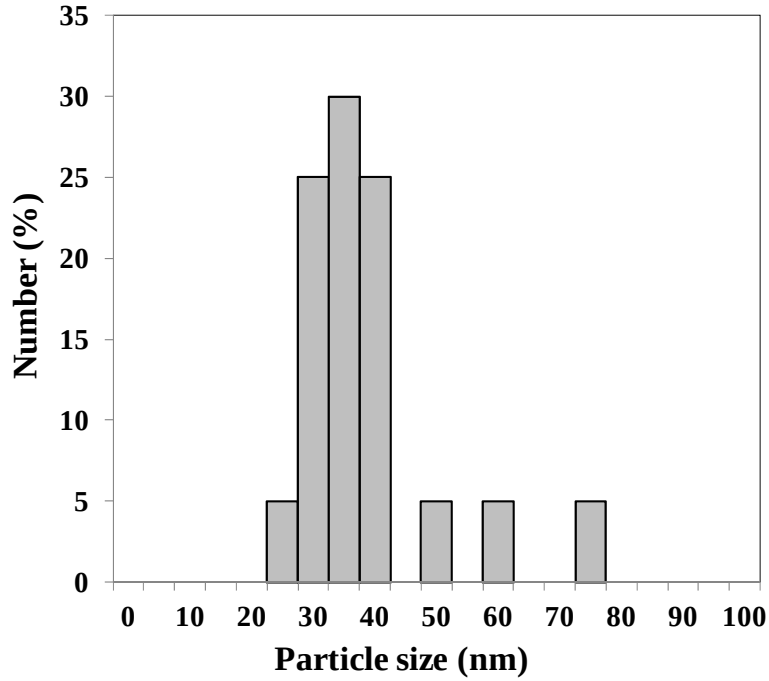
35
30
25
20
15
10
5
0
Number (%)
0 10 20 30 40 50 60 70 80 90 100
Particle size (nm)

(a)

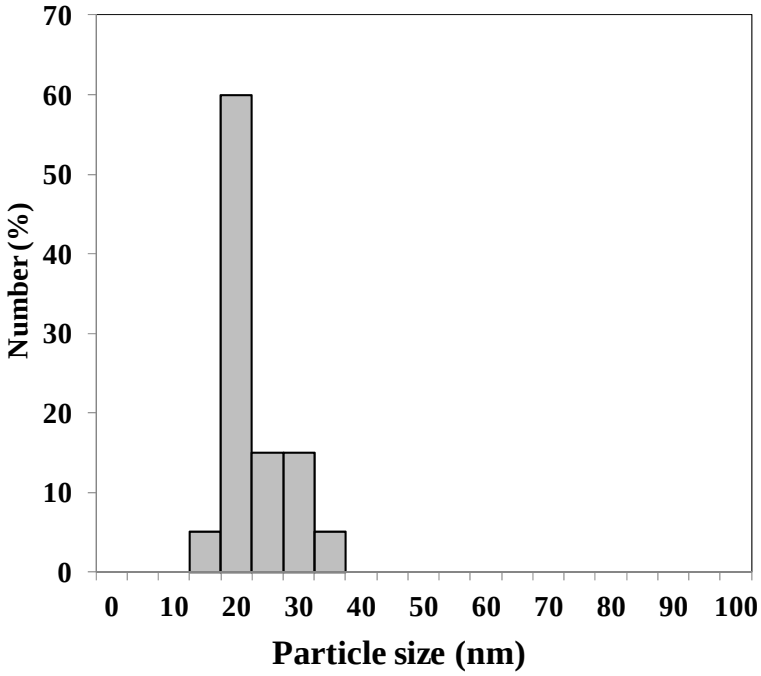
70
60
50
40
30
20
10
0
Number (%)
0 10 20 30 40 50 60 70 80 90 100
Particle size (nm)

(b)

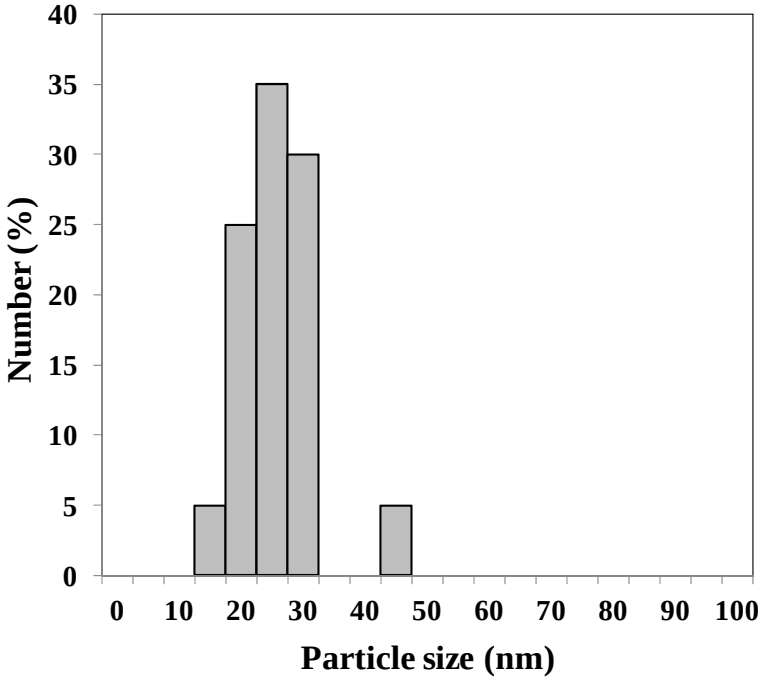

(c)

Fig. 4.23 Particle size distribution of ZnO synthesized using PAAs; (a) 0.05 wt% PAA(450k), (b) 0.5 wt% PAA(450k) and (c) 1 wt% PAA(450k)

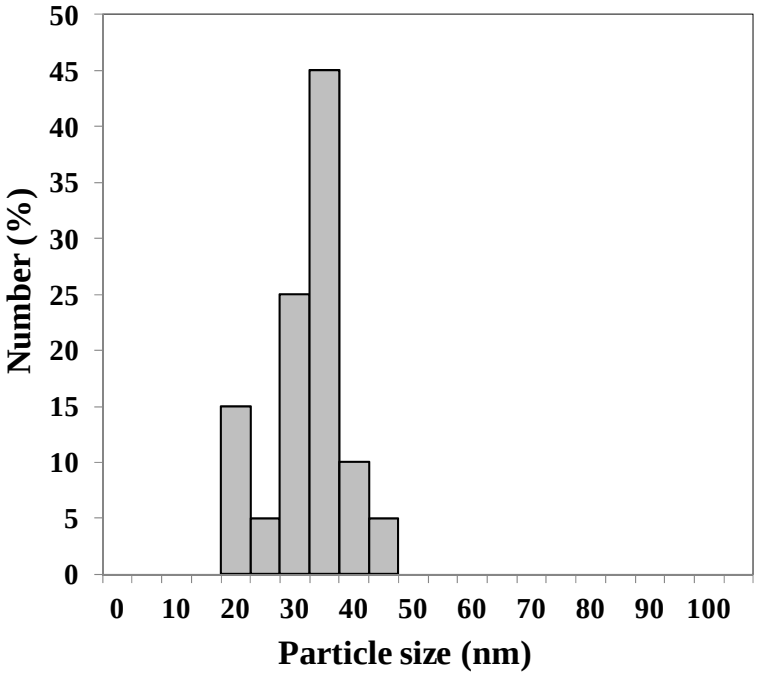

(a)

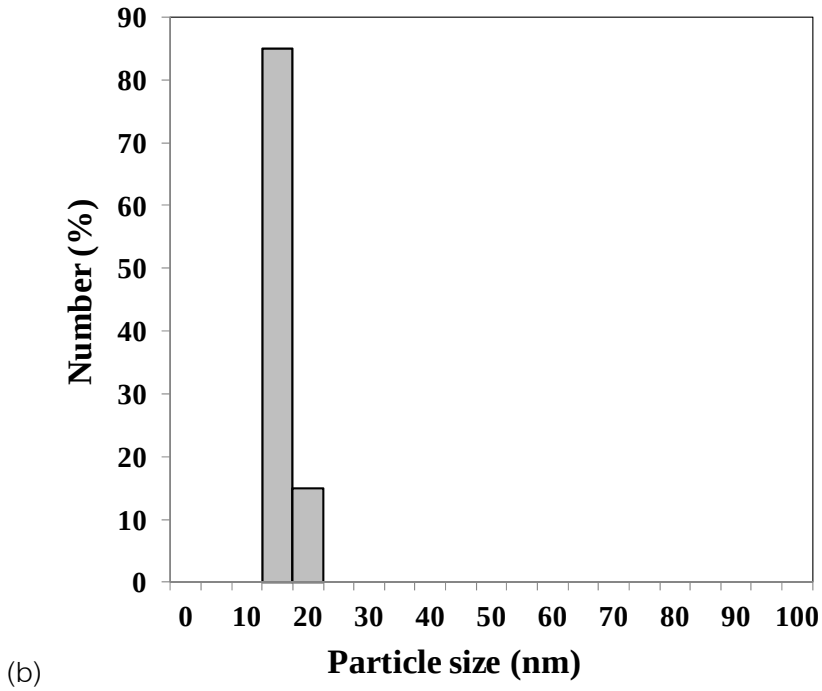

(b)

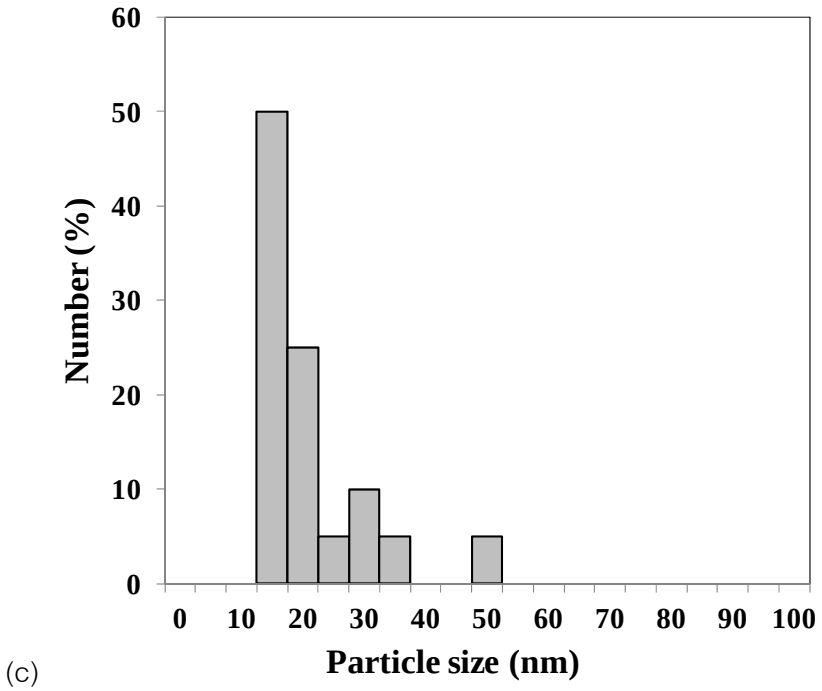

(c)

Fig. 4.24 Particle size distribution of ZnO synthesized using PAAs; (a) 0.05 wt% PAA(3000k), (b) 0.5 wt% PAA(3000k) and (c) 1 wt% PAA(3000k).

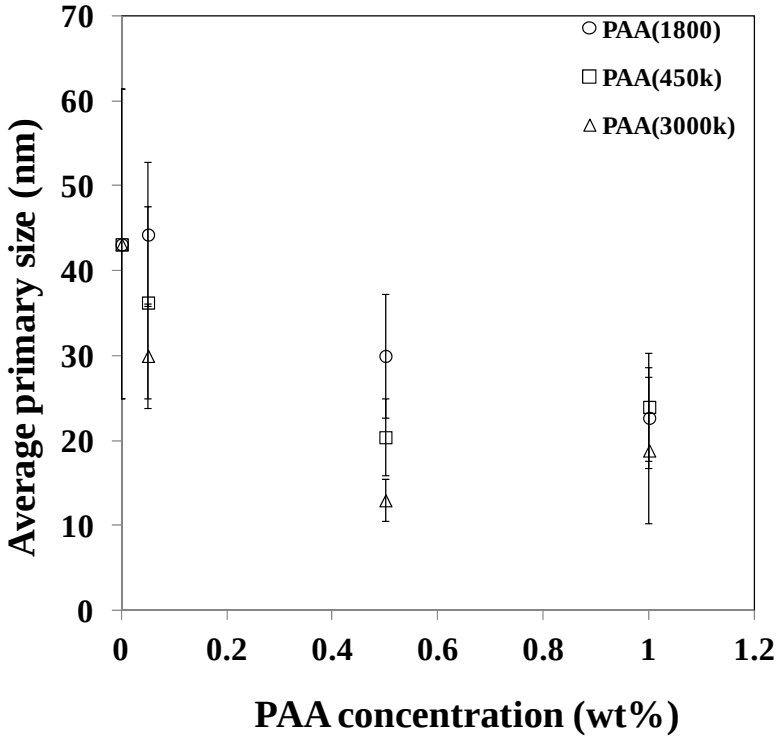

Fig. 4.25 The average primary size of ZnO synthesized using various PAA concentrations and molecular weights.

4.3.4. Specific surface area (BET)

The specific surface areas of ZnO synthesized with various PAA concentrations and molecular weights are shown in Table 4.5. It can be seen that specific surface area increases with the increasing PAA concentration and molecular weight. Since smaller particle sizes exhibit higher specific surface area than larger particles, results of specific surface area agree with primary size reported above.

Table 4.4 The specific surface area of ZnO synthesized with various PAAs.

wt%	Specific surface area (m^2/g)		
	PAA(1800)	PAA(450k)	PAA(3000k)
0	7.47	7.47	7.47
0.05	8.55	10.74	26.13
0.5	13.78	28.30	29.05
1	35.55	43.20	49.20

4.3.5. Zeta potential

Theoretically, zeta potential value indicated repulsive potential energy between particles. The magnitude of zeta potential exhibits surface charge and potential stability of particles in suspension. If all particles have a large negative or positive zeta potential, particles possess high repulsive force, which leads to long distance between particles and a well-dispersed suspensions [5, 15]. The pH of ZnO synthesized with various PAA molecular weights and concentrations when dispersed in aqueous suspension is shown in Table 4.6. Fig.4.26 shows zeta potential values of ZnO aqueous suspensions without pH adjusting. It can be seen that all ZnO particles exhibit positive surface charge, which is common at the observing pH around 7.5-8, which is lower than pH_{iep} of ZnO at 8.6 [31]. Zeta potential values of ZnO particles synthesized with various PAAs is shown in Table 4.7. It is shown that the zeta potential values increase with increasing PAA concentration. This could be due to the size effects on zeta potential. For smaller size, there is higher ion density surrounded the particle, leading to higher surface charge or higher zeta potential value comparing to large size [54]. The effect is much more pronounced when particle size decreases to less than 20 nm. Using 0.5-1

wt% PAA shifts most of the particle to the size around 20 nm and smaller, therefore, zeta potential values of those ZnO increases to 25 mV and higher. The result suggests that ZnO particles synthesized using 0.5-1 wt% PAAs should be well-dispersed in aqueous medium and provide a highly stable suspension, which is desired for most applications.

Table 4.5 pH values of synthesized ZnO in water

wt%	pH value		
	PAA(1.8k)	PAA(450k)	PAA(3000k)
0	8.21	8.21	8.21
0.05	7.56	7.61	7.77
0.5	7.42	7.86	7.78
1	7.67	7.99	7.89

Table 4.6 Zeta potential values of synthesized ZnO with various PAAs.

wt%	Zeta potential value (mV)		
	PAA(1.8k)	PAA(450k)	PAA(3000k)
0	10.40	10.40	10.40
0.05	15.34	19.97	20.70
0.5	24.70	24.78	26.23
1	26.65	27.23	28.13

To investigate the isoelectric point (IEP) of the synthesized ZnO particles, zeta potential as a function of pH are measured and illustrated in Fig. 4.27. For all synthesizing conditions, surface charge of ZnO is indicated as positive at pH <9 and negative at pH >9. ZnO particles synthesized with PAA exhibit higher zeta potential values both in positive and negative regions than the one synthesized without PAA. Using PAAs in synthesis process also shifts pH_{iep} of ZnO from 9 to the higher values. Therefore, in the region away from IEP, ZnO particles synthesized with PAA dispersants tend to disperse better in aqueous medium due to higher electrostatic force comparing to the one synthesized without PAA.

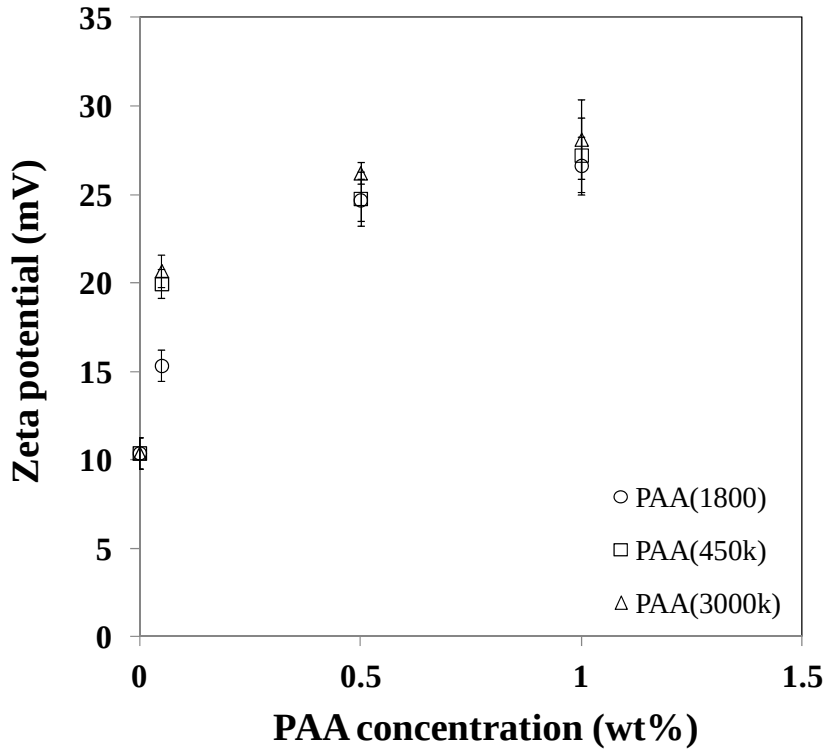

Fig. 4.26 Zeta potential value of ZnO synthesized with various PAA concentrations and molecular weights.

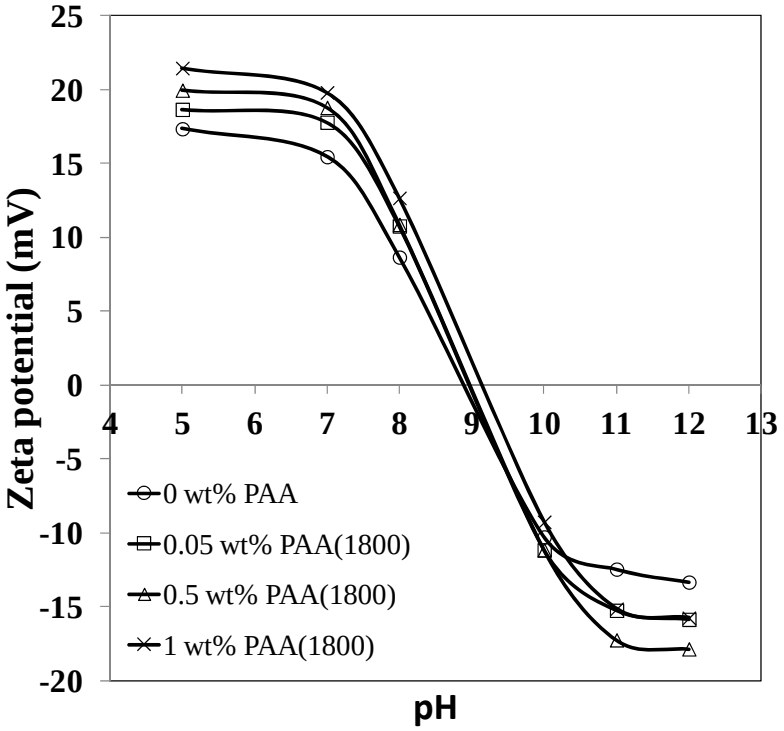
Zeta potential (mV)
25
20
15
10
5
0
-5
-10
-15
-20
4
5
6
7
8
9
10
11
12
13
pH
0 wt% PAA
0.05 wt% PAA(1800)
0.5 wt% PAA(1800)
1 wt% PAA(1800)

(a)

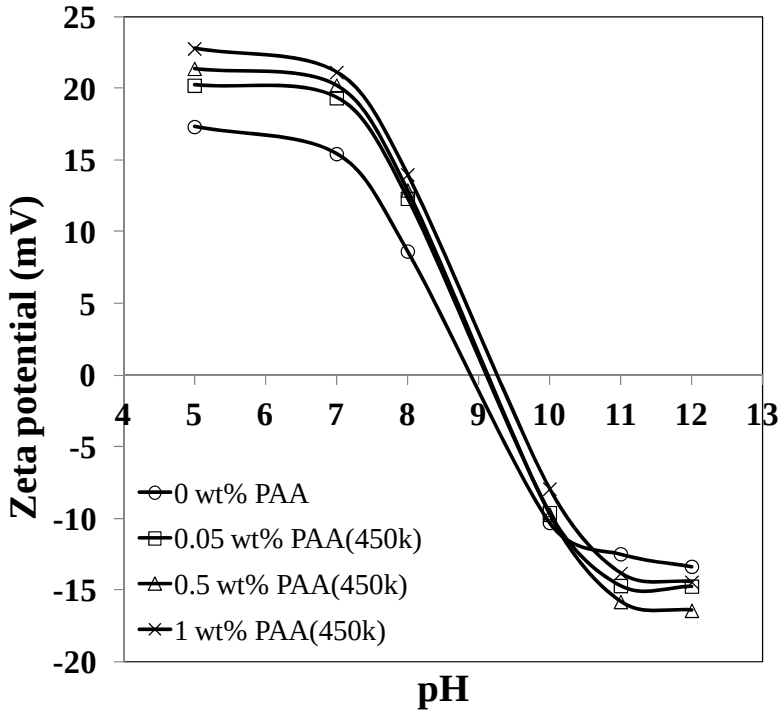
Zeta potential (mV)
25
20
15
10
5
0
-5
-10
-15
-20
4
5
6
7
8
9
10
11
12
13
pH
0 wt% PAA
0.05 wt% PAA(450k)
0.5 wt% PAA(450k)
1 wt% PAA(450k)

(b)

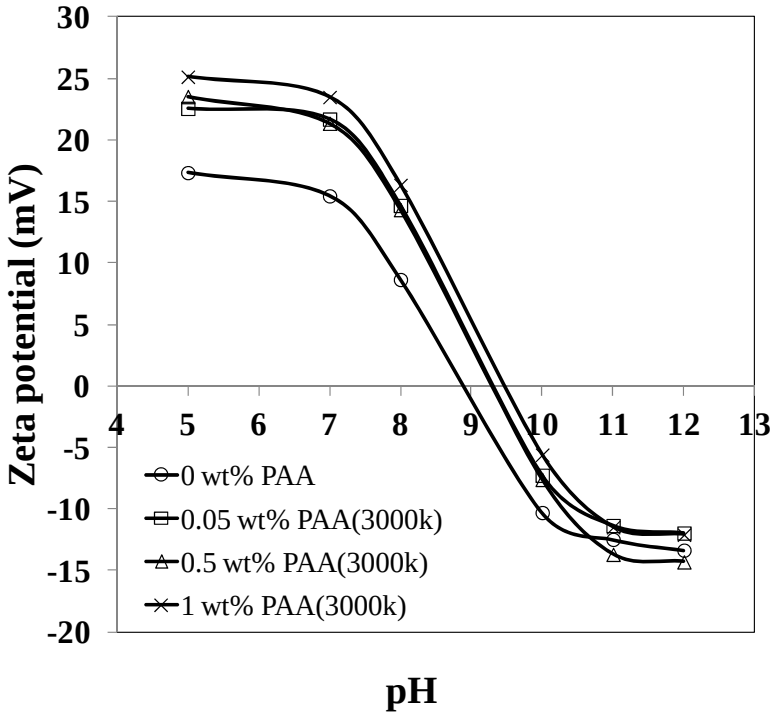

(C)

Fig. 4.27 Zeta potential value of ZnO synthesized with difference pH (a) PAA(1.8k), (b) PAA(450k) and (c) PAA(3000k).

4.3.6. Particle dispersion via Optical microscopy (OM)

OM images of synthesized ZnO particles dispersed in aqueous suspensions are shown in Fig.4.28. ZnO particles synthesized without PAA in Fig.4.28(a) show large agglomeration. Addition of PAAs in synthesis process decreases agglomerate size of nanoparticles and promoted particle dispersion as shown in Fig.4.28(b). Particles synthesized using PAA with higher concentrations exhibit better particle dispersion. This could be explained based on zeta potential results that show an increase in zeta potential value with increasing PAA concentration. Therefore, particles synthesized with 1 wt% PAAs are well-dispersed in aqueous medium due to high electrostatic repulsion between particles. On the other hand, particles synthesized

without PAA and with 0.05 wt% PAA(1.8k) are highly agglomerated due to low zeta potential of <20 mV.

(a)

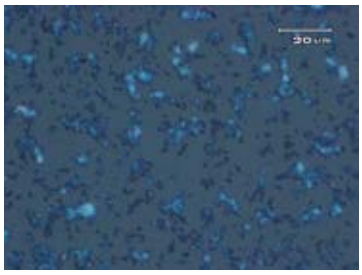

(b)

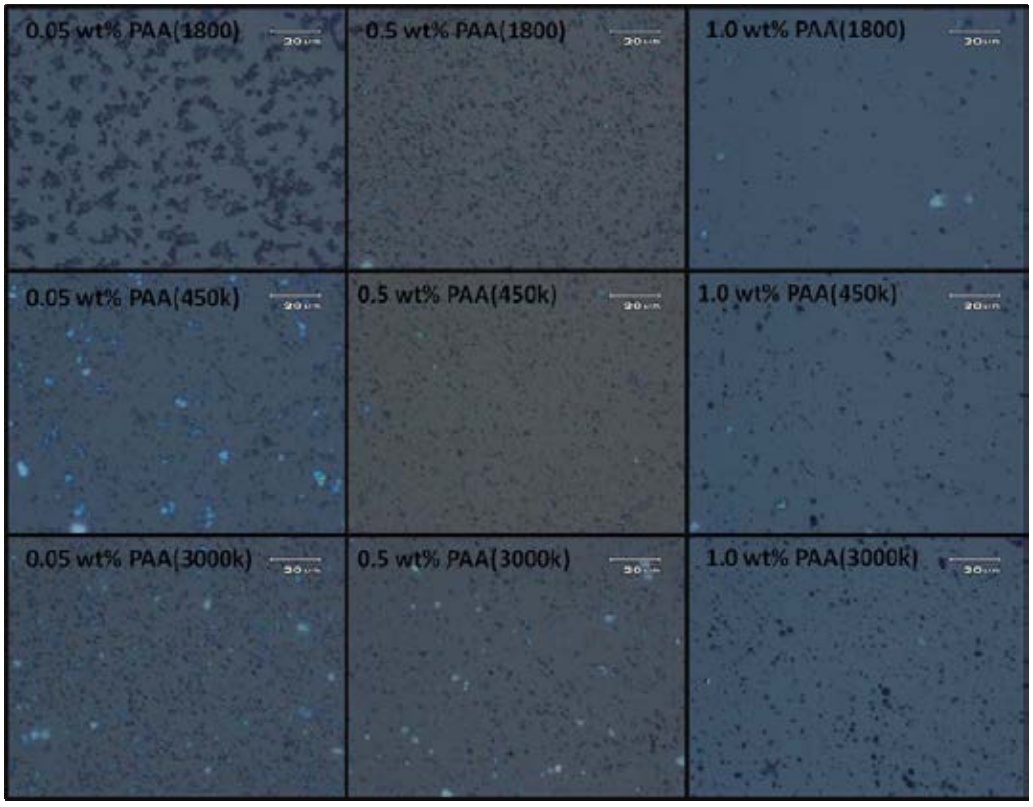

Fig. 4.28 OM images of ZnO particles synthesized (a) without PAA and (b)using PAAs of various molecular weights and concentrations as dispersant.

4.3.7. Particle size distribution of ZnO in suspension

Particle size distributions of synthesized ZnO particles in aqueous suspensions are shown in Fig.4.29. ZnO synthesized without PAA shows board size distribution of agglomerate sizes in the range of 0.5-100 μm . Addition of PAA(1.8k) (Fig.4.29(a)) decreases agglomerate size and increase volumes of small particles. At 1 wt% PAA(1.8k), most of the particles are smaller than 10 μm. PAA(450k) and PAA(3000k) provide similar effects (Fig. 4.29 (b, c)). The amount of large agglomerations decreases as PAA concentration increases.

Fig.4.30 shows the median agglomerate size of ZnO synthesized with various PAA concentrations and molecular weights. It can be seen that median agglomerate sizes of ZnO synthesized without PAA is 6.63 μm. With the increasing PAA concentration, the median size decreases for all molecular weights. The median sizes of 5.83, 6.32 and 6.38 μm are shown for 0.5 wt% of PAAs 1.8k, 450k and 3000k, respectively.. The minimum agglomerate sizes of 1.59, 2.0 and 2.55 μm can be obtained with 1 wt% of PAAs 1.8k, 450k and 3000k, respectively. Results are in agreement with zeta potential of particles synthesized by various concentrations and molecular weights of PAA. Without using PAA, particles show low zeta potential indicating low electrostatic repulsion between particles, leading to particle agglomeration. Particles synthesized with PAAs at concentrations of 0.5-1 wt% exhibit high zeta potential, resulting in high repulsive force between particles. In addition, adsorbed PAA chains could also provide steric stabilization, improving particle dispersion in the suspension. However, effects of PAA molecular weight on dispersion of synthesized ZnO nanoparticles are not clearly observed.

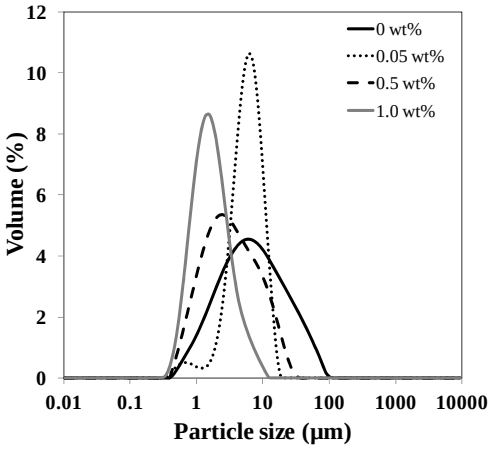

(a)

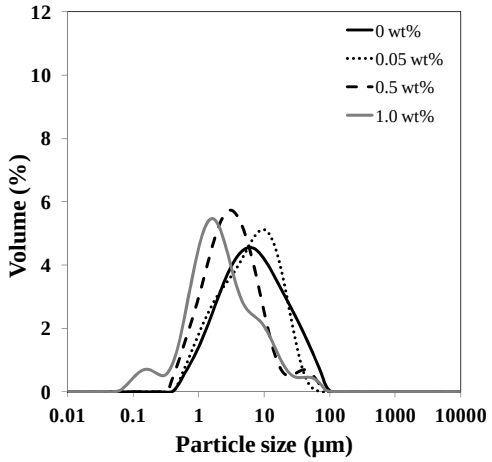

(b)

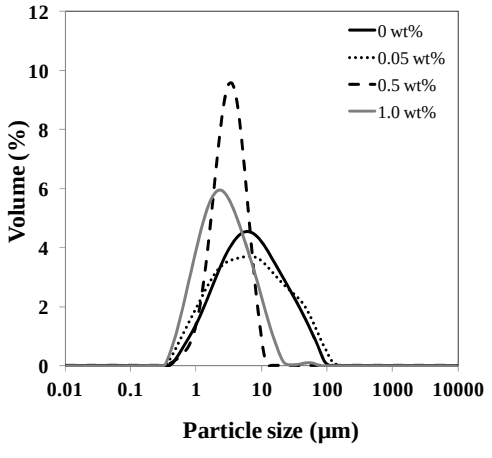

(c)

Fig. 4.29 Particle size distribution of ZnO synthesized with various concentrations of PAA; (a) PAA(1.8k), (b) PAA(450k) and (c) PAA(3000k).

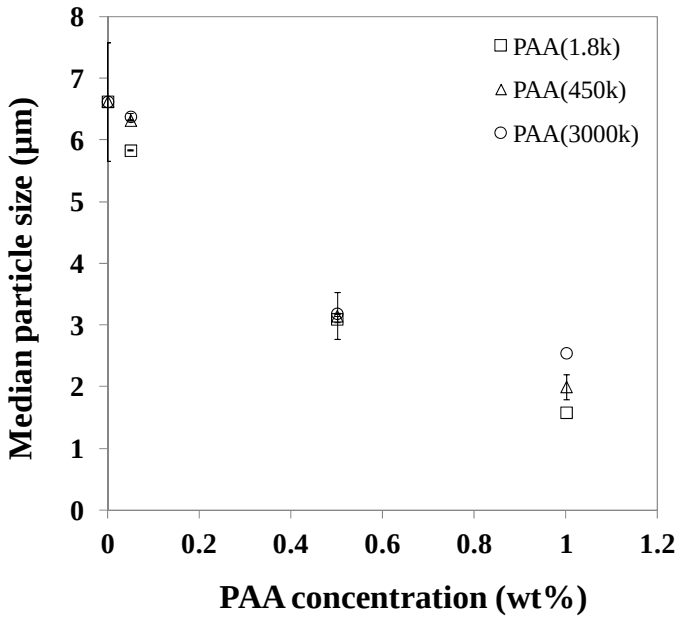

Fig. 4.30 The median particle size of ZnO synthesized with various PAA concentrations and molecular weights.

CHAPTER 5
CONCLUSIONS

5.1. Preparation and characterization of ZnO nanoparticle aqueous suspensions using various ZnO particle sizes and PAA molecular weights

(1) Addition of PAA as a dispersant in aqueous suspensions of ZnO nanoparticles promotes particle dispersion and stability of the suspension. Agglomerate size decreases with the increasing PAA concentrations for all molecular weights.

(2) Low molecular weight, short chain PAA(1.8k) is an effective dispersant for suspension of all ZnO sizes. Well-dispersed and highly stable suspensions can be produced with PAA(1.8k) at low concentration of 0.5 wt%.

(3) PAA(450k) can be used as a dispersant for suspensions of all ZnO sizes when using at high concentration of 3-5 wt%. Better particle dispersion is obtained for 174.56 and 224.54 nm-ZnO suspensions with 5 wt% PAA(450k) comparing to PAA(1.8k).

(4) High molecular weight, long chain PAA(3000k) can be used at high concentration of 5 wt% to disperse particles of 174.56 and 224.54 nm-ZnO suspensions. However, it is an inefficient dispersant for 65.31 nm-ZnO suspension.

(5) Addition of PAAs shifts zeta potential of ZnO from positive to negative values due to adsorption of COO^- groups on the ZnO surface. Addition of PAA(1.8k) provides higher zeta potential values than in the cases of PAA(450k) and PAA(3000k), which indicates stronger electrosteric stabilization. .

(6) FTIR spectra indicate adsorption of PAA on ZnO surface via interaction of COO^- with ZnO surface .

(7) Adsorption of PAA on the ZnO surface exhibits Langmiur isotherm. The adsorbed amounts of PAA increase with the increasing PAA concentrations for all ZnO sizes due to an increase in competitive adsorption. .

(8) Monolayer coverage of PAA on ZnO surface is higher with the longer chain PAA due to longer loop and tail lengths comparing to the shorter chain PAA.

(9) Area occupied per molecule of PAA on ZnO surface is evaluated. The results suggest that PAA adsorbs on large particles as loops and tails while mostly tails are formed on small particles.

5.2. Synthesis of ZnO nanoparticles by precipitation method using PAA of various molecular weights

(1) XRD patterns show that all synthesized ZnO particles obtained by precipitation method are hexagonal structure of the wurtzite

(2) FTIR results confirm the existence of PAA on ZnO particles synthesized using PAA as an additive.

(3) TEM images illustrate that all synthesized ZnO nanoparticles is nearly spherical.

(4) A board size distribution with average primary size of 43.14 nm is obtained for ZnO synthesized without PAA. Addition of PAA as well as an increase in PAA concentration and molecular weight significantly narrows size distribution and decreases primary size of ZnO particles. Average size of <20 nm can be obtained with PAA(3000k). This is due to prevention of crystalline growth by PAA adsorbed on ZnO surface.

(5) Specific surface area increases with increasing PAA concentration and molecular weight due to Primary particle size decreases.

(6) Synthesized ZnO particles exhibit positive surface charge. The zeta potential value of ZnO particles increase with increasing PAA concentration.

(7) Using PAAs in the synthesis process shifts pH_{iep} of ZnO from 9 to the higher values.

(8) ZnO particles synthesized using high concentrations of PAAs are well-dispersed in aqueous medium due to high repulsive interaction between particles.

REFERENCES

[1] Liufu, S.C. Xiao, H.N. and Li, Y.P. Effect of MA-Na copolymer adsorption on the colloidal stability of nano-sized ZnO suspension. Materials Letters. 59 (2005) : 3493-3497.

[2] Singh, B.P., Jena, J., Besra, L. and Bhattacharjee, S. Dispersion of nano-silicon carbide (SiC) powder in aqueous suspensions. Journal of Nanoparticle Research. 9 (2007) : 797-806.

[3] Paul, B., Claude, C., David, L. and Heinrich, H. Colloidal processing and sintering of nanosized transition aluminas. Powder Technology. 157 (2005) : 100-107.

[4] Lewis, J.A. Colloidal Processing of Ceramics. Journal of the American Ceramic Society. 83 (10) (2000) : 2341-2359.

[5] Srilomsak, S. Stabilization of Ceramic Slips I. Suranaree Journal of Science and Technology. 13 (3) (2006) : 259-270.

[6] Hackley, V.A. Colloidal processing of silicon nitride with poly(acrylic acid): I, adsorption and electrostatic interactions. Journal of the American Ceramic Society. 80 (1997) : 2315-2325.

[7] Kirby, G. H., Harris,D. J., Li, Q. and Lewis, J. A. Poly(acrylic acid)-poly(ethylene oxide) comb polymer effects on BaTiO3 nanoparticle suspension stability. Journal of the American Ceramic Society. 87(2) (2004) : 181-186.

[8] Das, K. K. and Somasundaran, P. Ultra-low dosage flocculation of alumina using polyacrylic acid. Colloids and Surfaces A: Physicochemical and Engineering Aspects. 182(1-3) (2001) : 25-33.

[9] Das, K. K. and Somasundaran, P. Flocculation-dispersion characteristics of alumina using a wide molecular weight range of polyacrylic acids. Colloids and Surfaces A: Physicochemical and Engineering Aspects. 223(1-3) (2003): 17-25.

[10] Liufu, S., Xiao, H. and Li, Y. Adsorption of poly(acrylic acid) onto the surface of titanium dioxide and the colloidal stability of aqueous suspension. Journal of Colloid and Interface Science. 281(1) (2005) : 155-163.

[11] Santhiya, D., Nandini, G., Subramanian, S., Natarajan, K. A. and Malghan, S. G. Effect of polymer molecular weight on the adsorption of polyacrylic acid at the alumina-water interface. Colloids and Surfaces A: Physicochemical and Engineering Aspects. 133(1-2) (1998) : 157-163.

[12] Jeon, S. J. and Hong, W. H. Effects of poly(acrylic acid) and poly(ethylene oxide) adsorption on the stability of alumina suspension. Korean Journal of Chemical Engineering. 20(5) (2003) : 916-921.

[13] Delaat, A. W. M., Vandenheuvel, G. L. T. and Bohmer, M. R. Kinenic aspects in the adsorption of polyacrylic acid salts onto $BaTiO_3$. Colloids and Surfaces a-Physicochemical and Engineering Aspects. 98(1-2) (1995).: 61-71.

[14] Dange, C., Phan, T. N. T. Andre, V., Rieger, J., Persello, J. and Foissy, A. Adsorption mechanism and dispersion efficiency of three anionic additives poly(acrylic acid), poly(styrene sulfonate) and HEDP on zinc oxide. Journal of Colloid and Interface Science. 315(1) (2007) : 107-115.

[15] Zhao, J., Wang, X., Chen, R. and Li, L. Dispersion of barium titanate in aqueous media. Ceramics International. 33(2) (2007).: 207-212.

[16] Suntako, R., Laoratanakul, P. and Traiphol, N. Effects of dispersant concentration and pH on properties of lead zirconate titanate aqueous suspension. Ceramics International. 35 (2009) : 1227-1233.

[17] Fazio, S., Guzman, J., Colomer, M.T., Salomoni, A. and Moreno, P. Colloidal stability of nanosized titania aqueous suspensions. Journal of the European Ceramic Society. 28 (2008) : 2171-2176.

[18] Yang, S. and Yan, D. Structure of Adsorbed Polymers on a Colloid Particle. Macromolecules. 39(12) (2006) : 4168-4174.

[19] Wikipedia, the free encyclopedia. Zinc oxide [online]. Avaliable from: http://www.wikipedia.org/wiki/zinc oxide. [2011, Aug 1].

[20] Aimable, A., Buscaglia, M.T., Buscaglia, V. and Bowen, P. Polymer-assisted precipitation of ZnO nanoparticles with narrow particle size distributuion. Journal of the European Ceramic Society. 30 (2010) : 591-598.

[21] Nano Materials Technology co., Ltd. Zinc oxide nano [online]. Avaliable from: http://www.nanomaterials.co.th. Accessed date Aug 1, 2011.

[22] Liu, H. and Xiao, H. Adsorption of poly(ethylene oxide) with different molecular weight on the surface of silica nanoparticles and the suspension stability. Materials Letters. 62 (2008) : 870-873.

[23] Degan, A. and Kosec, M. Influence of pH and ionic impurities on the adsorption of poly(acrylic) dispersant onto a Zinc Oxide surface. Journal of the American Ceramic Society. 86 (12) (2003) : 2001-2010.

[24] Santhiya, D., Subramanian, S., Natarajan, K. A. and Malghan, S. G. Surface Chemical Studies on the Competitive Adsorption of Poly(acrylic acid) and Poly(vinyl alcohol) onto Alumina. Journal of Colloid and Interface Science. 216(1) (1999) : 143-153.

[25] Srilomsak, S. Stabilization of Ceramic Slips II. Suranaree Journal of Science and Technology. 13 (3) (2006) : 268-281.

[26] Malvern Instruments Ltd. Zeta potential An Introduction in 30 Minutes [online]. Available from: www.nbtc.cornel.edu/faclities/downloads/Zeta %20potential%20-%20An%20introduction%20in%2030%20minutes.pdf. [2012, Aug 1].

[27] Zeta-Meter Inc. Zeta potential: a complete course in 5 minutes [online]. Available from: http://www.zeta-meter.com/5min.pdf. [2012, Sep 16].

[28] Shqau, K. Electrosteric dispersants used in colloidal processing of ceramics. Center for Industrial Sensors and Measurements. (2005) : 1-17.

[29] Zhao, J., Wang, X., Chen, R. and Li, L. Dispersion of barium titanate in aqueous media. Ceramics International. 33 (2007) : 207-212.

[30] Carty, W.M. Ceramic laboratory III manual CES205 Introduction to ceramic powder processing. New York State College of Ceramics at Alfred University, p.1-35. (1998)

[31] Ying, K. L., Hsieh, T. E. and Hsieh, Y. F. Colloidal dispersion of nano-scale ZnO powders using amphibious and anionic polyelectrolytes. Ceramics International. 35 (2009) : 1165-1171.

[32] Reed, J.S. Principles of Ceramics Processing. 2nd edition. New York, John Wiley & Sons, p.137-171. (1995)

[33] Sikong, L. Engineering ceramics [online]. Available form: http://www/mne.eng.psu.ac.th/staff/lek_files/ceramic/u2-5.htm. [2012, Sep 2].

[34] Moreno, R. The role of slip additives in tape-casting technology. American Ceramic Society Bulletin. 10 (71) (1992).

[35] Cann, M.C. Thermal polyaspartate as a biodegradable alternative to polyacrylate and other currently used water soluble polymers [online]. Available from: www.tiger.uofs.edu/faculty/CANNM1/polymer/polymermodule.html. [2005, Aug 15].

[36] Heizmen, P. C. and Rajagopan, P. Principle of colloid and surface chemistry., 3rd edition, New York, Marcel Dekker, Inc., p.331-336. (1997).

[37] Malvern Instruments Ltd. Laser Diffraction [online]. Available from: http://www.malvern.com/labeng/technology/laser diffraction/laser diffraction.htm. [2012, Sep 19].

[38] Malvern Instruments Ltd. Zeta potential theory [online]. Available from: http://www/nbtc.cornell.edu/facilities/downloads/Zetasizer%20chapter%2016.pdf. [2012, Sep 17].

[39] Thermo Nicolet Co. Ltd. Introduction to Fourier Transform Infrared Spectroscopy. Available from: http://mmrc.caltech.edu/FTIR/FTIRintro.pdf. [2012, Sep 19].

[40] Larkin, P. Infrared and Raman Spectroscopy Principles and Spectral Interpretation. New York, Elsevier Inc., p.1-62. (2011).

[41] Li, J. and Barron, A. R. Fourier Transform Infrared Spectroscopy of Metal Ligand Complexes [online]. Available from: http://cnx.org/content/m34660/lastest/#id6227878. [2012, Sep 23].

[42] Wikipedia, the free encyclopedia. Microscopy [online]. Available from: http://en.wikipedia.org/wiki/Microscopy. [2012, Sep 19].

[43] Traiphol, N., Suntako, R. and Chanthornthip, K. Roles of polymeric dispersant charge density on lead zirconate titanate aqueous processing. Ceramics International. 36 (7) (2010) : 2147-2153.

[44] Tang, E., Tian, B., Zheng, E., Fu, C. and Cheng, G. Preparation of zinc oxide nanoparticle via uniform precipitation method and its surface modification by methycryloxypropyltrimethoxysilane. Chemical Engineering Communications. 195 (5) (2008) : 479-491.

[45] Hong, R., Pan, T., Qian, J. and Li, H. Synthesis and surface modification of ZnO nanoparticles. Chemical Engineering Journal. 119 (2006) : 71-81.

[46] Aimable, A., Buscaglia, M. T., Buscaglia, V. and Bowen, P. Polymer-assisted precipitation of ZnO nanoparticles with narrow particle size distribution. Journal of the European Ceramic Society. 30 (2010) : 591-598.

[47] Malvern Instruments Ltd. Basic principles of particle size analysis [online]. Available from: http://golik.co.il/Data/BasicPrinciplesofParticlesize11269255113.pdf. [2012, Aug 13].

[48] Hu, Y., Jiang, X., Ding, Y., Ge, H., Yuan, Y. and Yang, C. Synthesis and characterization of chitosan–poly(acrylic acid) nanoparticles. Biomaterials. 23(15) (2002) : 3193-3201.

[49] Li, X., Chen, W., Bian, C., He, J., Xu, N. and Xue, G. Surface modification of TiO_2 nanoparticles by polyaniline. Applied Surface Science. 217(1–4) (2003) : 16-22.

[50] Liufu, S., Xiao, H. and Li, Y. Investigation of PEG adsorption on the surface of zinc oxide nanoparticles. Powder Technology. 145 (1) (2004): 20-24.

[51] Chibowski, S. and Winiewska, M. Study of electrokinetic properties and structure of adsorbed layers of polyacrylic acid and polyacrylamide at Fe_2O_3-polymer solution interface. Colloids and Surfaces A: Physicochemical and Engineering Aspects. 208 (1-3) (2002) : 131-145.

[52] Shengcong, L., Hanning, X. and Yuping, L. Adsorption of polyelectrolyte on the surface of ZnO nanoparticles and the stability of colloidal dispersions. Chinese Science Bulletin. 15 (50) (2005) : 1570-1575.

[53] Rodriguez-Paez, J., Caballero, A., Villegas, M., Moure, C. and Duran, P. Controlled precipitation methods: Formation mechanism of ZnO nanoparticles. Journal of the European Ceramic Society. 21 (7) (2001) : 925-930.

[54] Abbas, Z., Labbez, C., Nordholm, S. and Ahlberg, E. Size-dependent surface charging of nanoparticles. The journal of physical chemistry. 112 (2008) : 5715-5723.

APPENDICES

APPENDIX A

Properties of ZnO powder.

Product Name	ZoNoP (Zinc Oxide Nano Particles)	
Molecular formula	ZnO	-
Molecular Weight	81.39	g/mole
Appearance	White powder	-
Crystal Phase	Zincite (hexagonal)	-
Purity	99.5+	%
Average Particles Size	20-40	nm
Specefic Surface Area	26.22	m^2/g
Bulk Density	0.14	g/cc
True Density	5.6	g/cc
P.H.	7-8	-
Boiling Point	-	^0C
Melting Point	1975	^0C

XRD pattern of ZnO powder from Nano Materials Technology, Ltd.

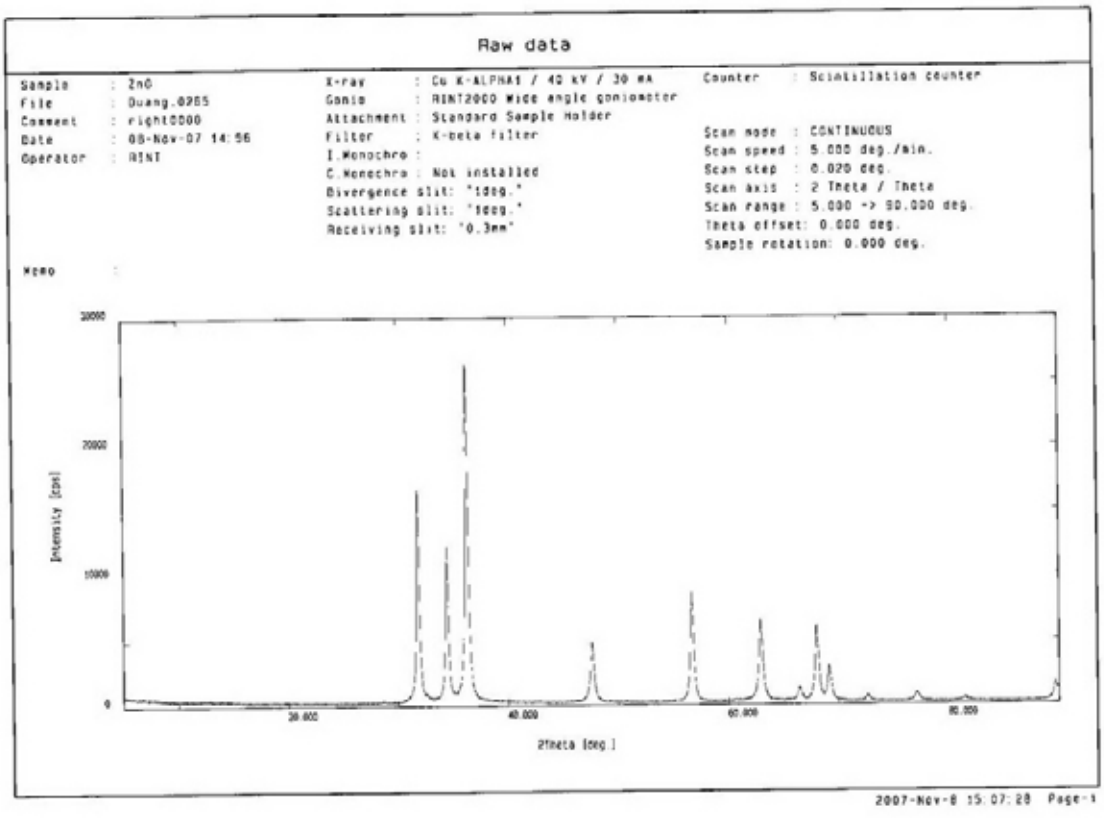

XRF report of ZnO powder

ศูนย์เครื่องมือวิจัยวิทยาศาสตร์และเทคโนโลยี จุฬาลงกรณ์มหาวิทยาลัย
อาคารสถาบัน 3 จุฬาลงกรณ์ ซอย 62 พญาไท กรุงเทพฯ 10330 โทร. 0-2218-8101, 0-2218-8032 โทรสาร (662) 254-0211
SCIENTIFIC AND TECHNOLOGICAL RESEARCH EQUIPMENT CENTRE CHULALONGKORN UNIVERSITY
CHULALONGKORN SOI 62 PHAYA-THAI ROAD BANGKOK 10330 THAILAND TEL. 0-2218-8101, 0-2218-8032 FAX : (662) 254-0211

Report No. 1123/2007 Page 1/1

Analysis Report

Sample:	ZnO nano
Sample owner:	Navaphattharakit Co., Ltd.
Objective:	To quantitate concentration of elements
Analysis Method:	Energy dispersive x – ray fluorescence spectrometry
Instrument:	X – ray fluorescence spectrometer, Oxford model ED 2000
Analysis date:	November 21, 2007

Results

Concentration (% by wt.)*		
Fe_2O_3	NiO	ZnO
0.03	0.04	99.73

*1.Quantitation method used theoretical formulas, "fundamental parameter calculations"
2. The concentration of elements is expressed as oxide equivalent

(Mr.Somboon Rhianphumikarakit)	(Mr.Utai Tiyawisutsri)	(Asst. Prof. Dr.Supongse Nimkulrat)
Analyst	Chief Scientist	Director

Remark : The results are good only for those samples analyzed.

SS/SN

The specific surface area (BET) of ZnO powder

THE PETROLEUM AND PETROCHEMICAL COLLEGE
CHULALONGKORN UNIVERSITY
SOI CHULA 12, PHAYA THAI ROAD, BANGKOK 10330, THAILAND
THE RESEARCH AFFAIRS

PPCSDWI-06-203/001.4

ANALYTICAL / TEST REPORT

Report no. 023/51

Sample owner : Navaphattarakit Co., Ltd.
Sample type : Zinc Oxide Nano
Number of sample : 1
Instrument used : Surface Area Analyzer (Quantachrome, Autosorb-1)
Date of receiving : November 8, 2007
Date of analysis : November 12, 2007
Result :

Sample name	Multipoint BET* (m^2/g)
Zinc Oxide Nano	26.22

* Specific surface area

Analyzed by :

(Ms. Jintana Chamnanmanoontham)
Researcher

Approved by : Suwabun Chirachanchai

(Assoc. Prof. Dr. Suwabun Chirachanchai)
Deputy Director for Research Affairs

N.B. The result is valid for sample analyzed only.

Properties of ZnO powder

Properties	
Molecular formula	ZnO
Molar mass	81.408 g/mol
Appearance	White solid
Odor	odorless
Density	5.606 g/cm^3
Melting point	1975 °C (decomposes)
Boiling point	2360 °C
Solubility in water	0.16 mg/100 mL (30 °C)
Band gap	3.3 eV (direct)
Refractive index(n_D)	2.0041
Thermochemistry	
Std enthalpy of formation $\Delta_f H^\ominus_{298}$	-348.0 kJ/mol
Standard molar entropy $S^\ominus_{298}$	43.9 J·K^{-1}mol

APPENDIX B

Standard JCPDS of ZnO (No.00-036-1451)

2 theta	h	k	l
31.77	1	0	0
34.42	0	0	2
36.25	1	0	1
47.54	1	0	2
56.60	1	1	0
62.86	1	0	3
66.38	2	0	0
67.96	1	1	2
69.10	2	0	1
72.56	0	0	4
76.96	2	0	2
81.37	1	0	4
89.61	2	0	3
92.78	2	1	0
95.30	2	1	1
98.61	1	1	4
102.95	2	1	2
104.13	1	0	5
107.43	2	0	4
110.39	3	0	0

APPENDIX C

Results from adsorption experiment in part of adsorption amount of PAA on ZnO particles

100% adsorption of PAA on ZnO surface

Size / MW of PAA		100 % Adsorption of PAA on ZnO surface (mg/m^2)		
		ZnO 65.31 nm	ZnO 174.56 nm	ZnO 224.54 nm
PAA(1.8k)	0.5 wt%	0.2021	0.4104	0.5863
	1 wt%	0.4162	0.8449	1.2072
	3 wt%	1.1891	2.4141	3.4491
	5 wt%	2.0215	4.1039	5.8635
PAA(450k)	0.5 wt%	0.2021	0.4104	0.5863
	1 wt%	0.3567	0.7242	1.0347
	3 wt%	1.3080	2.6555	3.7940
	5 wt%	2.0809	4.2246	6.0359
PAA(3000k)	0.5 wt%	0.1903	0.3863	0.5519
	1 wt%	0.4043	0.8208	1.1727
	3 wt%	1.1891	2.4141	3.4491
	5 wt%	2.0690	4.2005	6.0014

Amount of PAA adsorbed on ZnO surface

Size / MW of PAA		Amount PAA adsorbed on ZnO surface (mg/m^2)		
		ZnO 65.31 nm	ZnO 174.56 nm	ZnO 224.54 nm
PAA(1.8k)	0.5 wt%	0.0361	0.0180	0.0123
	1 wt%	0.0369	0.0185	0.0144
	3 wt%	0.0357	0.0178	0.0178
	5 wt%	0.0396	0.0198	0.0198
PAA(450k)	0.5 wt%	0.0691	0.0358	0.0275
	1 wt%	0.0699	0.0416	0.0333
	3 wt%	0.0700	0.0483	0.0499
	5 wt%	0.0749	0.0503	0.0503
PAA(3000k)	0.5 wt%	0.0856	0.0511	0.0404
	1 wt%	0.0904	0.0785	0.0547
	3 wt%	0.0862	0.0517	0.0862
	5 wt%	0.0949	0.0949	0.0949

The monolayer coverage of PAA adsorbed on ZnO

Size / MW of PAA	Monolayer coverage of PAA adsorbed on ZnO surface (mg/m^2)		
	ZnO 65.31 nm	ZnO 174.56 nm	ZnO 224.54 nm
PAA(1.8k)	0.0361	0.0185	0.0178
PAA(450k)	0.0691	0.0416	0.0499
PAA(3000k)	0.0856	0.0785	0.0862

Initial concentration of PAA for adsorption on ZnO surface

Size / MW of PAA	Initial concentration of PAA for adsorption on ZnO surface (mg/l)		
	ZnO 65.31 nm	ZnO 174.56 nm	ZnO 224.54 nm
PAA(1.8k)	24.48	50.40	144.00
PAA(450k)	24.48	43.20	158.40
PAA(3000k)	23.04	48.96	144.00

Data of Langmuir equation between $C/\left(n_2^s/W\right)$ as a function of C

Size / C		$C/\left(n_2^s/W\right)$		
		ZnO 65.31 nm	ZnO 174.56 nm	ZnO 224.54 nm
PAA(1.8k)	0.00034	28.0114	113.7360	238.3325
	0.0007	56.3889	228.9587	420.5868
	0.002	166.6667	676.7253	966.8663
	0.0034	255.0000	21035.3898	1479.3054
PAA(450k)	0.00034	14.6287	57.3256	106.7227
	0.0006	25.5080	87.0000	155.3757
	0.0022	93.4181	275.0000	379.8074
	0.0035	138.8768	420.0000	600.0719
PAA(3000k)	0.00032	11.1088	37.7629	68.2353
	0.00068	22.3638	52.2816	107.1739
	0.002	109.0684	233.3054	200.0000
	0.00348	109.0684	221.4280	316.3636

Values of slope (m), intercept (b) and equilibrium constant (K)

Value	M_W	Size		
		ZnO 65.31 nm	ZnO 174.56 nm	ZnO 224.54 nm
Slope (m)	1.8k	74961	304366	403577
	450k	39679	115144	153389
	3000k	31340	65118	76889
Intercept (b)	1.8k	5.83	23.672	126.51
	450k	2.24	18.692	55.868
	3000k	2.1	30.703	48.384
Equilibrium constant (K)	1.8k	12857.58	12857.64	3190.08
	450k	17714.63	6160.07	2745.56
	3000k	14906.06	2120.90	1589.14

Area occupied per molecule PAA on ZnO surface

Size / M_W of PAA	Area occupied per molecule (nm^2/molecule)		
	ZnO 65.31 nm	ZnO 174.56 nm	ZnO 224.54 nm
PAA(1.8k)	3.02	12.25	16.24
PAA(450k)	1.60	4.63	6.17
PAA(3000k)	1.26	2.62	3.09

APPENDIX D

XRD patterns of ZnO synthesized using 0.05 wt% PAA(1.8k).

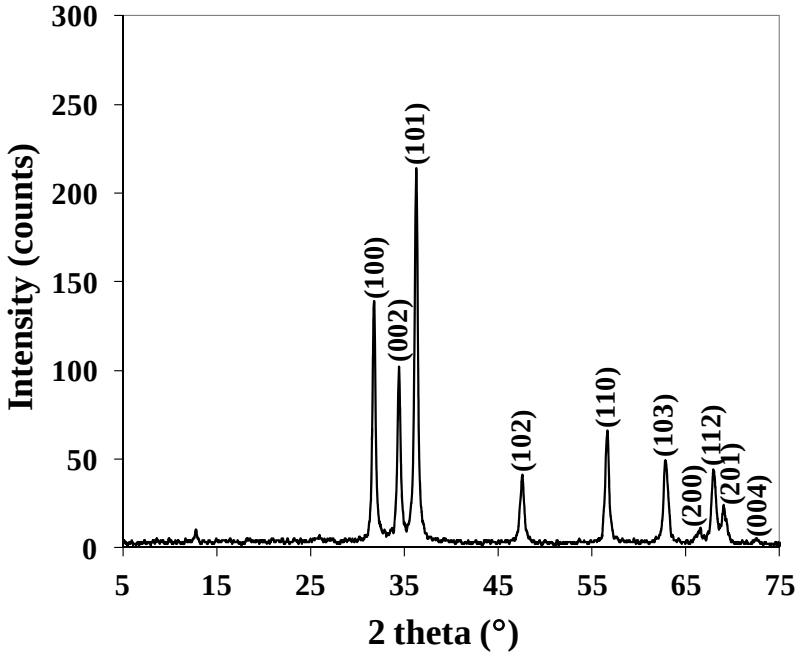

XRD patterns of ZnO synthesized using 0.05 wt% PAA(450k).

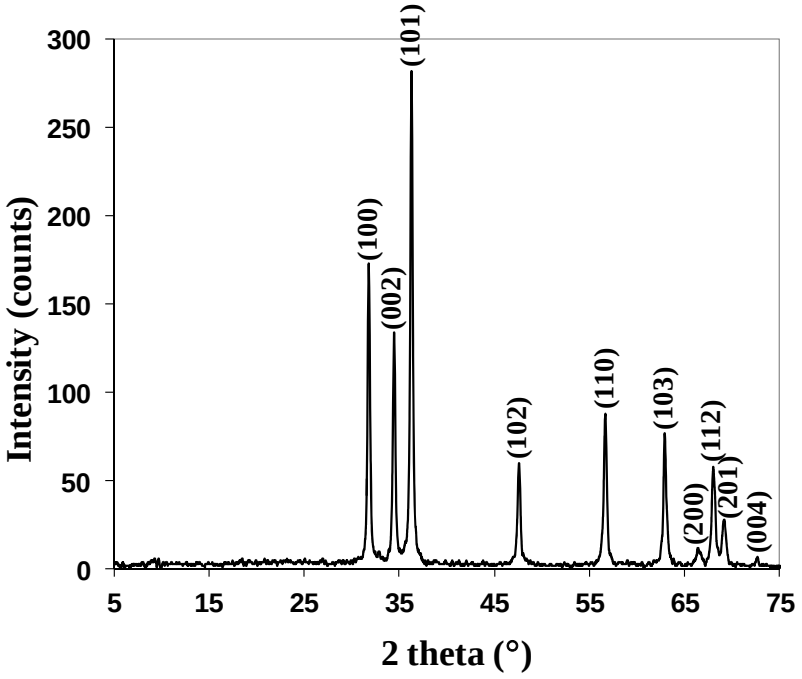

XRD patterns of ZnO synthesized using 0.05 wt% PAA(3000k).

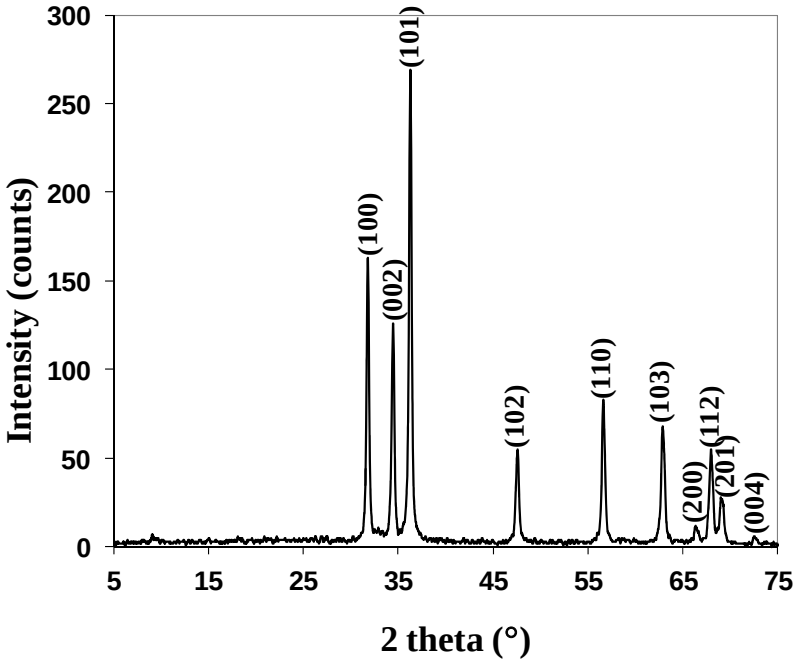

XRD patterns of ZnO synthesized using 0.5 wt% PAA(1.8k).

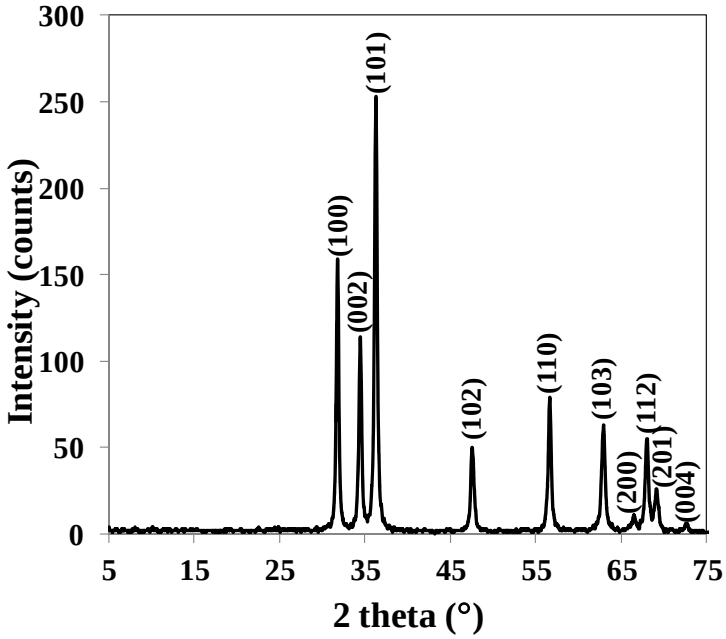

XRD patterns of ZnO synthesized using 0.5 wt% PAA(450k).

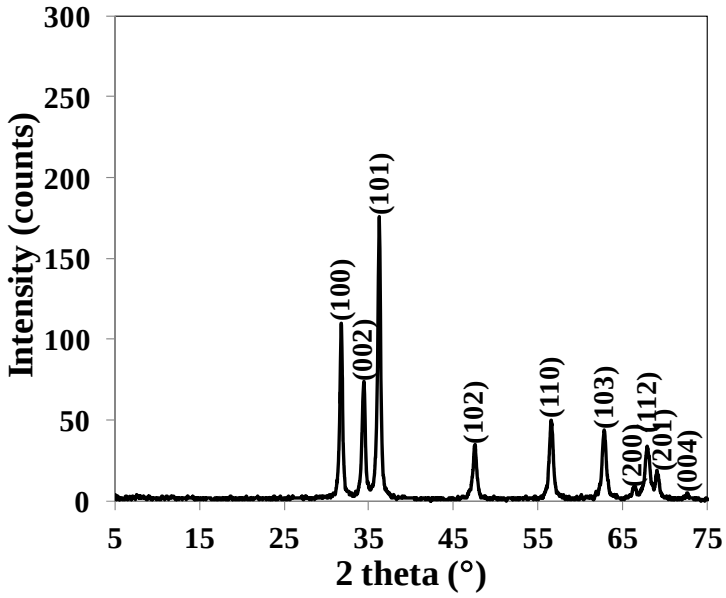

XRD patterns of ZnO synthesized using 0.5 wt% PAA(3000k).

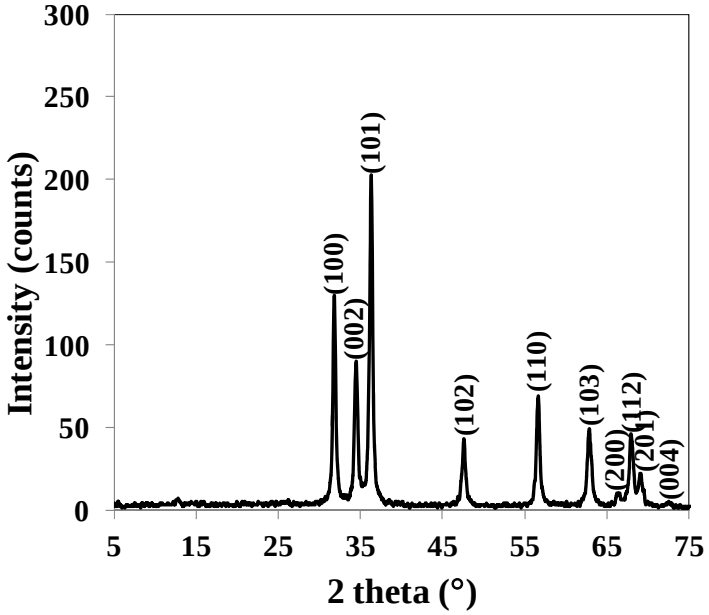

XRD patterns of ZnO synthesized using 1 wt% PAA(1.8k).

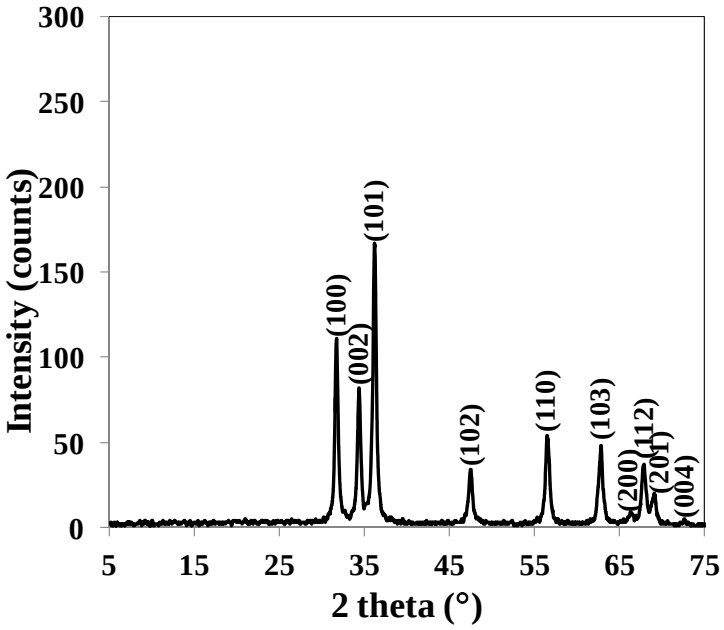

XRD patterns of ZnO synthesized using 1 wt% PAA(450k).

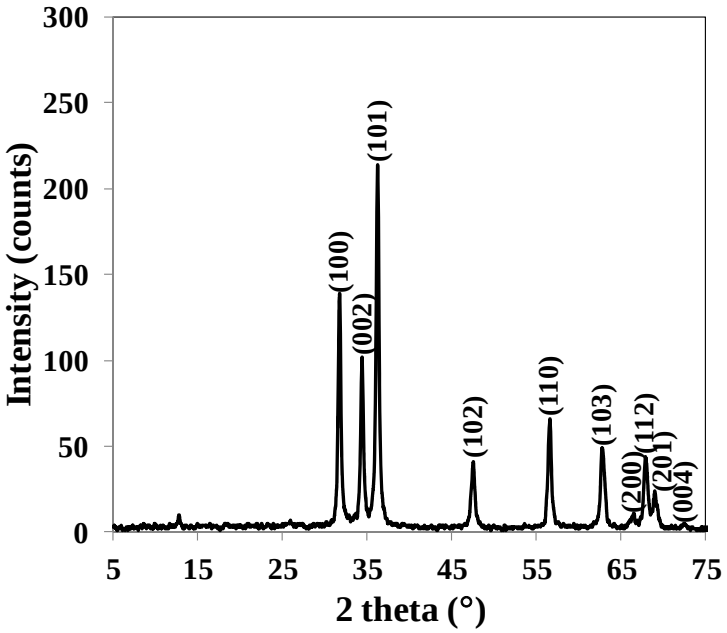

XRD patterns of ZnO synthesized using 1 wt% PAA(3000k).

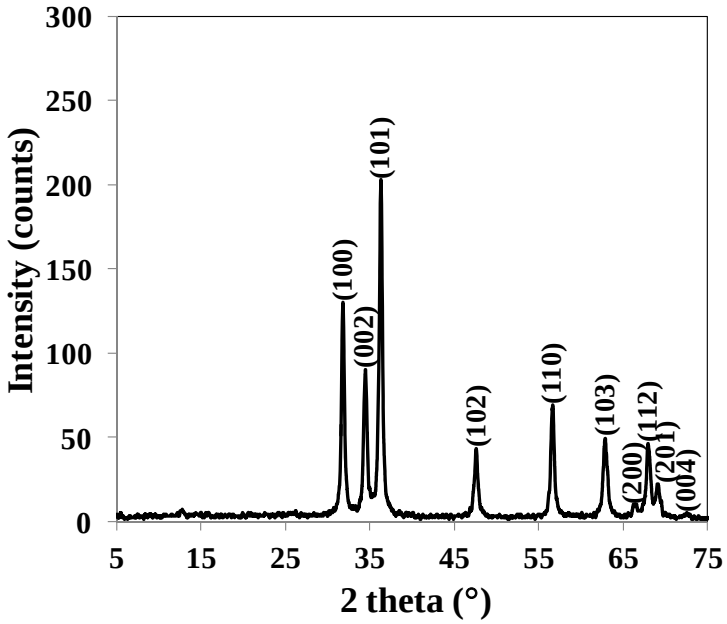

BIOGRAPHY

Miss Rudeerat Suntako was born in Pattani on March 30th, 1982. In 2004, she finished her Bachelor's Degree in Physics from the Department of Physics, Faculty of Science, Prince of Songkla University. In 2006, she finished her Master's Degree in Ceramic Technology from the Department of Materials Science, Faculty of Science, Chulalongkorn University. In 2007, she studied Doctoral's Degree in Materials Science from the Department of Materials Science, Faculty of Science, Chulalongkorn University and graduated in 2012.

Conference presentations

- **Rudeerat Suntako**, Pitak Laoratanakul and Nisanart Traiphol. Preparation of Lead Zirconate Titanate Aqueous Suspension and Properties of Ceramic Tape. 4th Mathematics and Physical Science Graduate Congress (MPSGC4). Faculty of Science, National University of Singapore, Singapore (2010).

-**Rudeerat Suntako**, Nisanart Traiphol. Aqueous dispersion of ZnO nanoparticle using Polyacrylic acid of various Molecular Weights. The 1st National Research Symposium on Petroleum, Petrochemicals, and Advanced Materials. Bangkok, Thailand (2010).

-**Rudeerat Suntako**, Nisanart Traiphol. Relationship of ZnO particle size and poly(acrylic acid) molecular weight: Effects on dispersion and stability of aqueous suspension. Commission on Higher Education Congress III: University Staff Development Consortium. Pattaya, Chonburi (2010).

-**Rudeerat Suntako**, Nisanart Traiphol. Synthesis of Zinc Oxide Nanoparticles using Polyacrylic Acid: Effects of Dispersant Molecular Weight. Pure and Applied Chemistry International Conference (PACCON2012). Chiangmai (2012).